INTEGRATION OF SINGLE-CELL ELECTROPERMEABILIZATION TOGETHER WITH ELECTROCHEMICAL MEASUREMENT OF QUANTAL EXOCYTOSIS ON MICROCHIPS

A Dissertation presented to
the Faculty of the Graduate School
at the University of Missouri-Columbia

In Partial Fulfillment of the Requirements for the Degree

Doctor of Philosophy

---

by
JAYA GHOSH

Dr. Kevin D. Gillis, Dissertation Supervisor

DECEMBER 2013

The undersigned, appointed by the dean of the Graduate School, have examined the dissertation entitled

INTEGRATION OF SINGLE-CELL ELECTROPERMEABILIZATION TOGETHER WITH ELECTROCHEMICAL MEASUREMENT OF QUANTAL EXOCYTOSIS ON MICROCHIPS

presented by Jaya Ghosh,

a candidate for the degree of Doctor of Philosophy,

and hereby certify that, in their opinion, it is worthy of acceptance.

Kevin D. Gillis, D. Sc., Department of Biological Engineering

---

Liqun (Andrew) Gu, Ph.D., Department of Biological Engineering

---

Shramik Sengupta, Ph.D., Department of Biological Engineering

---

Mahmoud Almasri, Ph.D., Department of Electrical and Computer Engineering

---

Michael R. Baldwin, Ph.D., Department of Molecular Microbiology and Immunology

ACKNOWLEDGEMENTS

This project is the result of the hard work, vision, and guidance of many people. I would like to take this opportunity to express my heartfelt thanks for each and every one of them.

First and foremost, I would like to thank my mentor Dr. Kevin Gillis who believed in my abilities and helped me in taking this step forward toward realizing my goals. His command on the subject, scientific passion and insights, integrity and intellectual honesty, problem-solving attitude and high performance expectations will always remain objects of inspiration for me. I am also deeply grateful to him and his family for welcoming every one of us in the lab with open arms and making us feel at home.

I sincerely thank my committee members Dr. Liqun (Andrew) Gu, Dr. Mahmoud Almasri, Dr. Shramik Sengupta and Dr. Michael Baldwin for their invaluable advice, insightful critiques and continuous encouragement.

A huge thank you to Dr. Mahmoud Almasri and Dr. Shubhra Gangopadhyay for training me and letting me use their cutting-edge facilities at the Department of Electrical and Computer Engineering. I am grateful to Dr. Michael Baldwin for the kind gift of Botulinum neurotoxin light chain /E and helpful discussions about the project. I thank Dr. Shramik Sengupta for the enlightening discussions about the grant writing process.

I am indebted to Dr. Xin (Alice) Liu not only for her contributions to this work but also for guiding me in developing an understanding of the subject. My heartfelt thanks to my fellow graduate students, colleagues at the Dalton Cardiovascular Research

Center, Department of Biological Engineering, and the Gillis Lab, especially to Dr. Barizuddin Syed and Dr. Jia Yao for their help, guidance and unwavering optimism.

I especially want to thank my family members who stood by me not only while I was working on this degree but also throughout my life. My grandfather and uncle taught me the value of education and their achievements inspired me to set higher goals for myself. My grandmother filled me with the goodness of life and taught me to be independent. I owe it to her from the very first step I took to venture out into this world. My mother taught me the values of perseverance, hard work and dedication. My aunt, elder brother and sister-in-law always guided and supported me like good friends. And thanks to my late father, who taught me the importance of happiness and dreams, and who I wish could be here today with me to share this prized moment. A special thanks to my dear friends Dr. Jhuma Das and Dr. Kamalika Mukherjee for their continuous support and help with the little everyday things of a graduate student's life.

TABLE OF CONTENTS

LIST OF FIGURES

LIST OF TABLES

Table Page

INTEGRATION OF SINGLE-CELL ELECTROPERMEABILIZATION TOGETHER WITH ELECTROCHEMICAL MEASUREMENT OF QUANTAL EXOCYTOSIS ON MICROCHIPS

Jaya Ghosh

Dr. Kevin D. Gillis, Dissertation Supervisor

ABSTRACT

An electrochemical microelectrode located immediately adjacent to a single neuroendocrine cell can record spikes of amperometric current that result from quantal exocytosis of oxidizable transmitter from individual vesicles. Using electroporation we have developed an efficient method where the same electrochemical microelectrode is used to electropermeabilize an adjacent chromaffin cell and then measure the consequent quantal catecholamine release using amperometry. Trains of voltage pulses, 5–7 V in amplitude and 0.1–0.2 ms in duration can reliably trigger release from cells using gold electrodes. Amperometric spikes induced by electropermeabilization have similar areas, peak heights and durations as amperometric spikes elicited by depolarizing high K^+ solutions. Uptake of trypan blue stain into cells demonstrated that the plasma membrane is permeabilized by the voltage stimulus. Robust quantal release is elicited upon electroporation in 0 Ca^{2+}/5 mM EGTA in the bath solution. Electropermeabilization-induced transmitter release requires Cl^- in the bath solution – bracketed experiments demonstrate a steep dependence of the rate of electropermeabilization-induced transmitter release on [Cl^-] between 2 and 32 mM. Using the same electrochemical electrode to electroporate and record quantal release of catecholamines from an individual chromaffin cell allows precise timing of the stimulus, stimulation of a single cell at a time, and can be used to load membrane impermeant substances into a cell.

CHAPTER 1

INTRODUCTION

Unique chemical and biological insights at the single-cell level have been made possible by advances in methodology enabling chemical measurements of very small volumes of analytes and at small spatial dimensions with high sensitivity and selectivity. Using a variety of methods and platforms, small analytes such as amino acids and neurotransmitter molecules as well as larger proteins and cell organelles have been quantified in single cells.

The use of microchip devices to study cellular systems is a research area that is growing at a rapid pace and poses numerous advantages. Microchip-based cellular analysis with electrochemistry as the basis for detection is used in a variety of systems including on-chip detection of quantal exocytosis from individual cells, electrochemical analysis of intracellular contents, use of integrated electrodes to assay cell confluency, etc … (Sims and others 2007; Ge and others 2010; Cans and others 2011; Johnson and others 2013). With the new appreciation of cellular heterogeneity in terms of variability in genetic composition, biochemistry, and physiology, traditional assays which yield data averaged across large groups of cells are being replaced by individual cell studies. Factors like variation in expression of genes, proteins and metabolites have been found to elucidate unique biological phenomena in single cells that are not detectable by bulk sampling procedures.

Technical specifications for single cell analysis are strict but various bioanalytical techniques have been developed to measure individual quantal neurotransmitter secretion

events at the single cell level (Wightman and others 1991; Chow and others 1992; De Toledo and others 1993; Chen and others 1994; Chen and others 1995; Finnegan and others 1996; Albillos and others 1997; Hochstetler and others 2000; Pothos 2002; Staal and others 2004; Zhang and others 2009). Studies reporting the use of carbon-fiber based microelectrochemical methods for measurement of neurotransmitters were reported as early as the late 1970s (Gonon and others 1978; Ponchon and others 1979). In the early 1990s, Wightman and coworkers (Leszczyszyn and others 1990; Kawagoe and others 1991) were the first to use carbon-fiber-based electrochemical methods for single-cell exocytosis studies. Adrenal glands of cattle and rats provided the first model secretory cells for electrochemical detection of quantal exocytosis because not only did they contain secretory vesicles that store catecholamines, but also because of their neuroectodermal origin and biochemical and functional similarities with true sympathetic neurons. In fact, compared to neurons, nonsynaptic cell models like the chromaffin cells are preferred for studying single-cell exocytosis because the release site on the neuroendocrine cell is easily accessible to the electrochemical microelectrodes.

Single cell electrochemical measurements have been done in primary as well as cell lines. Examples include catecholamine release from adrenal medullar chromaffin cells (Pihel and others 1996) and rat PC12 (pheocromocytoma) cells (Chen and others 1994), 5-hydroxytryptamine and histamine from mouse mast cells (Marszalek and others 1997), insulin from pancreatic β-cells (Barnett and others 1996), and metabolic molecules such as nitric oxide and hydrogen peroxide from single cells (Amatore and others 2008).

1.1 Exocytosis

Exocytosis is an essential vesicle trafficking process. It is the means by which cells direct intracellular vesicles to fuse with the plasma membrane and release their contents to the extracellular space, or, incorporate newly synthesized membrane proteins into the plasma membrane. Two types of exocytosis are seen in eukaryotic cells – non-Ca^{2+}-triggered constitutive exocytosis, and regulated exocytosis (Kelly 1985). In constitutive exocytosis, transport vesicles fuse with the plasma membrane constitutively to release their contents and no external stimulus is needed to trigger exocytosis by altering the level of a cytoplasmic second messenger. It is seen in all eukaryotic cells and is used to deliver newly synthesized proteins to the cell membrane and extracellular environment (Palade 1975; Schmoranzer and others 2000). Regulated exocytosis, on the other hand, is triggered by extracellular or intracellular signals such as cytoplasmic messengers including Ca^{2+}, cAMP, cGMP, etc. Ca^{2+}-dependent exocytosis is a process by which discrete vesicles fuse with the cell membrane and release their contents into the extracellular environment in response to an increase in intracellular Ca^{2+} concentration $[Ca^{2+}]_i$. Most neurons and neuroendocrine cells secrete hormones and neurotransmitters via Ca^{2+}-dependent exocytosis in response to Ca^{2+} influx as voltage-gated Ca^{2+} channels are opened by membrane depolarization.

By initiating secretion of neurotransmitters and hormones, Ca^{2+}-triggered exocytosis plays a fundamental role in cell-to-cell communication. On application of an appropriate stimulus, the vesicles fuse to the cell membrane and release their contents in order to trigger various responses in the target cell or environment. It is important to study the exocytosis mechanism in details as it plays an important role in various regular

neurological functions as well as in disease conditions. Parkinson's disease is a degenerative disorder of the central nervous system, which is characterized by symptoms like tremors, slowed movement, rigid muscles, impaired posture and balance, and is caused by the loss of dopaminergic neurons of the substanitia nigra in the brain and the resultant loss of dopamine release from neurons. L-3,4-dihydroxyphenylalanine (a.k.a. L-dopa or Levodopa), the precursor of dopamine, provides symptomatic relief for Parkinson's disease by increasing the amount of dopamine packaged into individual vesicles (Pothos and others 1996; Pothos and others 1998; Sulzer and others 2000; Pothos 2002; Gong and others 2003). In Huntington's disease, a neurodegenerative genetic disorder that typically becomes noticeable in mid-adult life, the amount of catecholamine secretion from each vesicle is diminished significantly although the number of secretion events remains the same. This affects muscle coordination and leads to cognitive decline and psychiatric problems in patients (Johnson and others 2007).

SNARE (Soluble N-ethylmaleimide-sensitive factor Attachment protein REceptor) proteins are a large family of proteins that play a primary role in vesicle fusion (Sudhof 1995; Neher 1998; Burgoyne and others 2003; Sørensen 2005; Jahn and others 2006; Jahn and others 2012). The synaptic proteins synaptobrevin, syntaxin 1 and SNAP-25 belong to the SNARE protein family. Clostridial neurotoxins, such as Botulinum Toxin types A and E (BoNT/A and BoNT/E), can inhibit the process of exocytosis and cause muscle paralysis and even death. Whereas effects of the neurotoxin can be lethal, local applications in very low doses can be helpful in treating various medical conditions. BoNT/A is best known for its use in cosmetic treatment (BOTOX®) whereby it temporarily improves the appearance of frown lines between the eyebrows and is also

used for treatment of uncontrollable movement disorders. The underlying working principle is that the toxin selectively blocks exocytosis of acetylcholine at a neuromuscular junction by cleavage of the SNARE protein SNAP-25, thus inhibiting acetylcholine-containing vesicle fusion with the cell membrane. By inhibiting acetylcholine release, the toxin causes flaccid paralysis of muscles, which can temporarily "relax" frown lines (Song 1998; Frampton and others 2003; Said and others 2003). BoNT toxin products are also used for treating excessive underarm sweating, migraine and other primary headache disorders, certain neurological disorders such as spasticity, and muscle pain disorders including cervical dystonia, eyelid spasms and crossed eyes (Boghen 1996; Kreyden and others 2000; McNeer and others 2000; Connolly and others 2003; Blumenfeld and others 2004).

Regulated exocytosis is highly conserved across several cell types including neurons, adrenal chromaffin cells, PC12 cell line (which is derived from a pheochromocytoma of the rat adrenal medulla), insulin-secreting pancreatic β-cells, platelets and a variety of immune cells such as mast cells and macrophages (Burgoyne and others 2003; Kim and others 2011). Our study focuses on chromaffin cells which are found mostly in the medulla of the adrenal glands. They secrete catecholamines (primarily epinephrine / adrenaline and some norepinephrine / noradrenaline), dopamine and a few other hormones (Fenwick and others 1978). The secreted adrenaline and noradrenaline play an important role in the fight-or-flight response whereby they directly increase heart rate, trigger the release of glucose from energy stores, and increase blood flow to skeletal muscle. Norepinephrine and dopamine act as neuromodulators in the central nervous system and hormones in blood circulation.

The biophysical and biochemical properties of exocytosis have been extensively studied but the detailed molecular mechanism and kinetics of exocytosis still continue to be challenging topics. Several powerful techniques with high sensitivity, signal-to-noise ratio and spatio-temporal resolution have emerged to help advance our understanding of this fundamental mode of intercellular communication. Platforms like carbon-fiber microelectrodes (CFEs) have been commonly used to study quantal exocytosis of electroactive transmitters such as catecholamines from individual cells (Wightman and others 1991). Though it is a robust technique, it is a low-throughput process involving manual positioning of an electrode adjacent to an individual cell surface using micromanipulators while observing the preparation under a microscope. Experiments are performed on one cell at a time and the carbon fiber electrodes have to be manually fabricated in small lots and need to be cut to expose a fresh surface or replaced frequently. Recently, in an effort to enable high-throughput experiments, microfabricated lab-on-a-chip devices have been developed with arrays of microelectrodes where cells can be targeted to individual electrodes thereby eliminating the need to manually bring electrodes to cells.

A common technique used to stimulate exocytosis is perfusion of cells with a secratogogue leading to depolarization of the cell membrane, opening of voltage-gated Ca^{2+}-channels, Ca^{2+} influx and Ca^{2+}-triggered release of neurotransmitter that is measured by on-chip electrochemical microelectrodes at the single-cell and single-vesicle level. Perfusion systems however, usually stimulate multiple cells and do not allow the stimulation to be timed precisely. In order to address these limitations, we have

developed an electrical stimulation approach that is integrated together with electrochemical measurement of quantal exocytosis on microchips.

1.2 Detection of exocytosis

Since individual secretory vesicles are small in size (25-500 nm), and the release event occurs in the milliseconds range, measurement of quantal exocytosis requires sensitive techniques of chemical analysis with high signal-to-noise ratios and high spatio-temporal resolution (Travis and others 1998). Commonly used techniques for exocytosis measurement include patch clamp, amperometry, and voltammetry.

Patch clamp is a powerful technique that allows electrophysiological study of single or multiple ion channels in cells. The technique can be applied to a wide variety of cells, but is especially useful in the study of excitable cells such as neurons, cardiomyocytes, and pancreatic beta cells. Erwin Neher and Bert Sakmann developed this technique (Neher and others 1976) in the late 1970s and early 1980s. This technique made it possible to record currents of single ion channels for the first time, and for their pioneering work, Neher and Sakmann received the Nobel Prize in Physiology and Medicine in 1991.

The basic working principle of patch clamp consists of using a glass micropipette with a very small open tip diameter to attach to a patch of cell membrane and record electrical activities going on in that patch or the whole cell (as shown in Fig 1.1). The patch pipette tip has a diameter of ~1 μm and is maneuvered to press gently against a cell. Suction is slowly applied to the inside of the pipette to pull a small patch of the cell membrane into the pipette tip. The patch and the pipette can form a tight seal with an

electrical resistance of over 1 GΩ, (hence it is called a gigaseal). The high resistance of this seal makes it possible to electrically isolate and measure with high signal-to-noise ratio the small currents (in the picoamp (10^{-12} A) range) generated due to ion flow through individual channels in the patch. The Food and Drug Administration uses this technique as the gold standard screening process for studying the interactions between drugs and ion channels during new drug discovery research. This is known as the cell-attached or on-cell patch configuration.

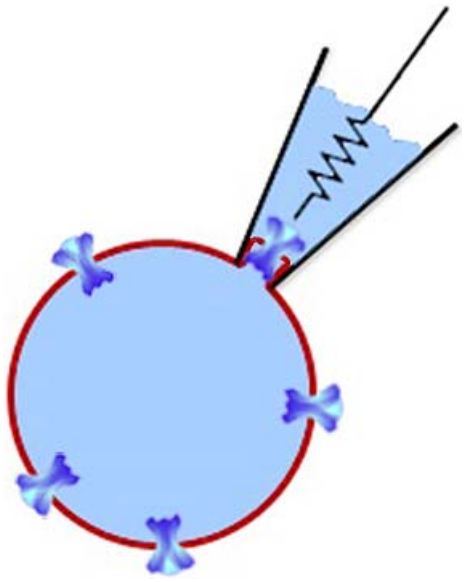

Fig 1.1 A schematic showing a single ion channel being recorded within the patch pipette

Several variations of the basic technique allow different modes of recording the electrical activity of the whole cell or the channels in the patch of membrane forming the seal. In the whole-cell patch clamp mode, the patch is ruptured by application of sudden suction pulses, and this allows recording of current throughout the whole cell. Also via diffusion, the intracellular solution can be exchanged for the solution contained in the glass pipette. In this study, we mainly employed whole-cell patch clamp recording in

order to measure action potentials as well as exocytosis-induced changes in membrane-area.

Action potentials are the physiological stimuli for secretion of hormones and neurotransmitters from most neurons and neuroendocrine cells. In neurotransmitter-secreting cells, Ca^{2+}-triggered exocytosis is known to be induced by action potentials (shown in flow-chart below) which can be triggered in cells using external stimuli.

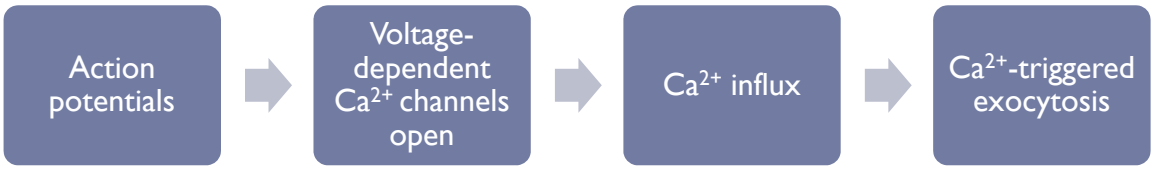

One widely used approach that is employed in neuroscience is to trigger an action potential using a transient electric field produced by a pair of extracellular electrodes.

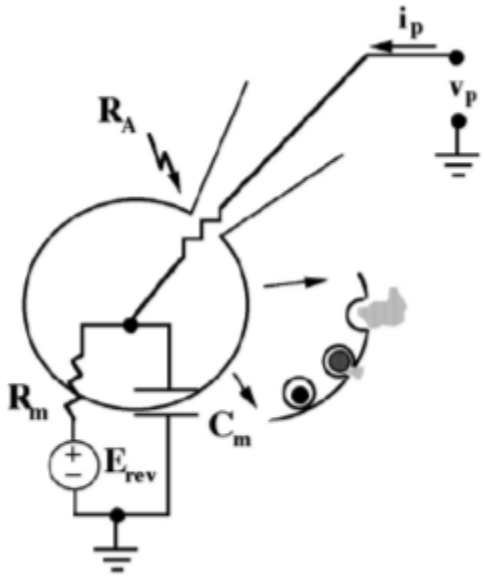

Fig 1.2 Equivalent circuit of a cell in the whole-cell patch clamp configuration

The capacitance of a cell membrane is proportional to its area. Upon fusion of vesicles, exocytosis leads to an increase in the cell membrane area, which in turn results in an increase in the measured capacitance. The whole-cell patch clamp technique can also be used to measure membrane capacitance changes and the equivalent circuit of a patch clamped cell in whole-cell mode is shown in Fig 1.2. The lipid bilayer of a cell membrane can be simplified as a membrane resistor (R_m) and a membrane capacitor (C_m) together with a cell resting potential (E_{REV}). The pipette electrode has series resistance (R_A). By applying a sinusoidal voltage (V_P) to the glass pipette electrode and measuring the current (I_P), membrane capacitance can be calculated using complex impedance analysis of the equivalent circuit (Gillis 1995; Marty and others 1995). Endocytosis, as opposed to exocytosis, leads to capacitance decreases due to membrane retrieval. With millisecond time resolution, cell membrane capacitance measurements provide detailed information about the time course of vesicle fusion. Though this method can help in understanding fusion pores dynamics, it does not directly measure release of neurotransmitter. For example, fusion of an empty vesicle produces similar capacitance changes to that of a transmitter-laden vesicle. A membrane capacitance change could also be induced by other membrane processes (Borges and others 2008) – some studies show that recovery of Na^+ channel from inactivation also accounts for non-exocytotic sources of capacitance change (Horrigan and others 1994).

In the 1950s, Sir Bernard Katz and colleagues pioneered the study of exocytosis at neuromuscular junction of frogs by recording the miniature endplate potentials generated by the release of acetylcholine molecules (Fatt and others 1950; Fatt and others 1950; Fatt and others 1952). These experiments led to the “quantal” hypothesis which states

that transmitter is released in discrete packets, now understood to be vesicles. However, it was only after the development of amperometry 40 years later that quantal release of neurotransmitter via exocytosis was directly measured. The Adams group was the first to work on the basic principles of monoamine oxidation at the electrode surface (Kissinger and others 1973; McCreery and others 1974). Following their work, Wightman's group (Leszczyszyn and others 1990; Chow and others 1992; Travis and others 1998) and others (Chow and others 1992) employed carbon fiber electrodes (CFEs) to detect quantal secretion of catecholamine from single vesicles of chromaffin cells. Potentially detectable chemicals include adrenaline, noradrenaline, dopamine, histamine and serotonin. Carbon fiber electrodes are mechanically rigid, chemically stable and highly conductive (Schulte and others 1996) making them the ideal candidate for electrodes used to measure quantal exocytosis. Released neurotransmitters are readily oxidized, and therefore can be detected using electrochemical techniques.

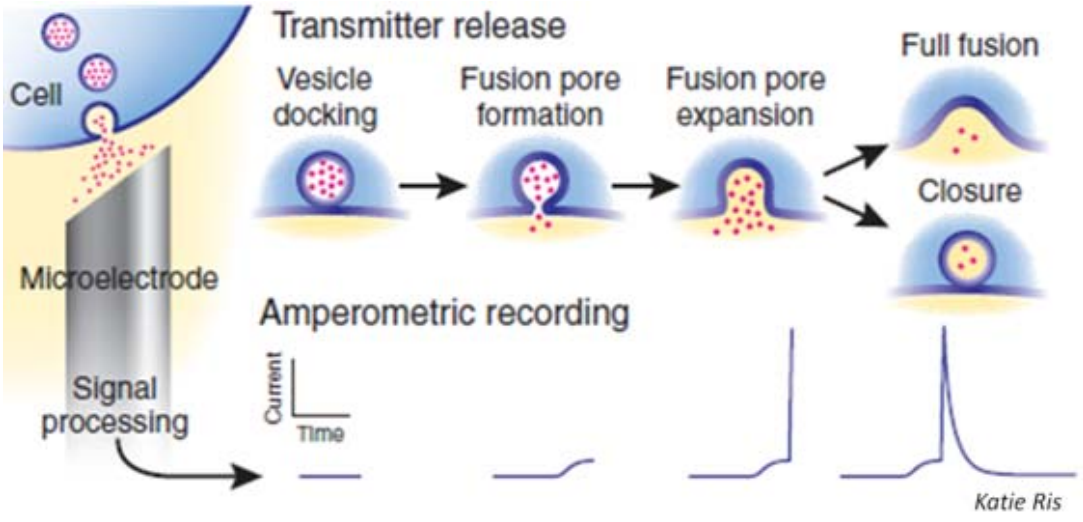

Fig 1.3 Illustration of carbon fiber amperometry in single cell quantal exocytosis measurement. Reprinted by permission from Macmillan Publishers Ltd: Nature Methods, (Evanko 2005), copyright 2005

Amperometry is the measurement of faradaic current while the measuring electrode potential is held at a constant value. This method allows the measurement of analyte with high time resolution but the identity and concentration of the analyte cannot be resolved. By holding a carbon fiber electrode at the constant potential (typically 600 – 700 mV), which far exceeds the redox potential of the released transmitter, a current can be recorded and the number of electroactive molecules along with the frequency of release can be known. In the oxidation process, each catecholamine molecule loses two electrons to the electrode and each spike in current represents a single-vesicle fusion event. The transmitter release process consists of multiple steps including fusion pore formation, fusion pore expansion and full fusion or closure of pore, which are evidenced by the foot signal, the steep rising phase of the amperometric spike and the slower exponential fall, respectively (as shown in Fig 1.3). Integration of the amperometric current indicates the amount of transmitter released from an individual vesicle. The time course of the spike provides important information about vesicle fusion event and release kinetics. With amperometry, millisecond time resolution and sensitivity of few tens of thousands of molecules can be achieved (Bruns and others 1995) if careful noise shielding and filtering are applied. Similarly, a foot signal (Chow and others 1992), provides information on the fusion pore geometry and its lifetime. It reflects the slow release of transmitter through a ~2 nm fusion pore before dilation of the pore leads to rapid release indicated by amperometric spikes (Alvarez De Toledo 1995; Lindau and others 2003).

As further demonstrated in Fig 1.4, important parameters can be extracted from recorded amperometric spikes. The maximum oxidation current, I_{max}, is the maximum

flux of neurotransmitters released during a vesicle fusion. Half-width $t_{1/2}$, is determined at 50% of I_{max} and describes how fast the molecules are released from the vesicle, and Q, the total charge, represents the area under the spike which can be used to calculate the total number of electroactive molecules released during a vesicle fusion event (Fig 1.4(a)). t_{foot} is an empirical measurement of the lifetime of the pore, Q_{foot}, the charge under the foot signal, can be used to calculate the number of molecules released through the pore, and I_{foot} describes the flux of neurotransmitter released during the duration of the foot signal. Fig 1.4(b) shows parameters of a typical pre-spike foot signal.

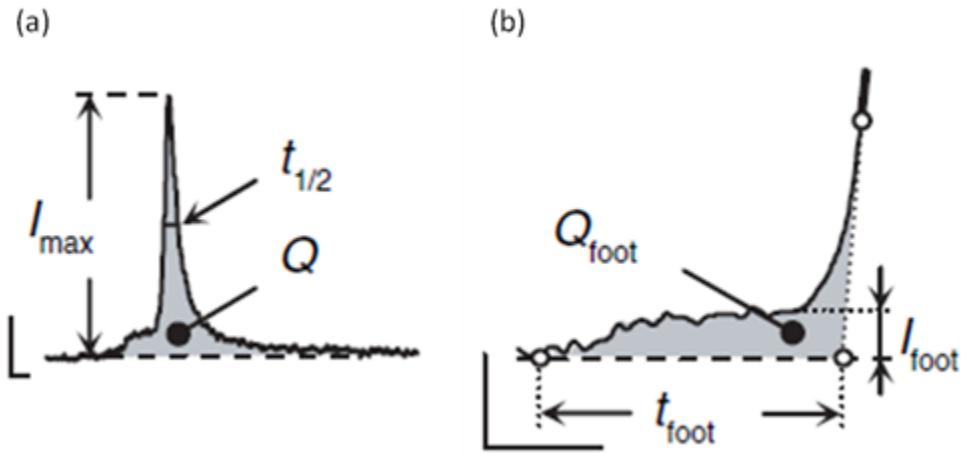

Fig 1.4 Relevant quantitative and kinetic parameters of an amperometric spike. (a) I_{max}, $t_{1/2}$ and Q. (b) Foot signal with Q_{foot}, t_{foot} and I_{foot}. Reprinted by permission from Macmillan Publishers Ltd: Nature Methods, (Mosharov and others 2005), copyright 2005

Patch amperometry (Albillos and others 1997) is a combination of patch clamp and carbon fiber amperometry techniques. Simultaneous measurement of membrane fusion capacitance and amperometric current from neurotransmitter oxidation was achieved by a novel technique that incorporated a carbon fiber microelectrode inside a traditional patch clamp pipette. Using the patch amperometry method, it is possible to

distinguish transient and full fusion events, and to analyze individual fusion pore openings and the role of the fusion pore in limiting release (Dernick and others 2003).

The methods described above have high sensitivity and spatial resolution but they have one disadvantage that is common to all of them. They require the manual positioning of the detecting microelectrode or patch pipette against an individual cell making the process labor intensive and low throughput. In addition, it is difficult to image the release site of the cell that is directly adjacent to the carbon fiber.

1.3 BioMEMS and on-chip amperometry

Micro-Electro-Mechanical Systems (MEMS), initiated in the 1970s, is a technology that uses miniaturized mechanical and electro-mechanical elements. These structures or devices are made using microfabrication techniques that were adapted from the semiconductor industry. As of 2002, the commercial market size of MEMS was over trillions of dollars (Madou 2002). MEMS devices have a number of relative advantages including batch fabrication at significantly reduced costs per unit. They can either be reusable or disposable making them ideal for different types of applications. MEMS devices are developed for a variety of platforms including mechanical, electrical, chemical as well as biological. Some popular examples of MEMS-devices are: silicon microphones (sound/voice sensor), gyroscopes, accelerometers (motion/position sensors), pressure-sensors, micromirrors (light actuator), Oscillators/Resonators, FR-MEMS switches (RF actuators), Ink-jet MEMS modules, Microfluidics & Bio-chips (Fluid actuators) and various other devices used in displays, IR sensing, fiber optics connectors, drug delivery systems, immunosensors, DNA arrays, etc. Medical and biomedical

application of MEMS reached over ten billion dollars in 2004 (Madou 2002) and Biomedical or Biological Micro-Electro-Mechanical Systems (BioMEMS) are now a heavily researched area with a variety of important applications to boast of. Areas of research and applications in BioMEMS range from diagnostics (DNA and protein microarrays), to various types of sensors, novel materials and biomaterials, microfluidics, tissue engineering, surface modification, implantable devices, and drug delivery systems (Bashir 2004). Some important commercial products include drug delivery patches from Cygnus Glucowatch, hand-held blood analyzers, on-line pressure monitoring from Motorola and Siemens, neural stimulating probes from the University of Michigan, pacemakers, and molecular diagnostic testing platforms like the Nanogen NanoChip™ (Madou 2002).

As with various other biological applications, microfabrication techniques are also being used by researchers to develop microchip platforms for single-cell electrophysiological (patch clamp on chip) and electrochemical (amperometry on chip) measurements. Over the last decade various designs in the form of planar or lateral patch clamp on a chip device have been implemented. Materials ranging from silicon, to quartz/glass, polyimide, Teflon, and PDMS have been used to fabricate these patch clamp devices. Integration with microfluidics has introduced functionalities and automation modules in patch clamp measurements. Some of the popular approaches used include small apertures in silicon nitride covered by silicon dioxide followed by chemical modification (Schmidt and others 2000), deposition of a plasma-enhanced chemical vapor deposition (PECVD) oxide film to narrow down the aperture and increase its depth (Sordel and others 2006), hydrophobic pores in silicon dioxide (Pantoja and others 2004),

hollow SiO_2 nozzles protruding out of plane and embedded in larger cavities to emulate the 3D profile of a patch pipette tip (Lehnert and others 2002), etching small apertures on pre-thinned fused quartz or borosilicate glass to enable formation of gigaseals (Fertig and others 2001; Fertig and others 2002; Fertig and others 2002; Fertig and others 2003), round patch apertures on a polyimide film milled by a focused ion beam and etched by O_2 plasma through a resist pattern (Stett and others 2003), apertures fabricated in amorphous Teflon (Teflon AF) sheets (Mayer and others 2003), and small apertures in PDMS (Klemic and others 2002). Some of these approaches result in high gigaseal success rates and while some offer medium throughput but high-quality recordings, others are relatively high throughput systems with only modest seals. A number of companies like Sophion, Nanion, Cytocentrics, Molecular Devices (Ionworks and PatchXpress featuring the technologies from Essen Instruments and the SealChip® of Aviva Biosciences) and more recently Fluxion Biosciences (Yobas 2013) are involved in the manufacture of commercial planar patch clamp platforms.

Planar electrochemical electrodes have also been developed. Various design considerations including i) different electrode materials, ii) surface modification to promote cell attachment, iii) assaying multiple cells using arrays of microelectrodes on-chip, iv) cell trapping methods, v) cell targeting methods, vi) developing different stimulation methods, and vi) simultaneous detection of amperometry and fluorescence imaging or TIRF, have been studied and explored thoroughly. The different electrode materials that have been used are gold (Chen and others 2003; Dittami and others 2010), platinum (Hafez and others 2005; Berberian and others 2009), graphite electrode on Si substrate (Parpura 2005) Indium Tin Oxide (ITO) (Amatore and others 2006; Sun and

others 2006), Nitrogen-doped Diamond-Like-Carbon (DLC:N) (Gao and others 2008; Barizuddin and others 2010), and boron-doped nanocrystalline diamond (NCD) on a sapphire wafer (Carabelli and others 2010). Spikes recorded on different kinds of electrodes have been compared to see how important spike parameters and sensitivity can vary from one material to the other (Kisler and others 2012). Electrode surfaces have been modified to improve sensitivity and specificity of target analyte molecules. Modification of Au electrodes with mercaptopropionic acid (MPA) has been shown to improve electrode performance by lessening passivation and increasing sensitivity (Spegel and others 2007). The Lindau group has worked on an arrangement with a group of four microelectrodes that allows for spatiotemporal localization of individual fusion pore openings on the surface of a single cell (Dias and others 2002; Hafez and others 2005). Microfluidic approaches for automated cell targeting and cell trapping have been explored (Gao and others 2009; Dittami and others 2010). Chemical and optical methods for cell stimulation together with electrochemical and fluorescence detection of amperometry have also been demonstrated (Amatore and others 2006; Chen and others 2008; Meunier and others 2011).

1.4 Cell-based electrochemical assay of Botulinum Neurotoxin (BoNT)

BoNTs are produced by the Gram-positive anaerobic soil bacterium *Clostridium botulinum* (Shukla and others 2005). They were first discovered as a contaminant of poorly preserved ham in the late 19th century. *C. botulinum* can grow in soil, spoiled food, wounds, and the human intestine. They can also be cultured in large scale in a laboratory. Due to the extreme potency, lethality and easy procurement, BoNTs have the potential to be very dangerous biological weapons and therefore represent significant

warfare and terrorism threat (Arnon and others 2001). BoNTs are one of the 6 category A agents listed as the highest risk threat agents for bioterrorism by the US Centers for Disease Control and Prevention (CDC) (Centers for Disease Control and Prevention 2003). Botulinum neurotoxins are potent metalloendoproteases capable of impairing transmitter release in neuronal and secretory endocrine cells via targeting and cleaving of various SNARE proteins at specific sites thereby inhibiting the process of exocytosis. It is a very powerful toxin and can be lethal in very minute doses (median lethal dose (LD_{50}) is 1-50 ng/kg of body weight (Band and others 2010)). Apart from being a dangerous biohazard agent and a potential weapon of biological warfare, BoNTs are also known for their multiple therapeutic uses in conditions such as strabismus, blepharospasms, migraine headaches, vocal cord dysfunction, diabetic neuropathy, etc. The most well-known application of BoNT serotype A is its use as a cosmetic anti-wrinkle agent, known commercially as BOTOX®.

BoNTs are made up of a light chain (LC) metalloprotease catalytic domain (50 kDa) and a heavy chain (HC), which consists of translocation and binding domains (100 kDa). After binding and internalization of the toxin via receptor-mediated endocytosis, translocation of the LC into the cytosol occurs followed by the final cleavage of SNARE complex proteins stage. The seven different serotypes of BoNTs have cleavage specificities – while types B, D, F, and G cleave synaptobrevin, types A, C, and E cleave SNAP-25, and type C cleaves syntaxin (Čapek and others 2010). Human botulism, mainly caused by BoNT/A, /B, /E and occasionally /F can happen through many factors like ingestion of contaminated food, wound infections, etc. The symptoms and manifestations of botulinum infection are identical for all serotypes and flaccid paralysis

occurs within 12 to 48 hours of intoxication. Muscle paralysis starts with facial muscles, and continues on to affect shoulders, arms and finally legs. Severe botulism leads to paralysis of respiratory muscles and respiratory failure (Kongsaengdao and others 2006). Treatment of botulism is mostly based on antitoxin administration in order to bind the toxin that has not yet been internalized into cells. Once the toxin enters into the cell, however, there is no way of reversing the onset of paralysis. This lack of treatment coupled with the extreme toxicity of BoNT makes detection and diagnosis of botulism in suspected cases an absolute necessity. Since the toxin plays an important role in therapeutic uses as well, it is also of commercial importance to assess the potency of BoNT-based products and standardize the assessment before they are approved for clinical use.

The potency of botulinum toxins is currently assessed with a mouse intraperitoneal injection assay. It has its inherent shortcomings but it remains the only accepted standard test to confirm active BoNTs (Solomon and others 2001). The mouse lethality assay has been used for analysis of complex matrices like bacterial cultures, serum, fecal, gastric and wound samples. It detects functionally active toxin only and is also highly sensitive and specific. However, it is time-consuming, imprecise, laborious, expensive, and requires an animal facility as well as the sacrifice of a large number of mice. A number of *in vitro* methods have been developed as alternatives to the mouse bioassay. The immunological methods based on binding of an antibody to the toxin are easier to perform and significantly faster, but lack in distinguishing between the active and inactive forms of the toxin. *In vitro* assays based on ELISA (Szílagyi and others 2000; Poli and others 2002; Stanker and others 2008; Volland and others 2008),

electrochemiluminescence immunoassay (Gatto-Menking and others 1995; Guglielmo-Viret and others 2005; Rivera and others 2006; Phillips and others 2008), immuno-PCR (Sano and others 1992; Wu and others 2001; Chao and others 2004), fluorescence-based biosensors (Ogert and others 1992; Kumar and others 1994; Singh and others 1996; Kostov and others 2009), and fluorescence endopeptidase assays (Schmidt and others 2001; Frisk and others 2009) have also been developed. Cell-based assays of BoNT are potentially very sensitive and relevant systems for evaluating toxicity. A FRET based cell assay (Dongo and others 2004; Parpura and others 2005), a cell-based assay with fluorescence read-out (Thyagarajan and others 2009), and action potentials recorded from neural cultures (Scarlatos and others 2008), are some examples of cell-based assays used for detection of BoNT. However, these assays are usually less sensitive and slower than the mouse *in vitro* assay.

1.5 Objectives and Overview

In an effort to enable high-throughput experiments, our group (Chen and others 2003; Sun and others 2006; Chen and others 2008; Gao and others 2008; Gao and others 2009; Sen and others 2009; Barizuddin and others 2010; Liu and others 2011; Yao and others 2012) and others are developing microfabricated devices with arrays of microelectrodes to measure the release of electroactive transmitter at the single-cell and single-vesicle level. These platforms are very different from the usual carbon fiber microelectrodes and can be modified to accommodate functionalities that cannot be implemented using CFEs. Use of photolithography in microchip fabrication also gives better control over electrode fabrication, and enables different electrode materials and insulation methods to be tested. Our microchips are ideal for high-throughput studies of

quantal exocytosis and have potential applications in drug discovery, assay of toxins like BoNT as well as basic science.

My research projects address two current unexplored areas in electrochemical measurement of quantal exocytosis on our lab-on-a-chip platform: the first one is developing an electrical method to trigger exocytosis in single chromaffin cells using the same underlying electrochemical microelectrode, and the second one is application of our microelectrode chip device in assaying toxins like botulinum neurotoxin that affect cellular exocytosis. Therefore, in Chapter 3, I focus on investigating the effect of transient voltage pulses applied by underlying planar microelectrodes on chromaffin cells using whole-cell patch clamp. I found that it is feasible to use an on-chip planar microelectrode to electrically stimulate action potentials, the physiological stimuli for Ca^{2+}-triggered exocytosis. Voltage pulses ranging from 1.5 V to 3 V lasting for 0.2 ms could successfully stimulate action potentials in both chromaffin and INS-1 cells and it was shown that they could be stimulated in single chromaffin cells using underlying planar electrochemical microelectrodes in an all-or-none fashion. In Chapter 4, I have integrated the process of electropermeabilization together with electrochemical measurement of neurotransmitter release from single chromaffin cells on the same microelectrode. A voltage pulse protocol consisting of 5-6 V (7-train) for duration of 0.1 ms led to selective permeabilization of an individual cell with precise timing. Surprisingly, robust quantal release was elicited upon electroporation in the absence of Ca^{2+} in the bath solution (0 Ca^{2+}/5 mM EGTA). In contrast, electropermeabilization-induced transmitter release required Cl^- in the bath solution in that bracketed experiments demonstrated a steep dependence of the rate of electropermeabilization induced

transmitter release on [Cl^-] between 2 and 32 mM. Finally, in Chapter 5, I present the work of assaying the inhibitory effect of botulinum neurotoxin on permeabilized chromaffin cells and using on-chip underlying electrochemical microelectrodes to record the resulting change in exocytotic frequency via amperometry. Results from comparing the rates of secretion in cells that were exposed to the light chain form of BoNT /E toxin with those that were exposed to an inactive form of the toxin (Null or RYM) showed that there is a modest decrease in secretion rate ($P<0.05$) in the presence of the active toxin in the bath solution.

CHAPTER 2

MATERIALS AND METHODS

2.1 Preparation of bovine adrenal chromaffin cells

Chromaffin cell preparation was modified from previously published protocols (Ashery and others 1999; Smith 1999) and has been described in details in a paper from our group (Yang and others 2007). In brief, fresh bovine adrenal glands were obtained from a local slaughterhouse (Davis Meat Processing LLC – Jonesburg, MO). The process consisted of isolating the glands from surrounding tissue/fat and keeping them in a Ca^{2+}-free and Mg^{2+}-free buffer solution (Buffer 1 solution) at room temperature while transporting to the lab. Adherent fat was trimmed from the glands using sterile scissors under a sterile culture hood. Blood inside each gland was washed out by injecting Buffer 1 solution into the opening of the renal vein with a 30 ml sterile syringe and then gently massaging the gland to let the solution out. This step was repeated several times until the solution coming out of the gland was comparatively clear. Collagenase P was dissolved in Buffer 1 solution at a concentration of 1 mg/ml and injected into each gland through the opening of the renal vein. The glands were placed in a sterile beaker and put in a 37 °C shaking water bath for 10 min. Then the glands were taken out, injected again with collagenase P and shaken for another 10 min. The collagenase digestion step allows isolation of the medulla from the outer cortex tissue. In another sterile Petri dish, the gland was cut open along the circumference of the cortex. The digested yellowish/whitish medulla was extracted carefully using scissors and put in Buffer 1 solution in another Petri dish. The medullae were then thoroughly minced into small pieces using a second

set of scissors. The medulla-containing solution was next filtered through a nylon mesh (70 μm opening). The filtered solution centrifuged at 140 g/1000 rpm for 10 min at room temperature. The supernatant was aspirated and the pellet was resuspended in 18 ml Buffer 1 solution. In another tube, percoll gradient solution was mixed with a 10-fold concentration Buffer 1 solution (pH = 4.5) at a ratio of 9:1 to make a solution with physiological tonicity and a pH of 7.2. The percoll solution was mixed with the cell solution at a 1:1 ratio and then centrifuged at 13,000 rpm for 45 min at 18 °C in a high speed centrifuge. Following centrifugation, the percoll gradient resulted in 4 layers: dead tissue constituting the top layer, norepinephrine and epinephrine secreting chromaffin cells in the middle two layers, and red blood cells in the bottom layer. The middle two layers were gently pipetted out and transferred to a tube. Buffer 1 solution was added to the tube and the cell mixture was centrifuged at 1000 rpm for 10 min. The supernatant was removed and the cell pellet was resuspended in Buffer 1 solution. Chromaffin cell culture media was added at a 1:3 ratio into the cell suspension to help cells adapt to normal Ca^{2+}-containing media. The suspension was centrifuged again at 1000 rpm for another 10 min and the supernatant was removed. Following this the cell pellet was resuspended in chromaffin cell culture media. Cell density was calculated by adding a drop of cell solution onto a hemocytometer. To make it easier to detach cells from the flask and to reduce cell clumping we cultured cells in Hibernate A media with calcium (BrainBits LLC, Springfield, IL, USA) in a refrigerator (4 °C) and used them 1–6 days after preparation.

2.2 Design, fabrication and testing of microdevice

2.2.1 Electrode material deposition

Device fabrication was carried out using a two-mask photolithographic process. Microscope slides (25 × 75 × 1 mm, Fisherbrand, Fisher Scientific, Pittsburgh, PA, USA) were used as a transparent substrate and the electrode material of choice was deposited.

A 110 nm-thick ITO film was sputtered onto the glass substrate using a magnetron sputtering system (ATC 2000-V, AJA International Inc. North Scituate, MA, USA) with an ITO target (90 wt% In_2O_3 and 10 wt% SnO_2, Williams Advanced Materials Inc, Buellton, CA, USA). The parameters for the sputtering process were adapted from Deng. et al., (Deng and others 2001). We used DC mode deposition at a power of 100 W, a working pressure of 2 mTorr, and a substrate temperature of 325 °C. Ar gas was introduced at a flow rate of 20 sccm, and O_2 was introduced at 0.2 sccm. The deposition time was 600 s. The transmittance spectrum for ITO-coated cover glass was measured using a UV-VIS recording spectrophotometer (UV-2401PC, Shimadzu, Kyoto, Japan). The conductance of the deposited ITO film was measured using a 4-point probe (S302, Lucas Labs, Gilory, CA, USA).

For the devices with gold as the electrode material, a semi-transparent 30 nm Au film was sputtered on top of an adhesion promoting Ti film (10 nm) using an RF magnetron sputtering system (ATC 2000-V, AJA international Inc., North Scituate, MA, USA, targets obtained from Kurt J. Lesker Company, Clairton, PA, USA). The deposition was performed at room temperature with a power of 100 W and a working pressure of 4 mTorr with an Argon gas flow rate of 20 sccm. The deposition rate for Ti and Au was 2

nm/min and 9 nm/min, respectively. The Au film was patterned using photolithography and wet etching into 72 conductive traces (36 on each half of the glass slide), 60 μm wide, with 2 mm diameter connection pads arranged around the circumference of the chip. The Au/Ti coated substrate was first cleaned with 2-propanol, then rinsed with deionized water and air-dried. The slide was then cleaned with air plasma at 10.5 W RF power level for 1 min (plasma cleaner/sterilizer, PDC-32G, Harrick Scientific Corp., Pleasantville, NY, USA).

DLC:N was deposited on top of transparent indium-tin-oxide (ITO, 15-30 nm thick) because the resistivity of DLC:N is high (~1 Ωcm). ITO-coated glass slides were obtained by sputter deposition as described above, or purchased from Sigma-Aldrich (St. Louis, MO USA) and were cleaned with acetone, methanol, and deionized water. The slide was blow dried with air and left on a hot plate for 2 min to remove the moisture. DLC:N was subsequently deposited on ITO surface using magnetron sputtering (ATC 2000-V, AJA international Inc., North Scituate, MA, USA) with 300 Watt DC power, a pressure of 2 mTorr, Ar flow of 10 sccm, N_2 flow of 10 sccm, and a temperature of 400 °C. The deposition rate was ~2 nm/min, and film thicknesses of ~40 nm were used for transparent electrodes with the microwell approach. The sheet resistance of DLC: N on ITO was measured using a four-point probe (S302, Lucas Laboratories, Gilroy, CA, USA) and was essentially identical to that of the underlying ITO film (70-100 Ω).

2.2.2 Electrode patterning and insulation

Transparent ITO electrodes were patterned on the ITO-coated cover slides using photolithography and wet-etching techniques adapted from Sun and Gillis (Sun and

others 2006). Briefly, we first rinsed the ITO-coated cover slide with 2-propanol, then sonicated for 20 min in acetone (Ultrasonic cleaner 1510, Branson, Danbury, CT, USA), then cleaned using air plasma (Plasma cleaner/sterilizer, PDC-32G, Harrick Scientific Corp., Pleasentville, NY, USA) for 1 min at the medium RF power level. Shipley S1813 positive photoresist (Rohm and Haas Electronic Materials, Philadelphia, PA, USA) was then spin-coated (single-wafer spin processor, Laurell Technologies Corp., North Wales, PA) onto the ITO-coated cover slide at 2500 rpm for 60 s to give a thickness of ~2 μm. The coated cover slide was baked on a hot plate at 115 °C for 2 min. Photoresist-covered cover slide was exposed to UV light through a high-resolution (20,000 dpi) transparency mask (CAD Art Services, Bandon, OR) and then developed in M351 (Rohm and Haas Electronic Materials) for ~1 min. It was then baked at 200 °C on the hot plate for 10 min. An acidic solution composed of 6 M HCl and 0.2 M $FeCl_3$ was used to wet etch the portion of the ITO film that was not protected by photoresist for 30 min, leaving 200 μm-wide ITO stripes, that widened to form connecting pads on the edge of the chip. The photoresist protection layer was then removed with an acetone wash. The cover slide with patterned ITO electrodes was rinsed with DD water and air-dried.

Au electrodes were also patterned by a wet-etch process (Fig 2.1). Shipley S1813 positive photoresist (Rohm and Haas electronic materials, Philadelphia, PA, USA) was spin-coated onto the Au/Ti substrate at 2500 rpm for 1 min resulting in a ~2 μm thick layer. The photoresist-covered Au/Ti slide was pre-baked on a hot plate at 115 °C for 2 min. Then it was exposed to UV light (15 mW/cm^2) through a high-resolution (20,000 dpi) transparency mask (CAD/Art Services Inc., Bandon, OR, USA) (Fig 2.1(a)) and developed in diluted M351 (4:1 dilution with deionized water) (MicroChem Corp,

Newton, MA, USA) for 1 min (Fig 2.1 (b)). Then the Au/Ti slide was post-baked at 150 °C on the hot plate for 10 min. Gold etchant solution (Sigma, St. Louis, MO, USA) was used for wet-etching the portion of Au/Ti film that was not protected by photoresist for ~10 s. TFTN solution (Transene Company Inc., Danvers, MA, USA) was then used to etch the Ti film at 85 °C for ~20 min. The S1813 photoresist was finally removed using PRS-3000 stripper (J.T. Baker, Phillipsburg, NJ, USA) (Fig 2.1(c)). Finally, the patterned device was rinsed with deionized water, and dried with compressed air.

The DLC:N/ITO film was patterned using photolithography and wet etching into 72 conductive traces (36 on each half of the glass slide), 100 μm wide, with 2 mm diameter connection pads arranged around the circumference of the chip. The DLC:N/ITO coated substrate was cleaned with 2-propanol, then sonicated for 10 min on each side in acetone (Branson Ultrasonic Corporation, model 1510, Danbury, CT, USA), and then rinsed with deionized water and air-dried. Finally, the slide was cleaned with air plasma at the medium power level for 1 min (plasma cleaner/ sterilizer, PDC-32G, Harrick Scientific Corp., Pleasantville, NY, USA). Shipley S1813 positive photoresist (Rohm and Haas electronic materials, Philadelphia, PA, USA) was spin-coated (Single-wafer spin processor, Laurell Technologies Corp., North Wales, PA, USA) onto the DLC:N/ITO substrate at 2500 rpm for 1 min resulting in a thickness of ~2 μm. The coated DLC:N/ ITO slide was prebaked on a hot plate at 115 °C for 2 min. The photoresist-covered DLC:N/ITO slide was exposed with UV light (15 mW/cm2) through a high-resolution (20,000 dpi) transparency mask (CAD/Art Services Inc., Bandon, OR, USA) and then developed in diluted M351 (M351:H_2O = 1:4; Micro-Chem Corp, Newton, MA, USA) for 1 min. Following development of the S1813 photoresist, the

unprotected DLC:N film was etched with air plasma (PDC-32G, Harrick Scientific Corp., Pleasantville, NY, USA) at the High power level for 15 min (40 nm films) or 18 min (120 nm films). Then, the underlying ITO was wet etched using 0.2 M $FeCl_3$ in 6 M HCl for 30 min. Subsequently, the S1813 photoresist was removed using PRS-3000 stripper. Finally, the patterned device was rinsed with deionized water and dried using compressed air.

We used the thick photoresist SU-8 2025 (MicroChem Corp, Newton, MA, USA) both to fabricate microwells and to insulate non-active areas of the conductive film. SU-8 was spin coated at 4000 rpm for 1 min to yield a film thickness of ~16 μm measured with a Tencor Alphastep 200 Profiler (San Jose, CA, USA) (Fig 2.2(a)). It was subsequently baked at 65 °C for 3 min and 95 °C for 5 min on hot plates. A second high-resolution (20,000 dpi) transparency mask was used to define a single 20 μm diameter microwell / electrode opening over each conductive trace as well as openings over each connection pad (Fig 2.2(b)). Following mask alignment using a microscope, the photoresist was exposed to UV light (11.7 mW /cm^2). Then it was post-baked at 65 °C for 1 min and 95 °C for 5 min on hot plates. It was then developed with SU-8 Developer (MicroChem Corp, Newton, MA, USA) for 10 min with mild agitation (Fig 2.2(c)). Finally, the device was baked on a hot plate at 150 °C for 2 hrs to seal small cracks on the surface of the SU-8 film.

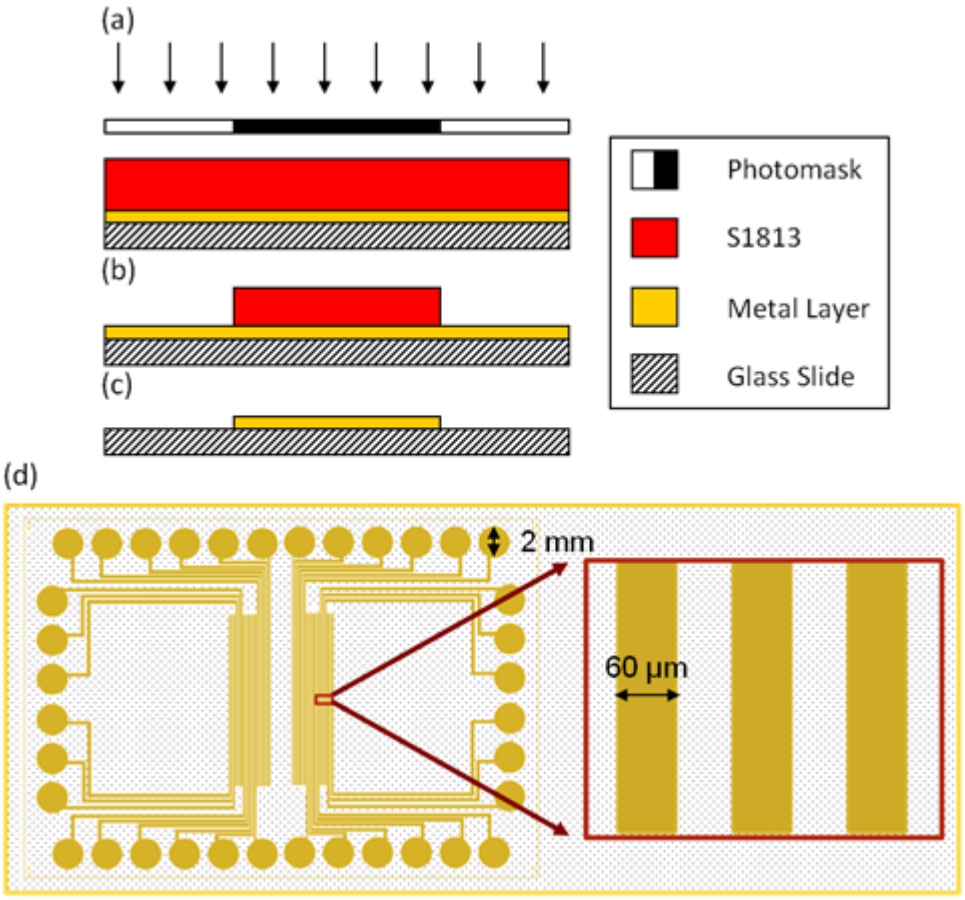

Fig 2.1 Cross section and top views of Au film patterning using photolithography and wet etching. (a) Positive photoresist S1813-covered Au/Ti slide exposed to UV light through a high-resolution transparency photomask. (b) Au/Ti slide with developed and patterned photoresist. (c) The part of Au/Ti film that is not protected by photoresist is wet-etched next using a gold etchant solution to pattern it. (d) Top view of patterned gold traces and connecting pads after completion of step (c)

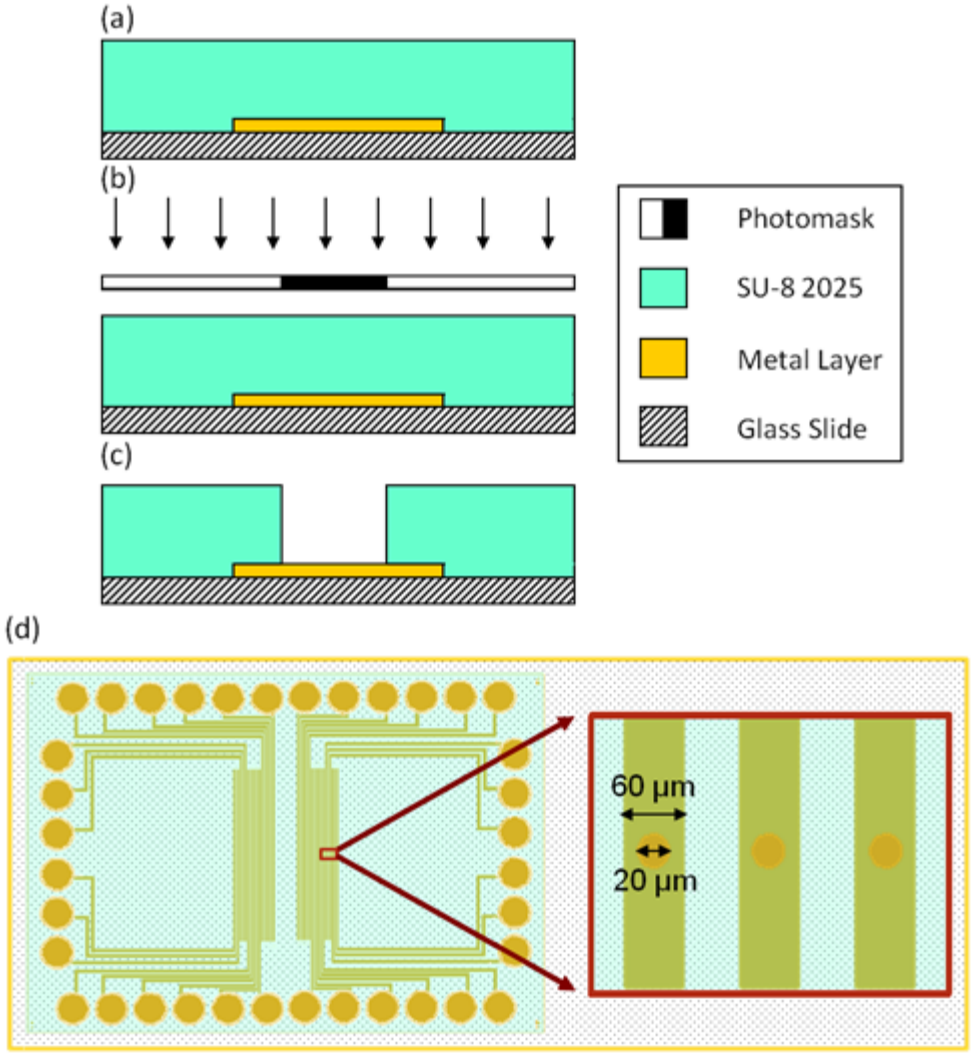

Fig 2.2 Cross section and top views of insulating patterned Au film (as shown in Fig 2.1) using photolithography and wet etching. (a) A negative photoresist (SU-8 2025) is spin-coated on patterned Au/Ti electrodes (thickness ~15-16 µm) such that the aspect ratio of the opening (20 µm diameter) is ~1. (b) Slide is exposed to UV light through a high-resolution transparency photomask. (c) Microwells are patterned on top of electrode traces leaving the non-active areas of the conductive film insulated. Also, areas over the bonding pads are defined by developing the SU-8 (d) Top view of insulated and patterned gold traces with defined microelectrodes and bonding pads after completion of step (c)

2.2.3 Microchip assembly

A 10:1 ratio of polydimethylsiloxane (PDMS) (Sylgard 184, Dow Corning) monomer and cross-linking agent was used to make PDMS gaskets for holding the cell-containing solution on the chip. The monomer was mixed with a curing agent, the mixture was degassed in a vacuumed dessicator and then poured into a plastic petri dish. After curing for 1 hr in a conventional oven at 80 °C, the PDMS was cut into small rectangular slabs with an opening in the middle serving as the PDMS gasket. It was then peeled off the petri dish and placed on top of the device to confine the drop of solution containing cells to the part on the device where the 36 working electrodes are located (Fig 2.3). The assembly was treated with air plasma for 1 min at 10.5 Watts power setting to enhance the sealing of the gasket to the chip. This air plasma also helped clean the device surface.

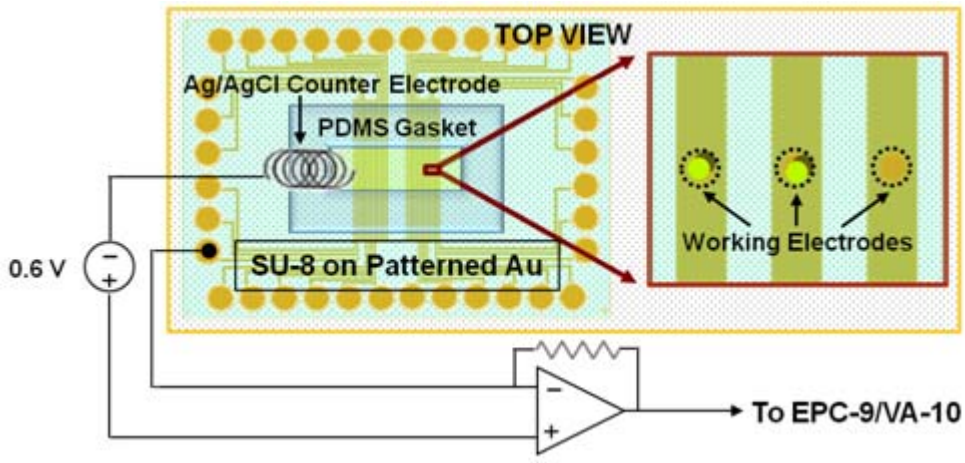

Fig 2.3 Top view of an assembled microchip with a PDMS gasket for holding cell-containing solution on top of insulated and patterned gold microelectrodes. Also shown is an amplifier connection made to a microelectrode via the connection pad and a Ag/AgCl ground/reference electrode in the drop of solution confined to the middle part of the chip by the PDMS gasket

2.3 Recording action potentials on the microchip

2.3.1 Electrical stimulation using planar patterned microelectrodes

Patterned ITO microdevices with 200 μm x 200 μm planar electrodes were used for stimulating action potentials in adjacent chromaffin cells. A smaller voltage change can be induced in the cell membrane by applying a larger brief voltage step to the underlying microelectrode via capacitive coupling. Changes in the cell's membrane potential in turn trigger action potentials in the excitable cells. Fabricated devices were cleaned with 2-propanol, rinsed with deionized water, air-dried and then sterilized via exposure to UV light. Finally chromaffin cells were plated and incubated at 37 °C for up to a few hours.

2.3.2 Electrophysiology

Whole cell patch clamp recordings of membrane potential were made in current-clamp mode using an EPC9 amplifier (HEKA, Lambrecht, Germany). Patch pipettes were fabricated from Kimax glass (Kimax-51, Kimble Glass Inc., Vineland, NJ) using a Flaming/Brown micropipette puller (Model P-97, Sutter instrument Co., Novato, CA). The pipette resistance typically ranged from 2 MΩ to 5 MΩ when filled with intracellular solution and was typically 5 MΩ to 10 MΩ in the whole-cell configuration. Voltage pulses were applied to patterned underlying electrodes in order to facilitate transient depolarization of the plasma membrane thus inducing action potentials in the chromaffin cells.

2.3.3 Solutions

The standard cell bath solution consisted of (in mM): 150 NaCl, 5 KCl, 2 $CaCl_2$, 1.2 $MgCl_2$, 10 HEPES, and 10 glucose, pH 7.2.The pipette solution used for the whole cell patch clamp experiments consisted of (in mM): 150 K-Gluconate, 1 EGTA, 10 HEPES, 4.6 $MgCl_2$, and 4 Na^+-ATP, pH 7.2.

2.4 Electropermeabilization

2.4.1 Trypan blue and propidium iodide assays to verify electropermeabilization in chromaffin cells

Electropermeabilization of the plasma membrane of cells was demonstrated by staining with trypan blue and propidium iodide. Trypan blue solution (0.4%, Sigma, St. Louis, MO, USA) was mixed with regular chromaffin cell medium at a ratio of 1:4. Following cell loading, 10–20 ml of this solution was added to 100 ml of cell solution on the device. Uptake of dye was evaluated by observing cells under a microscope within 10 min of staining. Propidium iodide stock solution was made by dissolving 400 µg of propidium iodide salt in 1 ml of standard cell bath solution. During experiments, 1 µl of propidium iodide stock solution was added to 100 µl of bath solution to attain a final concentration of ~4 µg/ml. Uptake of dye was evaluated within 5-10 min of staining and electropermeabilization of cells.

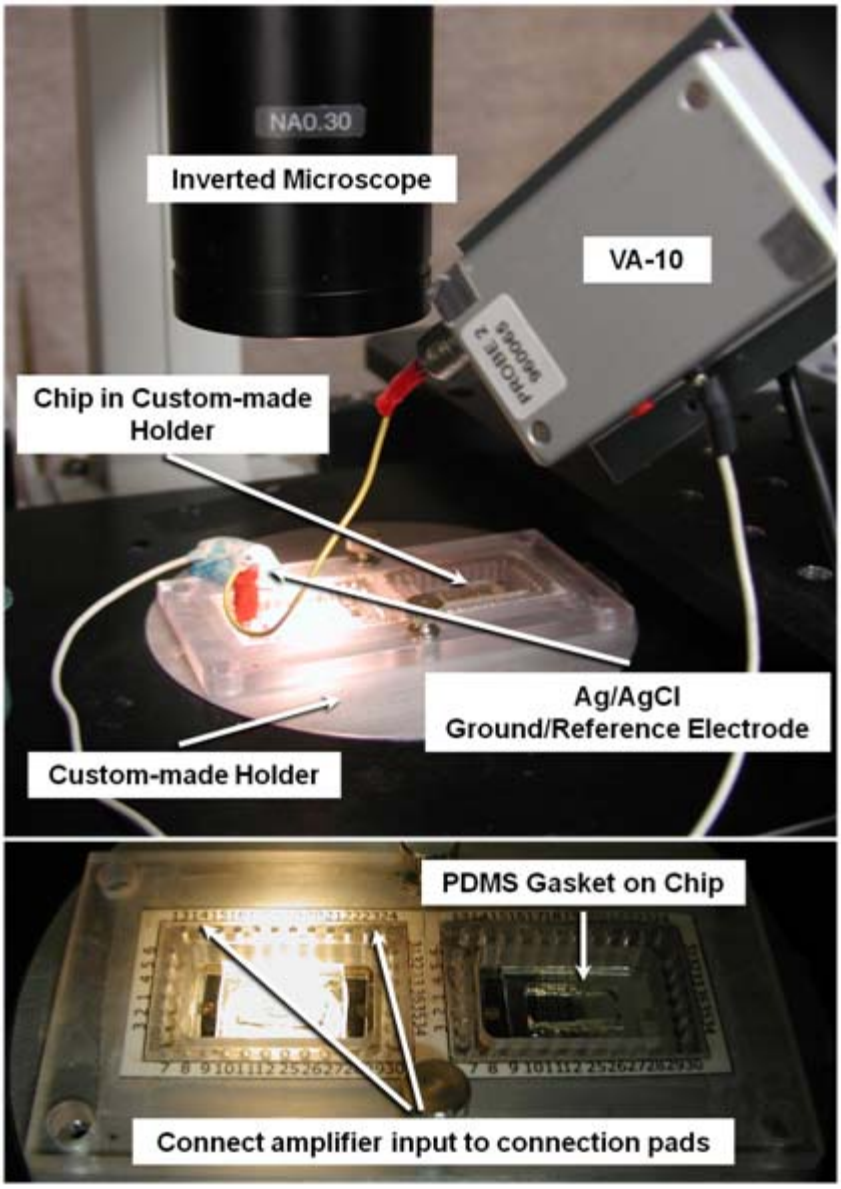

Fig 2.4 Photos of the device and recording configuration. Connection to the microfabricated device is made via the connection pads arranged around the circumference of the chip. The chip is mounted on a custom-made holder, which facilitates the connection of the amplifier input to a connection pad and insertion of a Ag/AgCl ground/reference electrode in the drop of solution confined to the middle part of the chip using the PDMS gasket. The chip plus holder is placed on an inverted microscope to observe cell docking to electrodes.

2.4.2 Electropermeabilization and subsequent recording of amperometric spikes using the same planar patterned microelectrode

Neurotransmitter release from a single chromaffin cell was induced as well as measured by the same planar Au working electrode. Voltage-stimulus protocols were adjusted to avoid formation of bubbles at the surface of the electrodes, presumably due to hydrolysis of water.

Voltage pulses led to current being passed through the microelectrode, which results in a voltage drop in the electrolytic solution surrounding the cell. This voltage gradient led to changes in the cell's membrane potential that produced electroporation upon dielectric breakdown of the cell membrane. For the stimulus-recording electrode approach to work, we needed the potentiostat to be capable of supplying a large enough current to induce electroporation, yet also be capable of resolving the picoamp-level currents associated with amperometric events. This was achieved by having a VA-10 potentiostat modified in collaboration with the manufacturer, NPI Inc (Tamm, Germany). The modification added a diode network in parallel with the op-amp feedback resistor such that the diodes "turned on" to bypass the feedback resistor to allow a large transient current to be supplied to the electrode in response to a voltage step. Once the capacitive current settled the diodes "turned off" to allow low-noise I–V conversion by the feedback resistor (Barbour and others 2000). The output of the VA-10 was sampled by the analog-to-digital converter of the EPC9 amplifier and recorded using Pulse software (HEKA, Lambrecht, Germany). During amperometric recording, the VA-10 potentiostat was held at a potential of 600 mV relative to an Ag/AgCl wire inserted in the solution that served as the counter/reference electrode. Amperometric signals were low-pass filtered with a

cut-off frequency of 2.9 kHz and sampled at a rate of 10 ksamples/s. Amperometric spikes were analyzed using the software of Segura et al. running on Igor Pro (Wavemetrics, Lake Oswego, OR, USA). Spike frequency was counted manually. Spikes were not included in the analysis if the peak current was less than 2 pA, had negative charges, multiple peaks or other irregular shapes, or 10–90% rise times of greater than 20 ms.

2.4.3 Intracellular Ca^{2+} measurements with Fura-4F

To load adrenal chromaffin cells with Ca^{2+} indicator dye Fura-4F AM, hibernate media was replaced with loading solution containing 10 μM of Fura-4F AM (stock 25.0 mM in DMSO). Chromaffin cells in hibernate were taken from a T25 flask, spun down at 100 g for 5 min, resuspended in 1 ml DMEM and the cell-containing solution was transferred to a 15 ml conical tube. After adding 10 μM Fura-4F (AM) and mixing gently, the cell suspension was incubated in a humidified incubator (37 ºC, 5% CO_2) for 45 min. Then the cell suspension was centrifuged at 100 g for 5 min. The supernatant was removed with a Pasteur pipette and vacuum, and the pellet was resuspended with 5 ml bath solution. The cell suspension was again centrifuged at 100 g for 5 min and the supernatant was removed with Pasteur pipette and vacuum. 1 ml bath solution was added in and the pellet was resuspended and ready for use. About 50 μl bovine adrenal chromaffin cells loaded with Ca^{2+} indicator dye Fura-4F (AM) were added into the cell reservoir on the microchip. After 10 to 20 min, cells would settle onto the DLC/ITO microchip surface with some randomly settling directly on top of the working electrodes. An inverted fluorescence microscope (IX50, Olympus America) with a 40X 1.15 NA water immersion lens (U-APO, Olympus America) was used to observe cells and the

transparent DLC/ITO electrodes. A monochromator (Poly II, TLL photonics) and a photodiode (TILL Photonics) were used together with the inverted fluorescence microscope to measure the fluorescent signal from the Ca^{2+} indicator dye to report $[Ca^{2+}]_i$ during the experiment. An EPC-9 amplifier (HEKA) and the corresponding software Pulse (HEKA) were used to record the amperometric and fluorescence data. The headstage of the EPC-9 amplifier was connected to a connection pad on the edge of the chip to activate one of the working electrodes. A Ag/AgCl wire inserted in the cell reservoir on the DLC/ITO microchip was used as the ground electrode and connected to the ground port on the headstage of EPC-9 amplifier. A 600 mV constant potential was applied to a working electrode during experiments.

2.4.4 Solutions

The standard cell bath solution consisted of (in mM): 150 NaCl, 5 KCl, 2 $CaCl_2$, 1.2 $MgCl_2$, 10 HEPES, and 10 glucose, pH 7.2. The Ca^{2+}-free solution was made with 0 $CaCl_2$ and 5 EGTA. The Na^+-free, Ca^{2+}-free solution consisted of (in mM): 135 KCl, 5 EGTA, 1.2 $MgCl_2$, 10 HEPES, and 10 Glucose, pH 7.2. Similarly, the Cl^--free, Ca^{2+}-free solution comprised of (in mM): 135 Na-glutamate, 5 EGTA, 1.2 $MgCl_2$, 10 HEPES, and 10 Glucose, pH 7.2. For the Cl^--dependency experiments we used Ca^{2+}-free solutions with varied Cl^--concentrations by equimolar substitution of Cl^- salts with glutamate salts. The free Ca^{2+} concentration in the bath solution was varied using the Ca^{2+} chelator DPTA (diethylenetriaminepentaacetic acid, K_d = 81 μM at pH 7.2 (Smith and others 1987)) titrated with Ca acetate rather than $CaCl_2$ to keep the concentration of Cl^- fixed. We tested electrodes as described previously (Liu and others 2011) by performing cyclic

voltammetry with a ferricyanide solution that consisted of 1 mM $K_3Fe(CN_6)$ in 0.1 M KCl, pH 3.0.

2.5 Using permeabilization to study the effect of Botulinum neurotoxin serotype E light chain on chromaffin cell exocytotic machinery

2.5.1 BoNT wild-type LC/E and inactive LC/E (RYM or Null form)

Botulinum neurotoxin was obtained in collaboration with Dr. Michael Baldwin from the Dept. of Molecular Microbiology and Immunology, University of Missouri. Protein expression and purification were carried out as described elsewhere (Baldwin and others 2004; Fu and others 2006). BoNT LC/E was constructed by amplifying DNA encoding LC fragments from Clostridium botulinum serotype E_{Begula} (Poulet and others 1992), (E. A. Johnson, University of Wisconsin Madison) and subcloning into pET-15b. Plasmids encoding LCs were transformed into *Escherichia coli* BL21 (DE3) RIL (Stratagene) and the cells were cultured overnight on L-agar with 100 µg/ ml ampicillin and 50 µg/ml chloramphenicol. Cells were inoculated into LB medium containing antibiotics and cultured at 30 °C for 2 h at 250 rpm when cells were induced with 0.75 mM isopropyl 1-thio-β-D-galactopyranoside (IPTG), and then cultured at 250 rpm overnight at 16 °C. Cells were harvested and broken with a French Press in 40 ml of cold buffer A (20 mM Tris-HCl (pH 7.9), 1 mM DTT, 10 mM imidazole, and 0.5 M NaCl) containing EDTA-free protease inhibitor cocktail (Sigma) and 2.5 µg/ ml DNAse I and 2.5 µg/mL RNAse I. The lysate was clarified by centrifugation at 20,000g for 20 min at 4 °C and passed through a 0.45 µm filter. The filtered lysate was applied to Ni-NTA resin (5 ml bed volume per 2 l of bacterial culture in buffer A). The column was washed with

25 ml of buffer A and eluted with 20 mM Tris-HCl, pH 7.9, containing 250 mM imidazole and 0.5 M NaCl. Peak fractions were pooled and subjected to gel-filtration on a Sephacryl S200 HR column (150 ml of resin equilibrated in 10 mM Tris-HCl (pH 7.9) and 20 mM NaCl). Peak fractions were pooled and subjected to anion exchange chromatography (10 ml of resin of DEAE-Sephacel with a 10 mM Tris-HCl (pH 7.9) with a 20-500 mM NaCl gradient). Peak fractions were pooled and dialyzed overnight into 10 mM Tris-HCl (7.6) and 20 mM NaCl with 40% glycerol (v/v).

A double mutation in LC/E, R362A/Y365F (RYM), was used to reduce the catalytic activity of BoNT to nondetectable levels, while not influence substrate binding affinity (Binz and others 2002). The RYM mutant was engineered using Quick Change techniques, and purified using the same procedure as the wild-type protein. Purified proteins were stored at -20 °C until ready to use.

2.5.2 Trypan blue assay to verify permeabilization of chromaffin cells in digitonin

Digitonin-induced permeabilization of the plasma membrane of cells was demonstrated by staining cells with trypan blue. Trypan blue solution (0.4%, Sigma, St. Louis, MO, USA) was mixed with regular chromaffin cell medium at a ratio of 1:4. Following cell loading, 10–20 ml of 20 μM Digitonin solution was added to 30-40 ml of a mixture of standard bath and Trypan blue solutions on the device. Uptake of dye was evaluated 10 min after staining.

2.5.3 Digitonin-permeabilization and amperometric recording of quantal exocytosis

Neurotransmitter release from a single chromaffin cell was induced by incubating digitonin-permeabilized cells in a solution containing 14.4 μM Ca^{2+}. Amperometric

spikes were measured by the underlying planar Au working electrodes. In order to verify that digitonin can effectively permeabilize chromaffin cells, we perfused cells in a digitonin-containing external solution using an application pipette and measured exocytosis using a planar electrode beneath the cell.

The BoNT LC/E and the inactive RYM mutant were introduced into permeabilized cells by including the proteins in the extracellular solution. Release of catecholamines from cells exposed to the wild-type LC/E toxin were compared with control cells that were not exposed to the toxin or that were incubated with the inactive RYM mutant.

The amperometric signal was sampled by the analog-to-digital converter of the EPC9 amplifier and recorded using Pulse software (HEKA, Lambrecht, Germany). During amperometric recording, the EPC9 potentiostat was held at a potential of 600 mV relative to an Ag/AgCl wire inserted in the solution that served as the counter/reference electrode. Amperometric signals were low-pass filtered with a cut-off frequency of 2.9 kHz and sampled at a rate of 10 ksamples/s. Amperometric spikes were analyzed using the software of Segura et al. running on Igor Pro (Wavemetrics, Lake Oswego, OR, USA). Spike frequency was determined manually.

2.5.4 Solutions

The standard BoNT buffer consisted of (in mM): 100 KCl, 45 K-Glutamate, 1.2 $MgCl_2$, 10 HEPES, pH 7.2. The digitonin-containing buffered Ca^{2+} solution was comprised of (in mM): 125 K-Glutamate, 0.02 Digitonin, 10 HEPES, 1.2 $MgCl_2$, 1.5 Na^{+}-ATP, pH 7.2. Solutions containing the active toxin or its null form were mixed with buffered Ca^{2+} solution containing digitonin and used in experiments.

CHAPTER 3

ELECTRICAL STIMULATION OF ACTION POTENTIALS FROM CHROMAFFIN CELLS USING A PLANAR ELECTROCHEMICAL MICROELECTRODE

3.1 Introduction to approaches used to electrically stimulate excitable cells and goal of project

Action potentials are the physiological stimuli for secretion of hormones and neurotransmitters from most neurons and neuroendocrine cells. In neurotransmitter-secreting cells, opening of voltage-dependent Ca^{2+} channels, influx of Ca^{2+} and subsequent Ca^{2+}-triggered exocytosis are induced by action potentials. Action potentials can be triggered in cells using external stimuli and one widely used approach that is employed in neuroscience is to trigger an action potential using a transient electric field. Studies on the relationship between action potential stimuli and the resultant exocytosis can provide in-depth biological information about cell secretion. For example, the Misler group discovered that chromaffin cell secretion has a steeper dependence on the action potential frequency than many nerve terminals (Zhou and others 1995). The Artalejo group showed that latencies between the onset of action potential stimuli and amperometric detection of quantal release of transmitters could be used to infer the distance between the L-type Ca^{2+} channel and the vesicle release sites (Elhamdani and others 1998).

Patterned electrodes on microchips have also been used to stimulate action potentials on adherent cells. The Stett group fabricated a silicon chip for capacitive stimulation of action potential (Fromherz and others 1995). The Fromherz group developed a semiconductor chip to apply voltage pulses to a neuron that was immobilized on the surface of the chip to elicit action potential in the neighboring neuron and the action potential was monitored by the underlying chip. Hence, the silicon-neuron-neuron-silicon circuit was used for presynaptic stimulation and recording, synaptic transmission, as well as postsynaptic recording (Zeck and others 2001). To our knowledge, however, patterned microelectrodes have not been demonstrated to elicit action potentials in small spheroidal neuroendocrine cells like chromaffin cells.

3.2 Stimulating action potential in single INS-1 and chromaffin cells using capacitive coupling on large chip microelectrodes

We sought to determine experimental conditions whereby action potentials could be elicited in an individual chromaffin or INS-1 cell by an adjacent electrochemical microelectrode as a method to stimulate, and subsequently record, exocytosis. Fig 3.1(c) shows how a smaller voltage change can be induced in the cell membrane potential (V_m) by applying a larger brief voltage step (V_e) via capacitive coupling.

Voltage pulses were applied to 200 μm x 200 μm planar electrodes (Figs 3.1(a) & (b)) while simultaneously monitoring the adherent cell's membrane potential using a patch-clamp pipette in the whole-cell current-clamp configuration (Fig 3.1(d)).

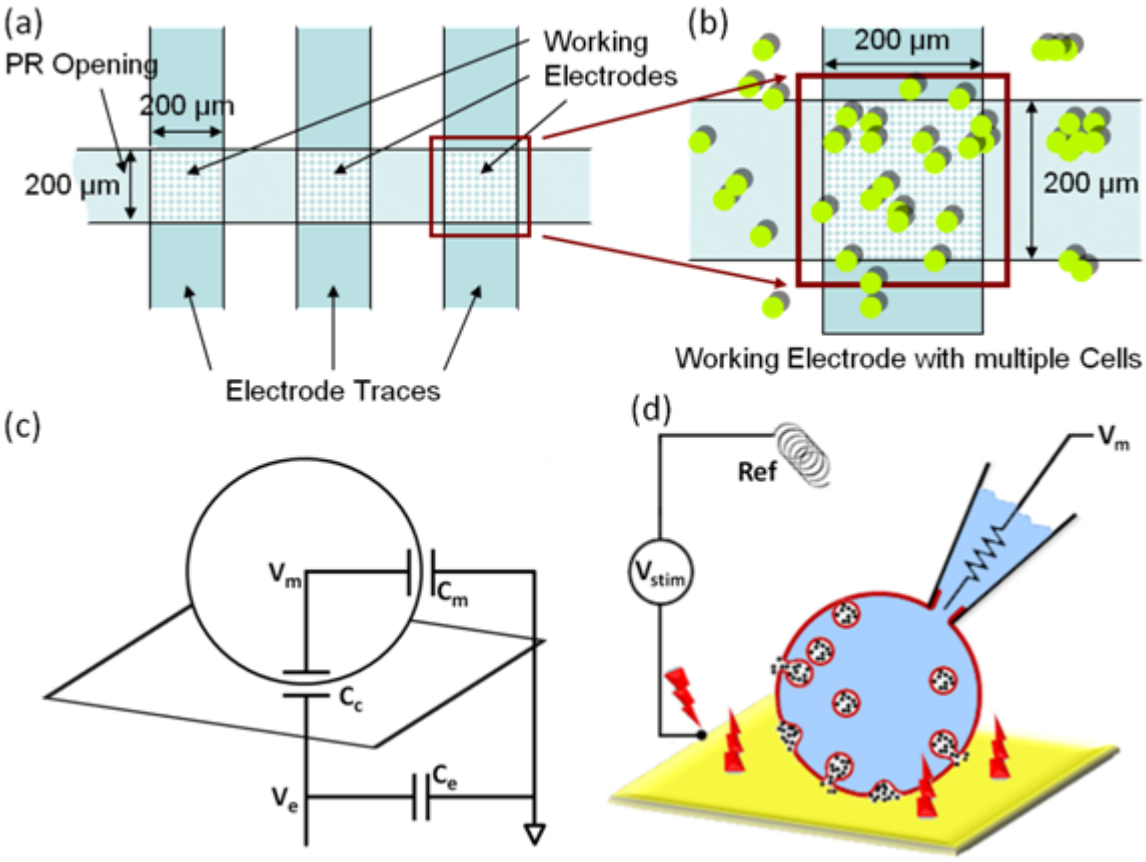

Fig 3.1 Stimulating action potential in single cells using capacitive coupling on large chip microelectrodes. (a) Schematic of 200 µm x 200 µm planar electrodes. Photolithography is used to define an opening in the photoresist insulation layer covering the underlying electrode trace. (b) The expanded portion on the right shows an individual working electrode with multiple cells. (c) Brief voltage step in V_e evokes a much smaller voltage change in V_m due to voltage divider formed from the series combination of the coupling capacitance (C_c) and cell membrane capacitance (C_m). (d) Schematic of a cell patch clamped in whole cell mode on a microelectrode. Voltage stimulus is applied using the underlying planar electrode and resulting action potentials are recorded using the patch pipette.

Fig 2.3 shows a schematic of a typical chip device with an array of cell-sized Au microelectrodes. The working electrode regions are openings in the patterned photoresist

insulation layer. A PDMS gasket is designed to hold the solution with cells on top of the working electrodes. The schematic in Fig 3.1(c) illustrates a voltage divider circuit formed by the series combination of the coupling capacitance (C_c) and cell membrane capacitance (C_m). The equation governing the voltage change is:

$$\Delta V_m / \Delta V_e = C_c/(C_m + C_c) \qquad \text{Eqn. 3.1}$$

Fig 3.2(a) below shows a light microscope image of chromaffin cells on an ITO electrode and Fig 3.2(b) shows a whole-cell patch clamped single chromaffin cell on the electrode.

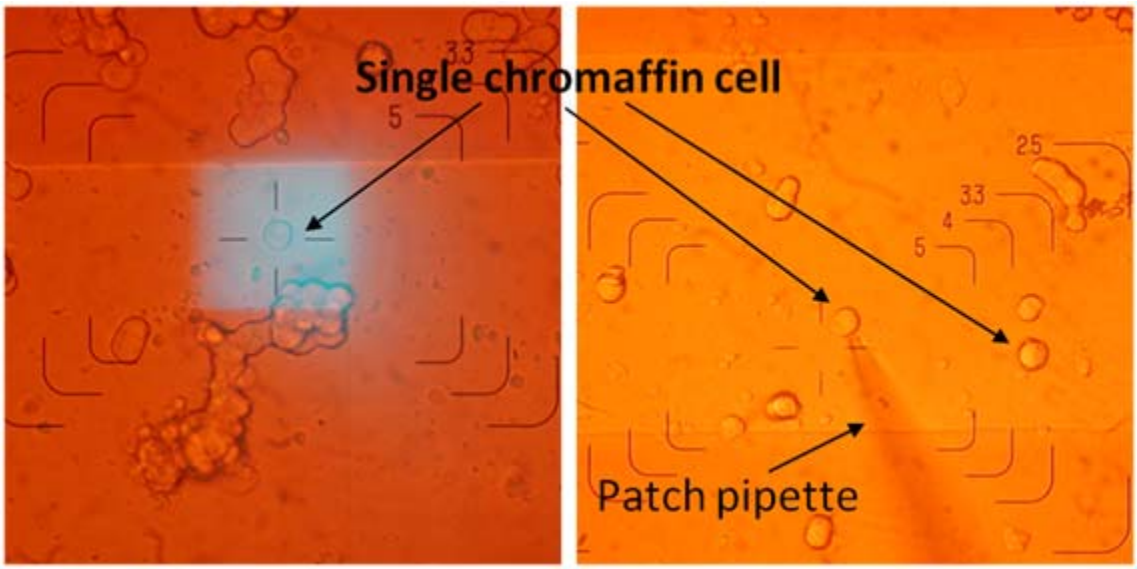

Fig 3.2 Microscopic images of single/clumped chromaffin cells on 200 µm x 200 µm planar ITO electrodes. (a) Light microscope image of an adhered single chromaffin cell. The bluish square window represents the use of a suitable wavelength of light (475 nm) from a monochromator in order to illuminate the otherwise transparent ITO electrode. (b) A single chromaffin cell on a working ITO electrode is whole-cell patch clamped using a patch pipette.

First, INS-1 cells as well as chromaffin cells were cultured on ITO electrodes on the chip. Single cells were then patch clamped and current was injected into the cell through the pipette. The resulting voltage responses (action potentials) were recorded in current clamp mode (Fig 3.3)

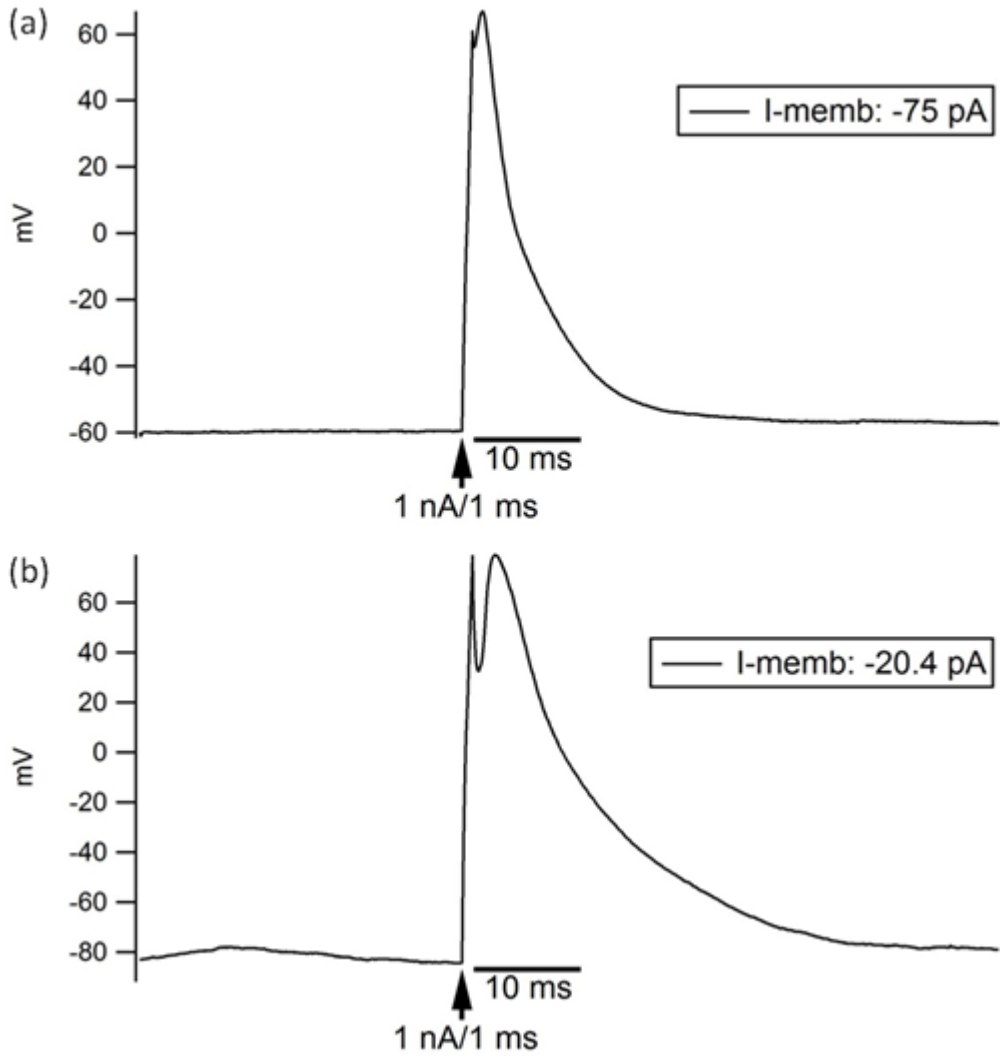

Fig 3.3 Action potentials resulting from injected current in single (a) INS-1 cell and (b) chromaffin cell and recorded using a patch pipette in whole cell current clamp mode

Once the excitability of the cells was established, INS-1 and chromaffin cells were stimulated using transient voltage pulses applied to the electrochemical

microelectrode located beneath the cell. Voltage protocols using varying voltage amplitudes and durations were tested until optimum voltage ranges were zeroed in on for each cell type. Voltage pulses between 1.5 V and 3 V lasting for 0.2 ms were found to reproducibly elicit action potentials in both chromaffin and INS-1 cells.

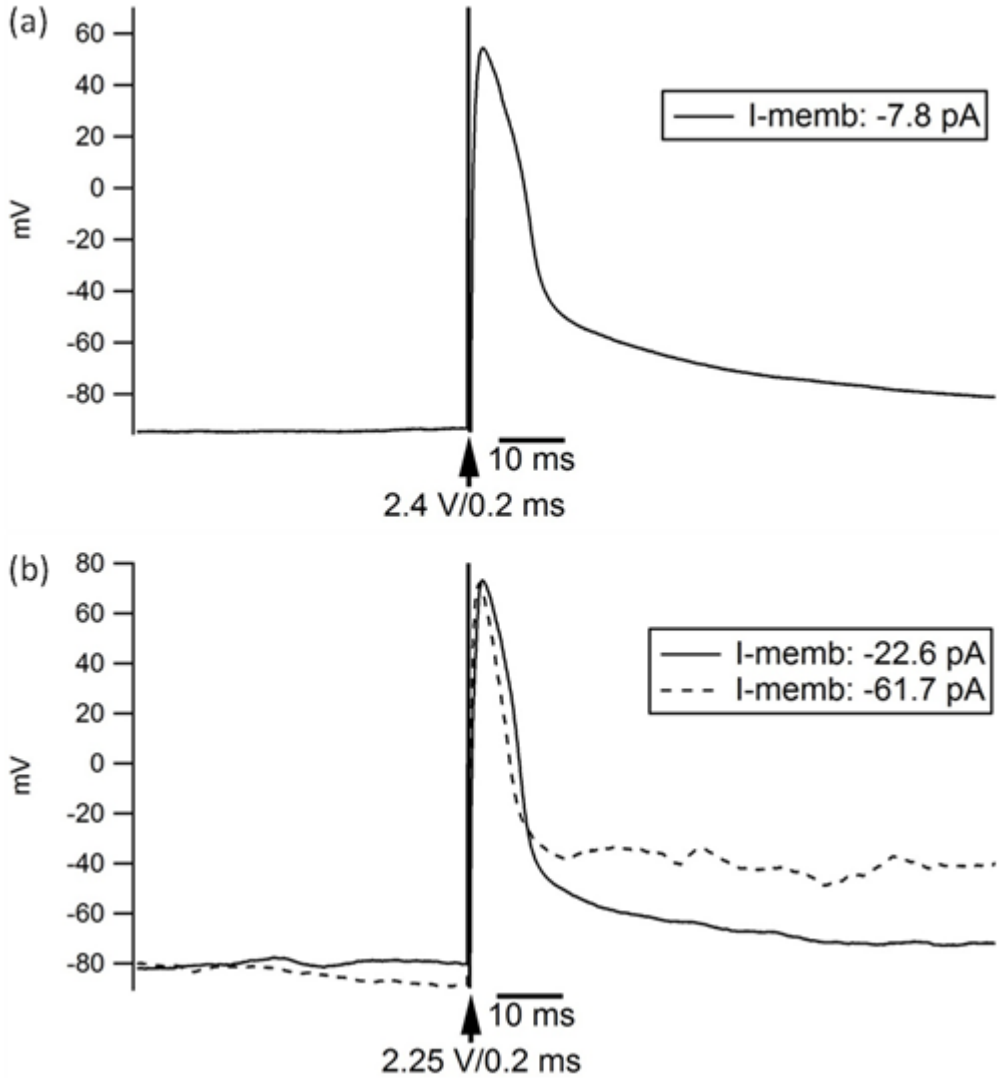

Fig 3.4 Action potentials induced by voltage pulses from underlying planar electrodes in single (a) INS-1 cell and (b) chromaffin cell and recorded using a patch pipette in whole cell current clamp mode

Fig 3.4 shows example traces from (a) a chromaffin and (b) an INS-1 cell where individual action potentials are evoked by transient voltage stimulations of 2.4 V/0.2 ms and 2.25 V/0.2 ms, respectively.

In order to induce exocytosis in a cell, a train of action potentials is required, therefore I tested protocols with trains of voltage pulses on chromaffin cells. The first protocol that was tested consisted of a train of three transient voltage pulses whose amplitudes and durations could be varied. Fig 3.5 is a representative trace showing action potentials that are induced by one such train consisting of three pulses.

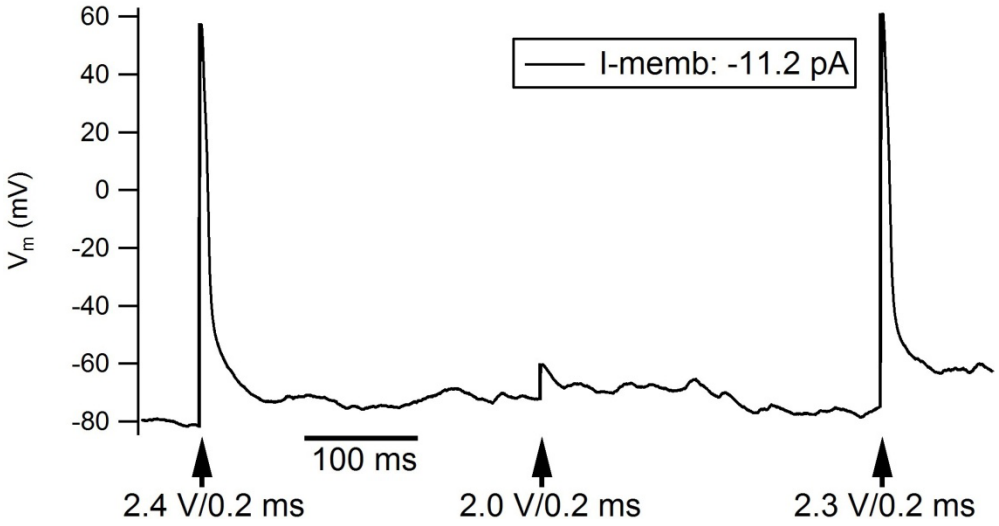

Fig 3.5 Action potential induced by transient voltages, 0.2 ms in duration, applied to the planar electrode beneath the pipette. Arrows indicate transient voltages of 2.4 V, 2.0 V and 2.3 V. Note that action potentials are stimulated in an all-or-none manner with a threshold stimulus between 2.0 and 2.3 V

Note that action potentials were induced in an all-or-none manner in that pulses with amplitudes of 2.4 or 2.3 V elicited action potentials whereas pulses to 2.0 V failed to induce an action potential. We found that the threshold for eliciting action potentials was

typically between 2.0 and 3.0 V for chromaffin cells that were well adhered to Au electrodes (2.23 ± 0.49 V, 0.2 ms pulse duration, n = 20 cells). Subsequent protocols with trains of more than three pulses were used to stimulate single chromaffin cells and responses were recorded. However, on repeated stimulation, precipitous drops in cell membrane potential resulting from a drop in membrane resistance occurred (Fig 3.6). A possible explanation of this phenomenon is that repeated stimulation leads to electropermeabilization of the cell membrane.

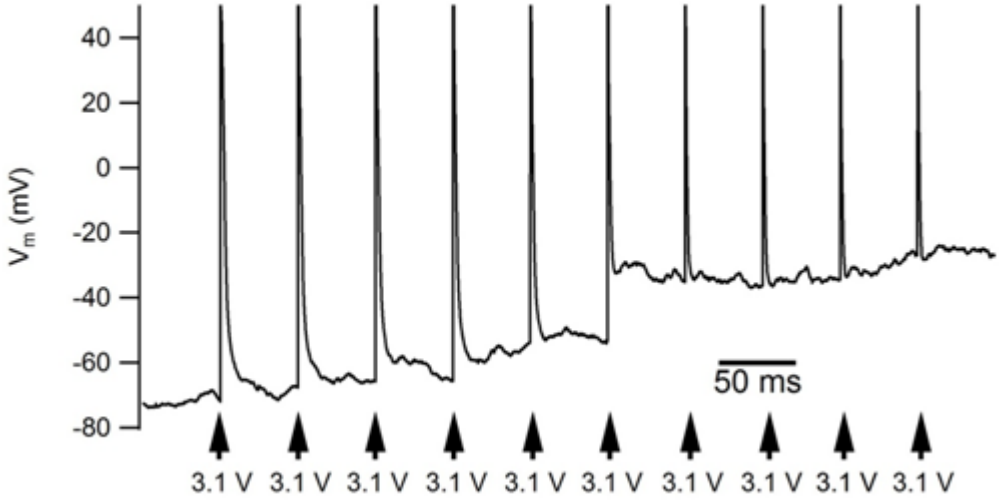

Fig 3.6 Trains of voltage pulses were applied to chromaffin cells in order to stimulate trains of action potentials that are required to induce an appreciable rate of exocytosis. However, a precipitous drop in membrane resistance was often observed on repeated stimulation or application of higher voltages. The figure denotes an example trace where action potentials were induced by transient voltages, 3.1 V in amplitude and 0.2 ms in duration, applied to the planar electrode. The abrupt rise in the intracellular voltage after the sixth pulse results from a drop in the membrane resistance.

3.3 Conclusion and discussion

Our "proof-of-concept" experiments showed that it is feasible to use an on-chip planar microelectrode to electrically stimulate action potentials, the physiological stimuli for Ca^{2+}-triggered exocytosis. Voltage pulses ranging from 1.5 V to 3 V lasting for 0.2 ms could successfully stimulate action potentials in both chromaffin and INS-1 cells. Using protocols with trains of three voltage pulses up to 2.4 V for a duration of 0.2 ms, it was shown that action potentials could be stimulated in single chromaffin cells using underlying planar electrochemical microelectrodes in an all-or-none fashion. The abrupt drop in membrane resistance that was often observed on repeated stimulation or application of higher voltages, however suggested that electropermeabilization of the cell membrane is occurring with these types of stimuli. Since electropermeabilization proves to be an effective way to induce quantal release from individual cells, we turned our attention to optimizing this approach.

CHAPTER 4

ELECTROPERMEABILIZATION OF SINGLE CHROMAFFIN CELLS FOLLOWED BY EXOCYTOSIS MEASURED USING THE SAME PLANAR ELECTRODE

4.1 Introduction to the different types of approaches used to stimulate exocytosis in neuroendocrine cells and goal of project

In neurons and endocrine cells, individual secretory granules discharge their neurotransmitter content during the process of quantal exocytosis. Although carbon fiber amperometry (Wightman and others 1991; Chow and others 1992; Travis and others 1998; Borges and others 2008) has been extensively used to monitor the time course of this catecholamine release, it is a low-throughout process. Recently, in an effort to enable high-throughput experiments, our group and others have developed microfabricated devices with arrays of microelectrodes to measure the release of electroactive transmitter at the single-cell and single-vesicle level (Chen and others 2003; Sun and others 2006; Spegel and others 2007; Chen and others 2008; Spegel and others 2008; Barizuddin and others 2010; Dittami and others 2010; Liu and others 2011). With existing systems the most common way of stimulating exocytosis is by perfusion of cells with a secratogogue (Barizuddin and others 2010; Liu and others 2011) leading to depolarization of the cell membrane, opening of voltage gated Ca^{2+}-channels, Ca^{2+} influx and Ca^{2+}-triggered exocytosis. Perfusion systems, however, often stimulate multiple cells and do not allow precise timing of the stimulus. In contrast, extracellular electrodes can also be used to directly depolarize cells and can potentially stimulate individual cells with very precise

timing (Fromherz and others 1995; Zeck and others 2001; Dittami and others 2010). Significantly, Dittami and Rabbitt demonstrated cells undergo exocytosis when forced through a narrow constriction in a microfluidic channel in proximity to a recording electrode, perhaps due to cell depolarization.

Another approach to stimulate exocytosis in neuroendocrine cells is by permeabilizing the cell membrane using either high electric fields or chemical agents that disrupt the integrity of the cell membrane (Holz 1988; Hay and others 1992). Following permeabilization, exocytosis can be elicited by including Ca^{2+} or other secretagogues in the bath solution that subsequently diffuse into the cell. Permeabilizing the plasma membrane bypasses the normal excitation pathway and allows one to sort out whether a drug or protein mutation affects exocytosis through a direct effect on exocytosis as opposed to an effect on the membrane potential mediated by ion channels. It also allows one to introduce membrane-impermeable substances into the cell, such as peptides or antibodies, to modulate protein function or second-messenger cascades.

A number of groups have implemented cell electroporation on a microchip, usually by applying a high electric field in a microfluidic channel or through a narrow aperture (reviewed in (Olofsson and others 2003)). Recently the Orwar group has induced electroporation at the single-cell level using carbon-fiber electrodes, thus demonstrating the feasibility of electroporation using polarizable microelectrodes suitable for electrochemistry (Ryttsen and others 2000).

We cultured cells on an open-volume microelectrode array and selected electrodes with a single adherent cell. We then tested the feasibility of using the same electrode to

stimulate a cell and subsequently record release from the cell using amperometry. This stimulus-recording electrode approach allows selective stimulation of a single cell, measurement of quantal transmitter release within 1 s after permeabilization in order to capture rapid kinetic features of exocytosis, and can distinguish quantal release of transmitter from vesicles (evident as amperometric spikes) from release of cytosolic transmitter or other electroactive compounds (which result in a slowly changing background faradaic current) (Cahill and others 1995). A schematic of the approach is shown in Fig 4.1.

4.2 The same electrochemical electrode can be used to stimulate and record quantal transmitter release

The same planar electrochemical electrode was used to stimulate the cell and record the electrochemical signal that results from oxidation of released transmitter. Fig 4.2 depicts a representative trace with amperometric spikes resulting from quantal transmitter release induced by electropermeabilization of a single cell on a gold microelectrode.

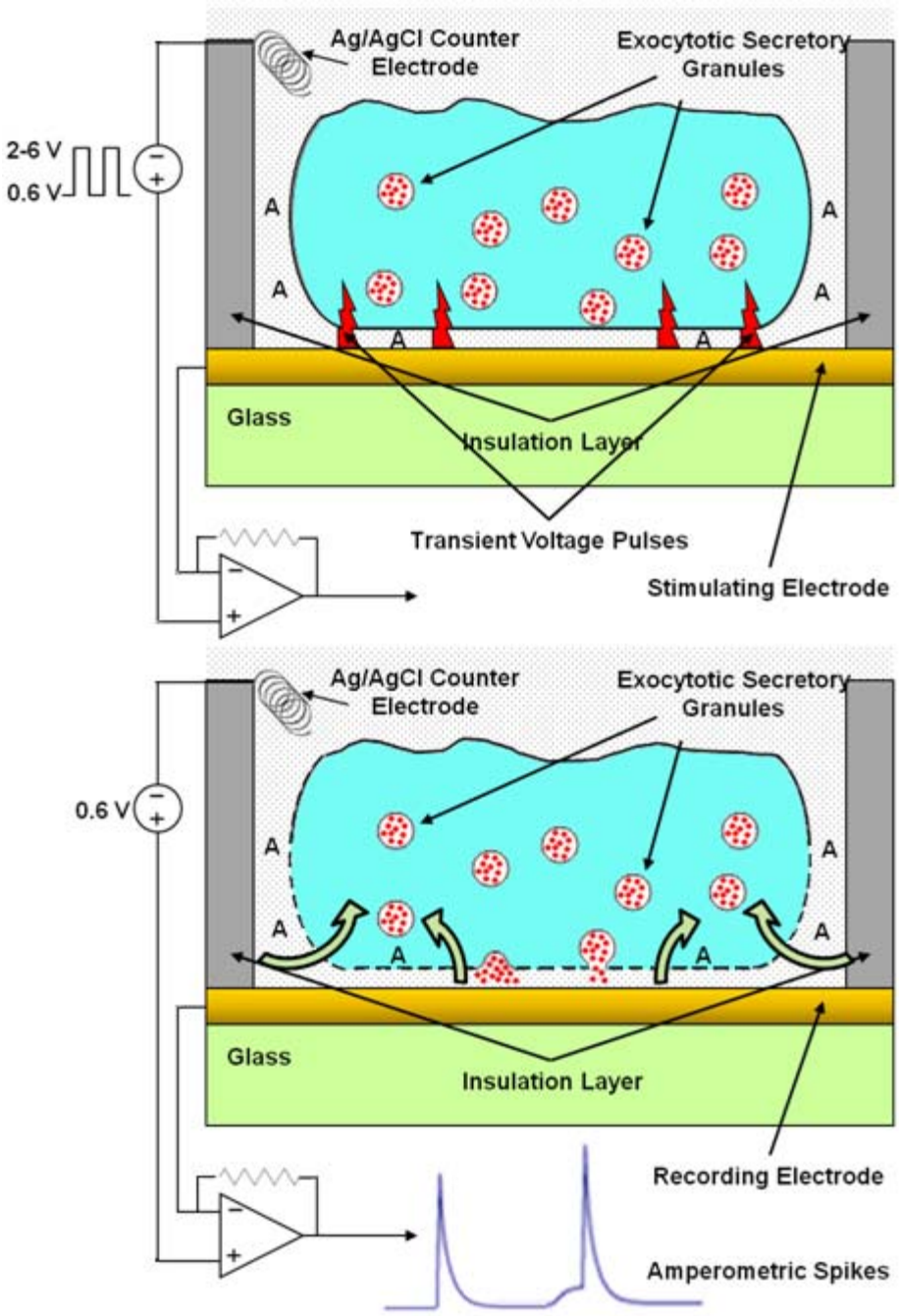

Fig 4.1 Schematic of novel stimulus-recording electrode (labeled stimulating electrode and recording electrode, respectively) approach where the same electrochemical microelectrode on-chip is used to electropermeabilize as well as record amperometric spikes from a single chromaffin cell

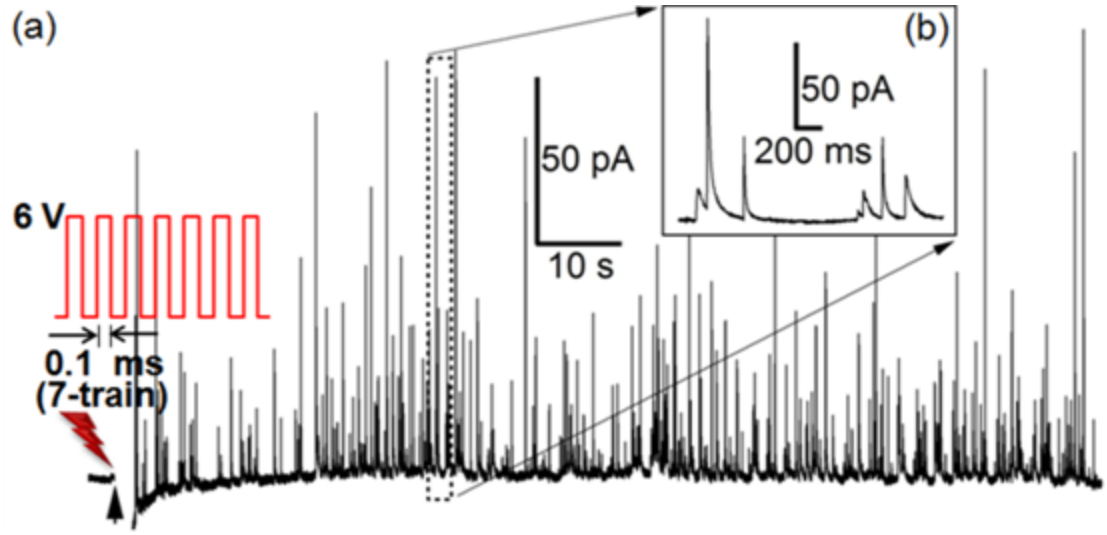

Fig 4.2 Trains of voltage pulses result in robust quantal transmitter release. Representative amperometric spikes following a train of voltage pulses that permeabilize the cell membrane of a single chromaffin cell on a Au microelectrode. The inset (b) is an expanded view of the amperometric spikes within the dashed box in part (a)

The amperometric spikes have amplitudes (I_{max}), durations ($t_{1/2}$) and areas (Q) that are consistent with previous reports of quantal exocytosis (Table 1 (Wightman and others 1991; Chow and others 1992; Elhamdani and others 2001; Yang and others 2007)). Thus the electrochemical signal that follows stimulating pulses is consistent with quantal exocytosis of chromaffin granules.

Table 1 Mean ± standard deviation of four descriptive spike parameters: half width ($t_{1/2}$), time to peak (t_p), charge (Q) and amplitude (I_{max}). Data obtained from cells electropermeabilized on gold microelectrodes in solutions containing a range of chloride concentrations

$t_{1/2}$ (ms)	**t_p (ms)**	**Q (pC)**	**I_{max} (pA)**
1.4±11.5	11.0±2.9	2.2±1.6	64.1±39.5

# of Cells = 9, # of Spikes = 771

A range of stimuli are able to elicit electropermeabilization and quantal release. Pulses with durations less than 0.2 ms were used in order to prevent bubbles from forming on the surface of electrodes. Individual or trains of voltage pulses from the holding potential used for amperometry (~0.6 V) to test potentials of 4–7 V were found to trigger massive quantal release from single chromaffin cells. Steps to lower potentials led to transient release i.e. secretion that terminated within 10 s of seconds. On the other hand, larger voltage steps or pulse trains led to release lasting for minutes.

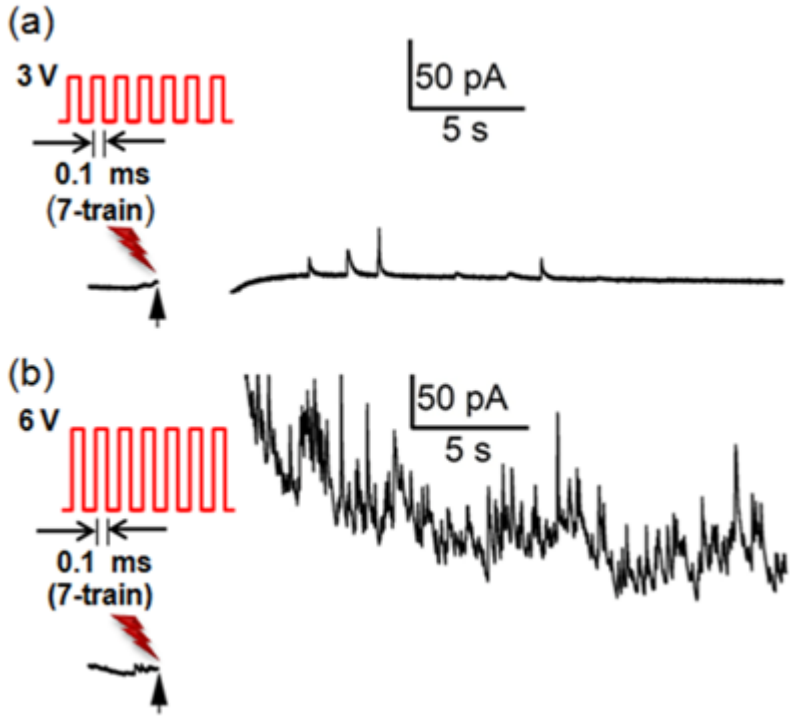

Fig 4.3 Increasing the amplitude of the stimulus voltage train leads to a greater frequency and duration of quantal transmitter release. (a) Representative trace showing infrequent spikes over a 30 s recording interval when the cell is stimulated by voltage pulse to 3 V (7 pulses, 0.1 ms in duration). (b) A subsequent stimulation train to 6 V leads to massive quantal release in the same cell that continues for minutes

Fig 4.3(a) provides a sample response to a train of seven pulses to +3 V, 0.1 ms in duration. Note that only a handful of release events are elicited before the response terminates. A subsequent train of pulses to +6 V in the same cell elicits a massive response (Fig 4.3(b)) that lasts for a number of minutes. Fig 4.4 shows a response from a different cell where a train of 7 pulses of 6V amplitude and 0.1 ms duration elicits massive release of neurotransmitter lasting for at least 5 minutes. Note that both modest and massive stimulation can be useful for studies of exocytosis. Whereas transient electropermeabilization could leave the cell more intact to allow probing the cell over prolonged intervals, prolonged permeabilization would be necessary to study the dependency of exocytosis on external factors like changing concentrations of a molecule of interest in the external solution.

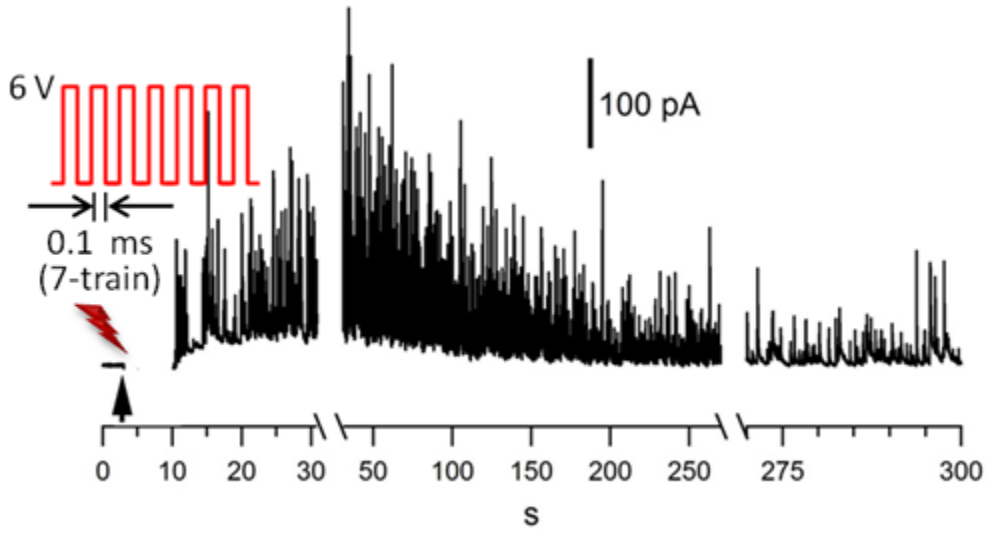

Fig 4.4 Massive stimulations of cells may result in thorough electropermeabilization which in turn leads to release of neurotransmitter over a prolonged period. Representative trace showing robust exocytosis lasting for 5 minutes due to electropermeabilization by a stimulation train to 6 V

The electropermeabilization of the plasma membrane was validated next by observing the uptake of membrane-impermeant dyes. Trypan blue is a commonly used membrane- impermeant stain that is excluded from viable cells. Since it cannot cross the plasma membrane before electropermeabilization, viable cells remained unstained. However, following stimulation, permeabilization of the plasma membrane allows the dye to enter the cell where it accumulates in the nucleus giving it a blue color. Propidium iodide is another known membrane-impermeant nucleic acid stain that is excluded from viable cells. However, the increase in membrane permeability that results from electroporation allows the dye to enter the cell. Once it enters the cell, the dye binds to the nucleic acids and its fluorescence is enhanced 20- to 30-fold. Propidium iodide staining indicates that the cell has become receptive to entry of exogenous molecules that would otherwise be excluded.

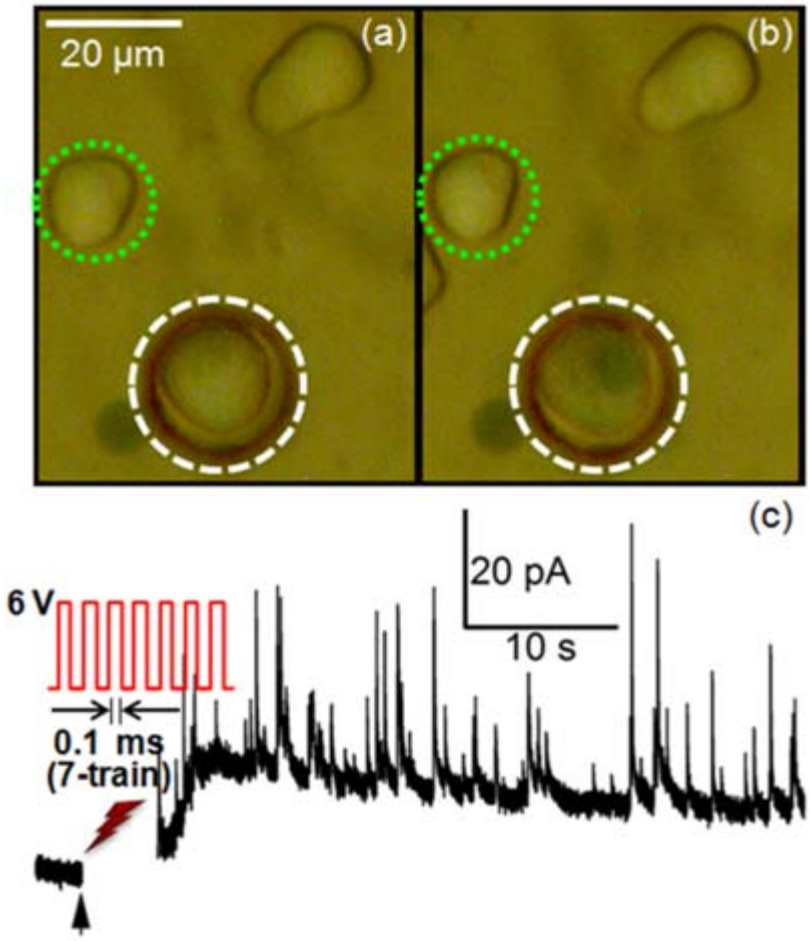

Fig 4.5 Uptake of the cell-impermeant dye Trypan blue demonstrates that the stimulation protocol leads to selective permeabilization of the cell adjacent to the electrode. (a) Photomicrograph with two viable chromaffin cells (encircled) sitting in a standard bath solution containing trypan blue before electropermeabilization. The upper cell encircled in green is sitting on the SU-8 insulation layer whereas the cell encircled in white is sitting on the working electrode. (b) A few minutes after application of the stimulating pulse to the working electrode, the cell sitting on the electrode has taken up the dye, indicating electropermeabilization, whereas the green encircled cell not directly adjacent to the electrode remains intact. (c) Amperometric spikes resulting from electropermeabilization of the cell adjacent to the electrode.

Fig 4.5(a) depicts two chromaffin cells; one directly over the electrode (white dashed circle) and another cell not adjacent to an electrode (green dashed circle). Neither cell took up the trypan blue present in the bath, indicating that they are viable cells. After application of the voltage pulse (Fig 4.5(b)), the cell over the electrode takes up the stain, indicating electropermeabilization has occurred, whereas the control cell remains unstained. This indicates that the stimulation is specific and addressable to the single-cell level. Fig 4.5(c) indicates amperometric spikes recorded from the stained cell in Fig 4.5(b) in response to the voltage pulse and demonstrates that the cell remains viable enough to secrete transmitter via quantal exocytosis. Similarly, Fig 4.6(a) depicts a chromaffin cell sitting on a working electrode. Fig 4.6(b) is the corresponding fluorescence image showing that the cell (yellow dashed circle) did not take up the propidium iodide stain present in the bath, indicating a viable cell. After application of the voltage pulse (Fig 4.6(c)) to the electrode, the nucleus of the cell is stained red (Fig 4.6(d)), indicating that electropermeabilization has occurred. Other cells in the vicinity do not pick up the dye (data not shown). Fig 4.6(e) shows representative amperometric spikes recorded from the stained cell in Fig 4.6(d) in response to stimulation.

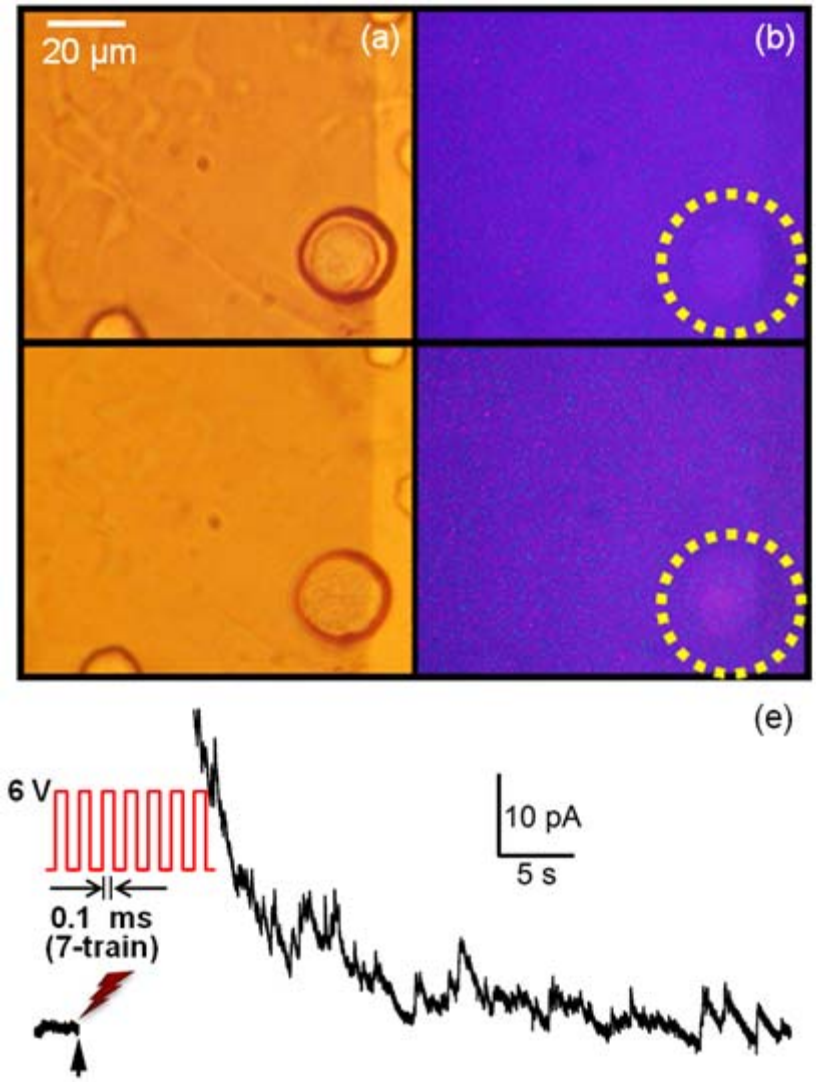

Fig 4.6 Uptake of the cell-impermeant dye propidium iodide demonstrates that the stimulation protocol leads to selective permeabilization of the cell adjacent to the electrode. (a) & (b) Images of a viable chromaffin cell (encircled in b) sitting on an electrode in a standard bath solution containing propidium iodide before electropermeabilization. (c) & (d) A few minutes after application of the stimulating pulse, the cell sitting on the electrode has taken up the dye, indicating occurrence of electropermeabilization, (e) Amperometric spikes resulting from electropermeabilization of the cell adjacent to the electrode.

4.3 Voltage pulses do not degrade the electrochemical electrodes

The experiments depicted in Figs 4.2–4.6 demonstrate that, following a voltage pulse, the electrochemical electrode could recover within several seconds and remain sensitive enough to record amperometric spikes with typical features. We next sought to determine if the voltage pulses alter the sensitivity of the electrodes or increase measurement noise.

Our experiments indicated no change in the noise (standard deviation) resulting from brief (sub ms) pulses to +10 V. In order to test for changes in electrode sensitivity, we recorded cyclic voltammograms (CVs) using the test analyte ferricyanide before and after applying voltage pulses (Fig 4.7). During the CV the voltage is scanned from +0.7 V to -0.5 V and a reduction peak is observed at ~+0.1 V as the ferricyanide is reduced to ferrocyanide. This reaction is reversed as the voltage is scanned in the positive direction, resulting in an oxidation peak. The voltage difference between the oxidation and reduction peaks (ΔE_p) is a measure of electron-transfer kinetics. Note in Fig 4.7 that applying several 0.2 ms pulses to +10 V in between CV measurements has little effect on ΔE_p or other features of the CVs, therefore there is no apparent degradation of the electrochemical sensitivity of the electrode. In fact, ΔEp decreases slightly after application of a voltage pulse, perhaps because the voltage pulse oxidizes, and thus removes, a thin layer of gold on the surface of the working microelectrode, thus cleaning the electrode surface.

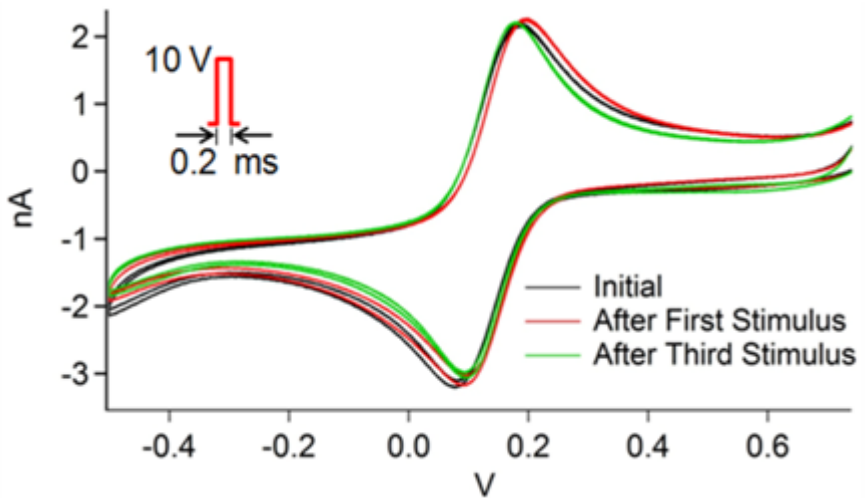

Fig 4.7 Voltage pulses do not reduce the sensitivity of the electrochemical electrode to a test analyte. Cyclic voltammograms were acquired at 1 V s^{-1} using a 1 mM ferricyanide ($K_3Fe(CN)_6$) solution in 0.1 M KCl, pH 3. The Au electrode was 20 mm in diameter. In between CVs the solution was exchanged to a normal extracellular solution and voltage pulses (+10 V for 0.2 ms) were applied

4.4 Electropermeabilization-induced quantal release is dependent on $[Cl^-]_e$, but not $[Ca^{2+}]_e$

Under physiological conditions, exocytosis is triggered in excitable cells by entry of Ca^{2+} into the cell through ion channels. Therefore it would seem likely that electropermeabilization of the plasma membrane triggers exocytosis by providing an alternative pathway for Ca^{2+} to enter cells from the extracellular solution. In order to test this hypothesis we performed experiments using extracellular solutions with no added Ca^{2+} together with 5 mM of the Ca^{2+} chelator EGTA to buffer the free Ca^{2+} concentration into the subnanomolar range. Experiments were also carried out using 2 mM BAPTA instead of EGTA as the Ca^{2+} chelator. We were surprised to find that robust exocytosis

can be elicited with voltage pulses applied to cells bathed in this "Ca^{2+}-free" solution (Fig 4.8(a)). In contrast, Ca^{2+}-free solutions do not support substantial exocytosis when chromaffin cells undergo large-scale electropermeabilization in a cuvette (Knight and others 1982) or are permeabilized with chemical agents such as digitonin (Dunn and others 1983). Cell depolarization also fails to elicit exocytosis in Ca^{2+}-free solutions (Neher and others 1982).

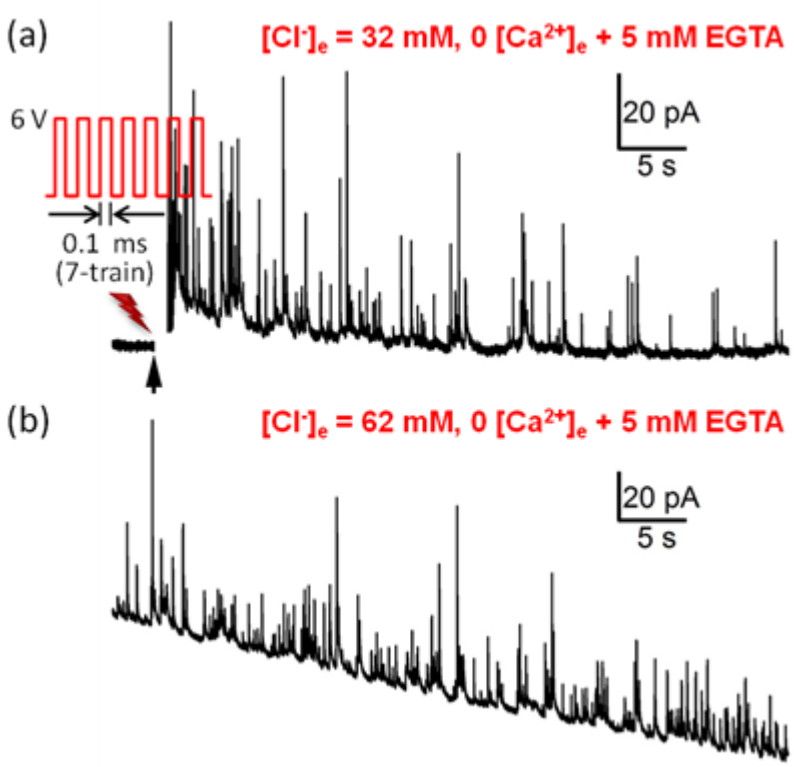

Fig 4.8 Quantal transmitter release is dependent on the Cl^- concentration in the bath. Representative experiments from the same cell. (a) A lower spike frequency is observed following electropermeabilization in a solution containing 32 mM Cl^- (Note that the frequency is higher initially but drops gradually with time). (b) Washing with a solution containing 62 mM Cl^- greatly increases the rate of quantal transmitter release. Changes in Cl^- concentration were made by equimolar substitution of glutamic acid for Cl^-

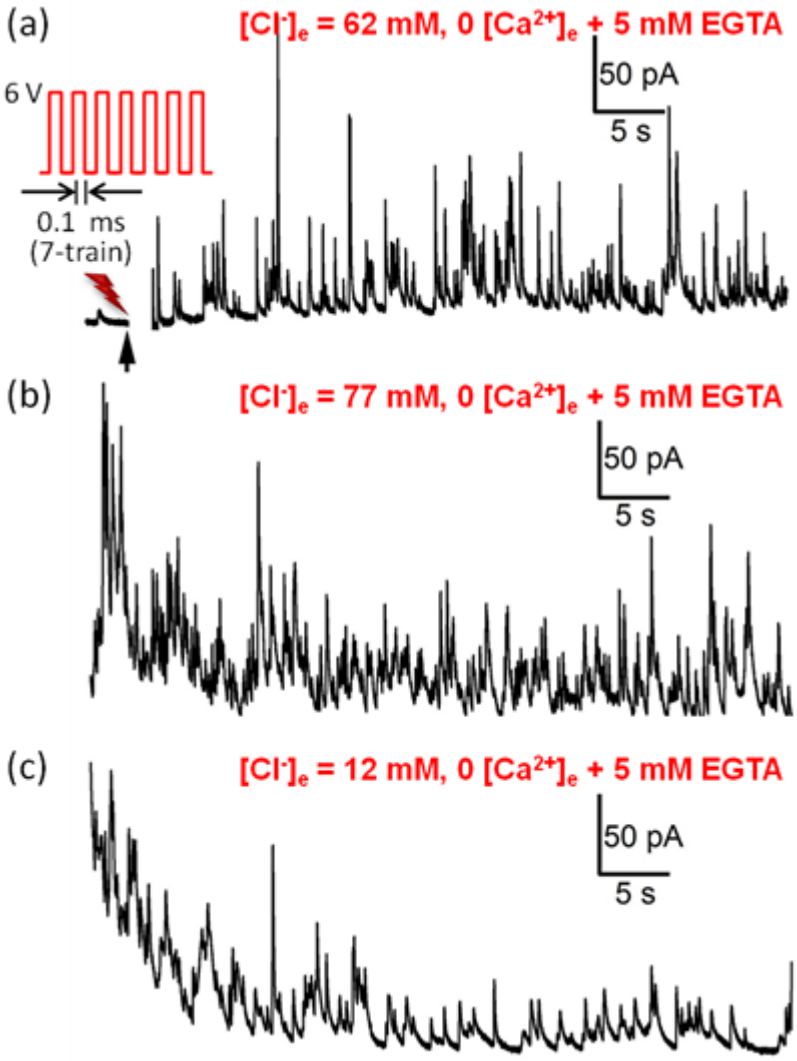

Fig 4.9 Representative experiments from the same cell on Cl^--dependency of exocytosis. (a) A higher spike frequency is observed following electropermeabilization in a solution containing 62 mM Cl^-. (b) Wash with a solution containing 77 mM Cl^- results in a comparable rate of release. (c) A final wash with a solution containing only 12 mM Cl^- leads to a lower rate of release. Changes in Cl^- concentration were made by equimolar substitution of glutamic acid for Cl^-

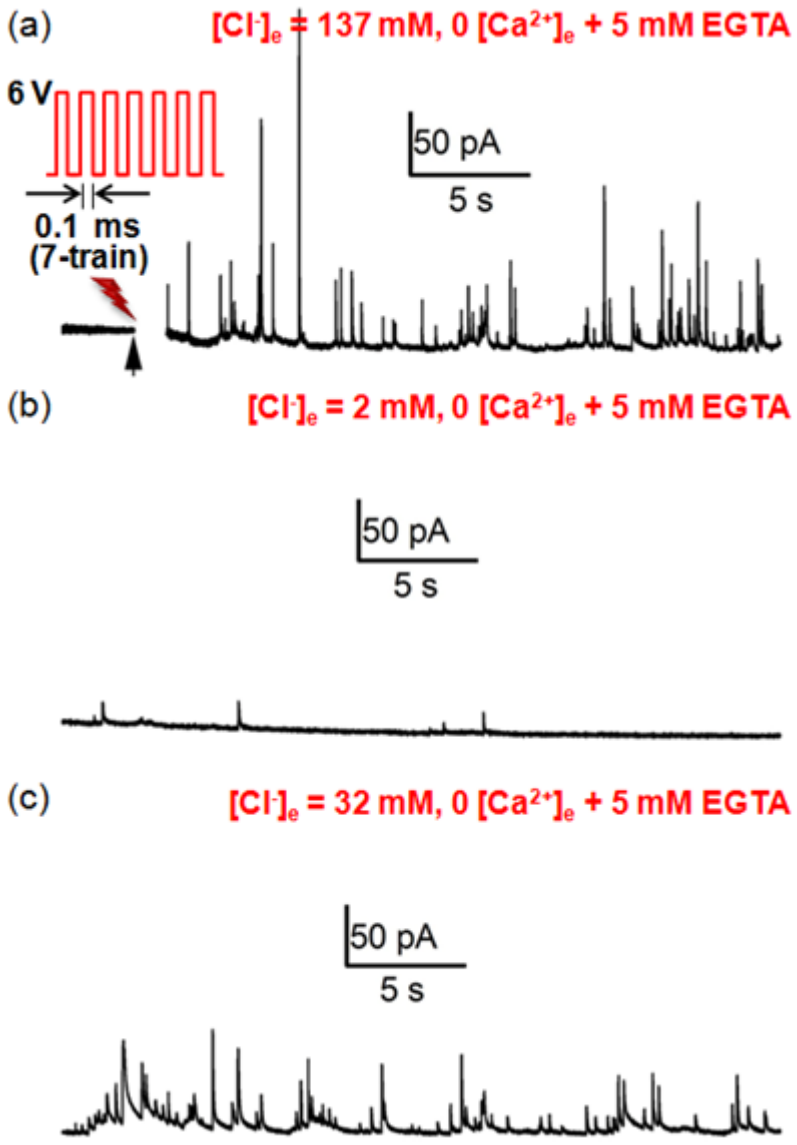

Fig 4.10 Quantal transmitter release is dependent on the Cl^- concentration in the bath. Representative bracketed experiment from the same cell. (a) A high spike frequency is observed following electropermeabilization in a solution containing 137 mM Cl^-. (b) Wash with a solution containing 2 mM Cl^- greatly reduces the rate of quantal transmitter release. (c) Exchange of the bath solution for one containing 32 mM Cl^- restores a high rate of transmitter release. Changes in Cl^- concentration were made by equimolar substitution of glutamic acid for Cl^-

Whereas extracellular Ca^{2+} is not essential, we found that mM concentrations of Cl^- are necessary to support robust quantal transmitter release in response to our electropermeabilization protocol. Fig 4.8(a) depicts a sample experiment where neurotransmitter release is elicited in a "Ca^{2+} free" solution containing 32 mM Cl^- (with equimolar substitution of glutamic acid for Cl^-). However, subsequent wash with a solution containing a higher Cl^- (62 mM) leads to a higher rate of release (Fig 4.8(b)). Fig 4.9(a) depicts another sample experiment where robust release is elicited in a solution containing 62 mM Cl^-. Subsequent wash with a solution containing 77 mM Cl^- leads to a comparable rate of release (Fig 4.9(b)). A final wash with a solution containing only 12 mM Cl^- leads to a lower rate of release (Fig 4.9(c)). Fig 4.10a depicts a third sample experiment where robust release is elicited in a solution containing 137 mM Cl^-. However, subsequent wash with a solution containing only 2 mM Cl^- leads to a much lower rate of release (Fig 4.10(b)). Subsequent wash with a solution containing 32 mM Cl^- restores a robust rate of secretion (Fig 4.10(c)). In experiments from 5 cells following the same protocol, the rate of quantal release was reduced from 4.1 ± 1.2 to 0.11 ± 0.05 spikes s^{-1} upon reduction of Cl^- from 137 to 2 mM. Subsequent wash with 32 mM Cl^- returned the rate of release to 0.53 ± 0.49 spikes s^{-1}. The lower rate of release at 32 mM Cl^- compared to 137 mM Cl^- (Fig 4.10) may be partially or completely explained by a slow "rundown" of exocytosis following electropermeabilization (also see (Knight and others 1982)), nevertheless, these bracketed experiments demonstrate a steep dependence of the rate of transmitter release on Cl^- between 2 and 32 mM using our approach to stimulate exocytosis.

During exocytosis, vesicles fuse with the cell membrane to release their content into the extracellular space. The fusion of a vesicle with the plasma membrane leads to transient incorporation of the vesicle membrane with the cell membrane and this leads to an increase in the membrane area. This phenomenon can be monitored electrically as an increase in surface membrane capacitance (Neher and others 1982). Thus, during whole cell patch clamp experiments, introduction of free Ca^{2+} in the pipette induces exocytosis, which in turn results in a membrane capacitance increase. Although electropermeabilization-induced exocytosis can occur in the absence of Ca^{2+}, patch clamp experiments with chromaffin cells depicted in Fig 4.11 confirm that Ca^{2+} in the intracellular solution is essential to cause increases in membrane capacitance.

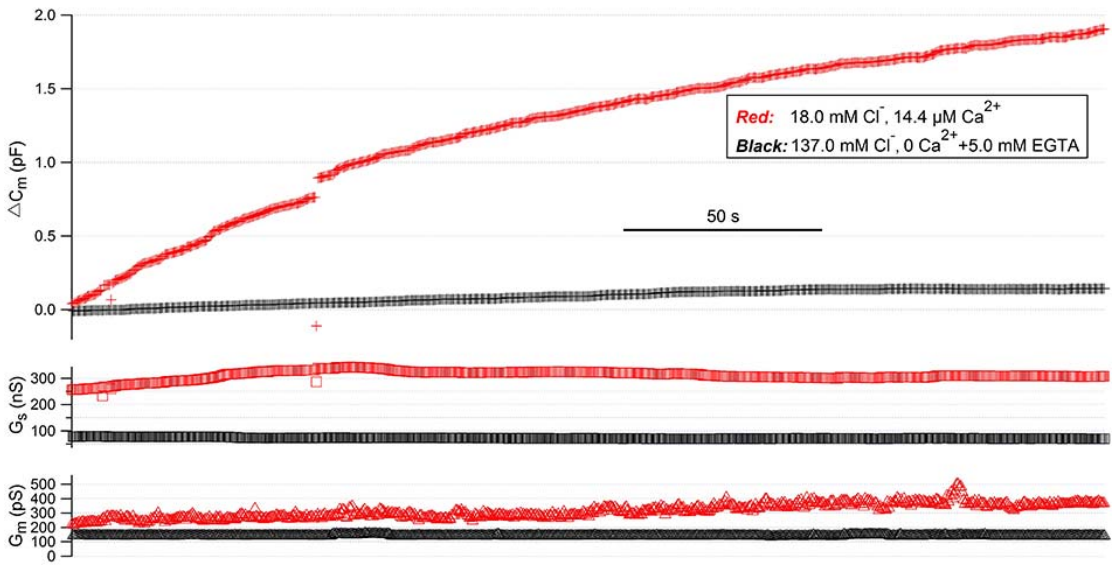

Fig 4.11 Ca^{2+}-free, Cl^--containing solutions do not elicit massive exocytosis in chromaffin cells. Capacitance measurements from whole-cell patch clamp recordings show that buffered 14.4 µM Ca^{2+} in the pipette can elicit exocytosis but absence of Ca^{2+}, even in the presence of 137 mM of Cl^- does not induce increases in capacitance. In contrast electropermeabilization-induced exocytosis leads to robust exocytosis in the presence of 0 Ca^{2+} and EGTA

Thus, in a chromaffin cell, whereas 14.4 μM Ca^{2+} in the pipette can elicit massive neurotransmitter release, Cl^- in the absence of Ca^{2+} fails to elicit exocytosis during whole-cell patch clamp recording (Fig 4.11).

A possible explanation for why extracellular Ca^{2+} is not needed to stimulate exocytosis in our experiments is that the pulse protocol leads to release of Ca^{2+} from intracellular stores, either through direct intracellular electroporation, heating, or other mechanisms. In order to address this we performed preliminary experiments measuring changes in intracellular Ca^{2+} concentration ($[Ca^{2+}]_i$) in response to voltage pulses. Fig 4.12(a) presents a sample experiment, representative of three cells, where $[Ca^{2+}]_i$ increases in response to the voltage pulses when the extracellular solution contains 2 mM $CaCl_2$. This is consistent with the hypothesis that electroporation allows substantial influx of Ca^{2+} from the bath solution. An additional two cells, however, did not show a prominent $[Ca^{2+}]_i$ response, perhaps because the electropermeabilization was transient. In contrast, Fig 4.12(b) shows a sample trace, representative of 5 cells, where a voltage pulse protocol that reliably evokes exocytosis does not lead to a discernible increase in $[Ca^{2+}]_i$ if the bath solution contains 0 Ca^{2+}/5 mM EGTA. This suggests that release of Ca^{2+} from internal stores is not prominent under these experimental conditions, although we cannot exclude the possibility that spatially local release of Ca^{2+} occurs that escapes detection in our system.

Whereas the absolute dependence of quantal transmitter release on Ca^{2+} appears to be lost following electropermeabilization under our experimental conditions, we next sought to determine if Ca^{2+} can modulate the rate of Cl^--dependent release. We therefore set the Cl^- concentration to 30 mM, which is a concentration where the rate of release is

roughly half maximal in a low Ca^{2+} solution. Keeping $[Cl^-]_e$ fixed to 30 mM, cells were first electropermeabilized in a 0 Ca^{2+}, 5 mM EGTA solution and then the cells were washed with a solution containing 97.7 µM free Ca^{2+} buffered with DPTA.

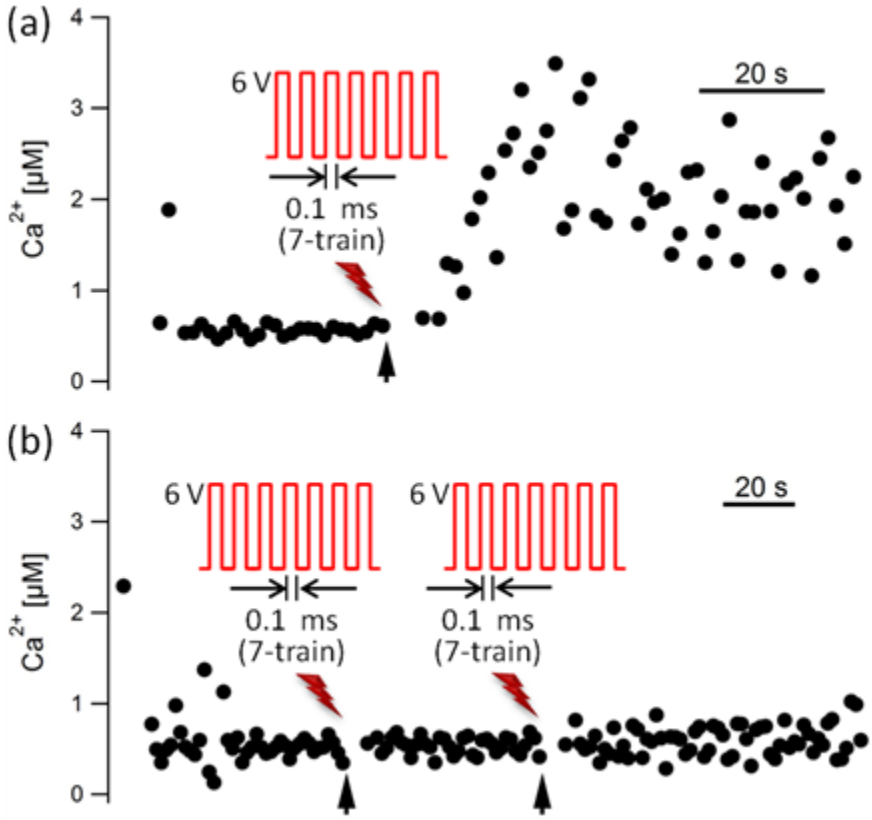

Fig 4.12 Release of Ca^{2+} from internal stores is not prominent under our experimental conditions. (a) Denotes an example where the stimulus protocol leads to a clear increase in $[Ca^{2+}]_i$ when the bath contained 2 mM $CaCl_2$. Similar increases in $[Ca^{2+}]_i$ were seen in two other cells, whereas two other did not show a clear increases in $[Ca^{2+}]_i$. (b) shows a sample recording where the stimulus protocol lead to no discernible increase in $[Ca^{2+}]_i$ when the bath solution contained zero added Ca and 5 mM EGTA. Similarly, no discernible $[Ca^{2+}]_i$ increases were seen in four other cells in response to the stimulus protocol

Fig 4.13(a) below depicts a sample experiment where neurotransmitter release is elicited in an optimum Cl^- (32 mM), "Ca^{2+} free" solution. However, subsequent wash with a solution containing a higher Ca^{2+} shows negligible change in rate of release (Fig 4.13(b)). Likewise, Fig 4.14(a) depicts a sample experiment where neurotransmitter release (at a comparatively lower rate) is elicited in an optimum Cl^- (32 mM), "Ca^{2+} free" solution.

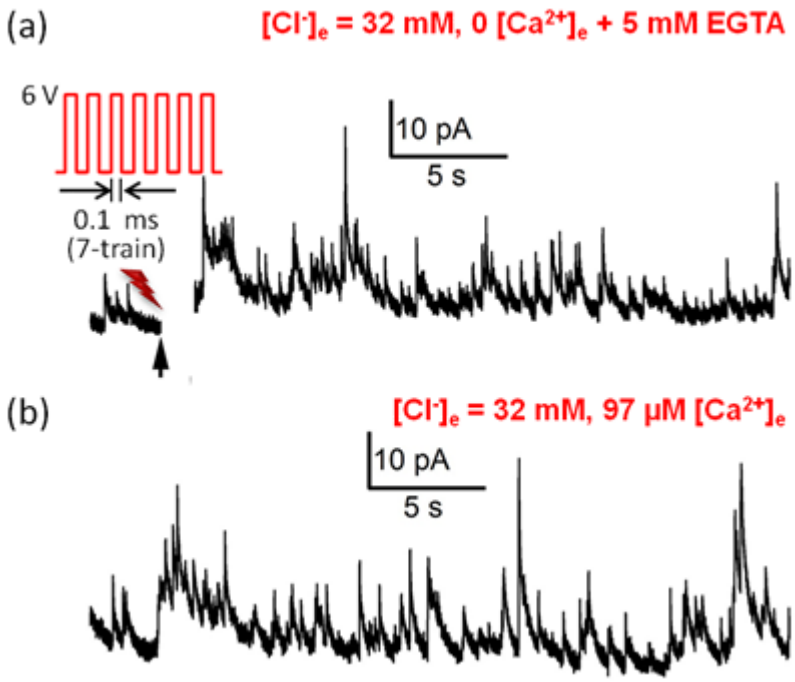

Fig 4.13 Ca^{2+} plays little to no role in modulating the rate of Cl^--dependent release in electropermeabilized chromaffin cells. (a) A high spike frequency is observed following electropermeabilization in a solution containing 32 mM Cl^- and 0 Ca^{2+}/EGTA. (b) No significant increase in spike frequency is noted on exchange of the bath solution for one containing 32 mM Cl^- but higher buffered Ca^{2+} (97 µM)

However, subsequent wash with a solution containing a higher Ca^{2+} shows a slight decrease in rate of release (Fig 4.14(b)). From (n = 7 cells), the spike frequency was 1.90

± 0.42 in the Ca^{2+}-free solution and 1.93 ± 0.50 in the Ca^{2+}-containing solution. Thus, surprisingly, Ca^{2+} is found to play little role in triggering or modulating quantal transmitter release when electropermeabilization is induced under our experimental conditions.

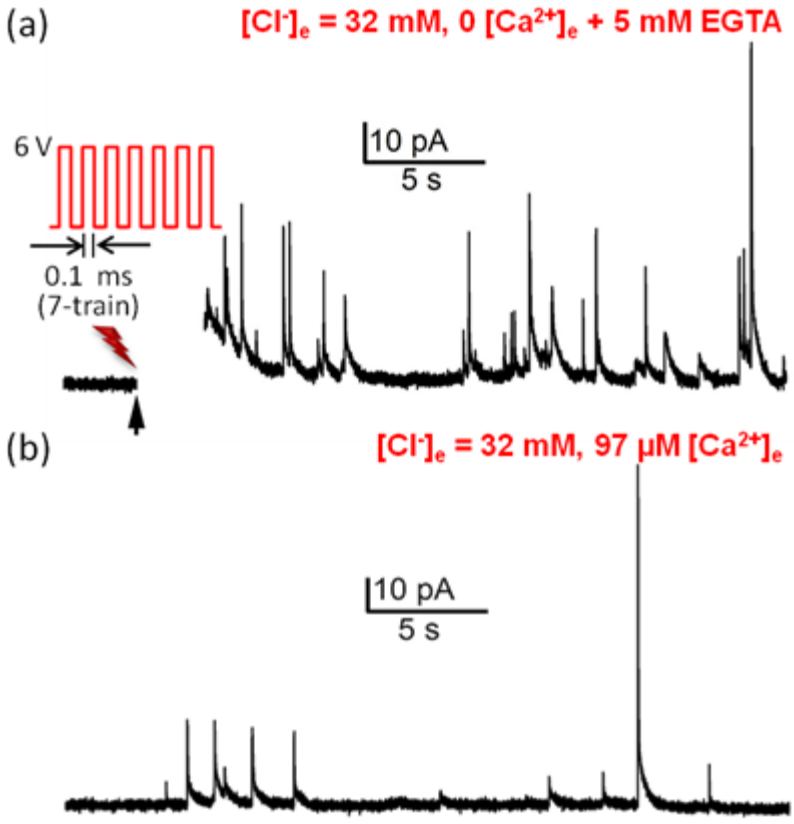

Fig 4.14 Ca^{2+} plays little to no role in modulating the rate of Cl^--dependent release in electropermeabilized chromaffin cells. (a) A low spike frequency is observed following electropermeabilization in a solution containing 32 mM Cl^- and 0 Ca^{2+}/EGTA. (b) A small decrease in spike frequency is noted on exchange of the bath solution for one containing 32 mM Cl^- but higher buffered Ca^{2+} (97 µM)

4.5 Conclusion and discussion

As noted previously, the amperometric spikes obtained under Ca^{2+}-free conditions have amplitudes and time courses that are typical for exocytosis events from chromaffin cells (Table 1). Thus Cl^--stimulated, electropermeabilization induced "quantal" catecholamine release almost surely occurs from individual chromaffin granules. Our experiments cannot resolve, however, whether the release occurs via bona fide exocytosis or by lysis of secretory granules as they approach the membrane/electrode surface.

Of further note is the fact that the dependence of transmitter release on $[Cl^-]_e$ occurs after the electroporation step since manipulation of $[Cl^-]_e$ after electroporation modulates the rate of ongoing transmitter release in a reversible manner (Fig 4.10). We speculate that the dependence of vesicle release on Cl^- may be mediated by ClC Cl^- channels on the vesicle membrane (Maritzen and others 2008). It is interesting to note that Cl^--containing solutions have previously been reported to support lysis of secretory granules isolated from chromaffin cells (Holz 1986).

We have developed an approach where the same electrochemical electrode located immediately below a cell can be used to stimulate and record quantal release of catecholamines from an individual chromaffin cell via electroporation. The voltage-pulse protocol leads to selective permeabilization of an individual cell with precise timing. Mild stimuli support reversible electroporation, which may in the future allow transfection of cells to express proteins of interest followed by on-chip measurement of exocytosis from transfected cells.

CHAPTER 5

CELL-BASED DETECTION OF BONT LC/E IN PERMEABILIZED CHROMAFFIN CELLS USING ON-CHIP ELECTROCHEMICAL MEASUREMENT OF QUANTAL EXOCYTOSIS

5.1 Introduction to existing methods for detection of botulinum neurotoxin (BoNT)

Botulinum neurotoxins (BoNTs) are one of the most toxic substances known to human. With a median lethal dose (LD50) of 1-50 ng/kg of body weight (Band and others 2010), they are the cause of botulism, a life-threatening neuroparalytic disorder (Dembek and others 2007). BoNT intoxication is marked by flaccid paralysis originating from an inhibition of neurotransmitter release from motor neurons. On a molecular level, BoNTs impair transmitter release in cells by cleaving several isoforms of the three SNARE proteins that are critical for vesicle fusion with the plasma membrane (Schiavo and others 2000).

BoNTs are produced by the gram positive anaerobic soil bacterium Clostridium botulinum (Shukla and others 2005). Strains of C. botulinum are classified into seven types, A to G, according to the antigenic properties of BoNTs they produce. These are large proteins with a molecular weight of 150 kDa. After synthesis, the BoNT complexes remain relatively inactive (Cai and others 2007) until they are activated by protease nicking to form a dichain molecule made up of a light chain (LC) and a heavy chain (HC) linked by a single disulfide bond and many other non-covalent interactions between the

two peptide chains. (Singh 2000). The LCs are zinc-endopeptidases, which cleave specific proteins involved in vesicle docking and fusion, whereas, the HCs play an accessory role by helping in cell binding and translocation through the plasma membrane and into the cytosol (Li and others 1999; Simpson 2004; Montecucco and others 2005; Singh 2006). Fig 5.1 shows how neurotransmitter release occurs at a neuromascular junction and how the light chain of BoNT disrupts the vesicle fusion process by cleaving the SNARE proteins.

Each of the 7 different serotypes cleaves a unique peptide bond located on one of the SNARE proteins (Schiavo and others 1992; Blasi and others 1993; Breidenbach and others 2004). BoNT/A and /E cleave synaptosomal associated protein of 25 kDa (SNAP-25), at positions 197–198, and 180–181, respectively. Human botulism is caused mainly by BoNT/A, /B, /E and occasionally /F. However, the duration of induced muscle paralysis varies from one serotype to the other. Muscle paralysis caused by BoNT/A can last for several months while BoNT/E has been observed to have relatively short-lived effects (Eleopra and others 1998). Although it is known that BoNTs are a dangerous biohazard agent capable of causing widespread casualties, these toxins are used in important therapeutic applications. A wide variety of conditions including cervical dystonia, strabismus, blepharospasms, hemifacial spasms, hyperhidrosis, myofacial pain, migraine headaches, vocal cord dysfunction, diabetic neuropathy, anal fissure and multiple sclerosis are treated using BoNT toxin products. Additionally, the most well-known application of BoNT serotype A is its use as a cosmetic anti-wrinkle agent, known commercially as BOTOX® (Fig 5.2).

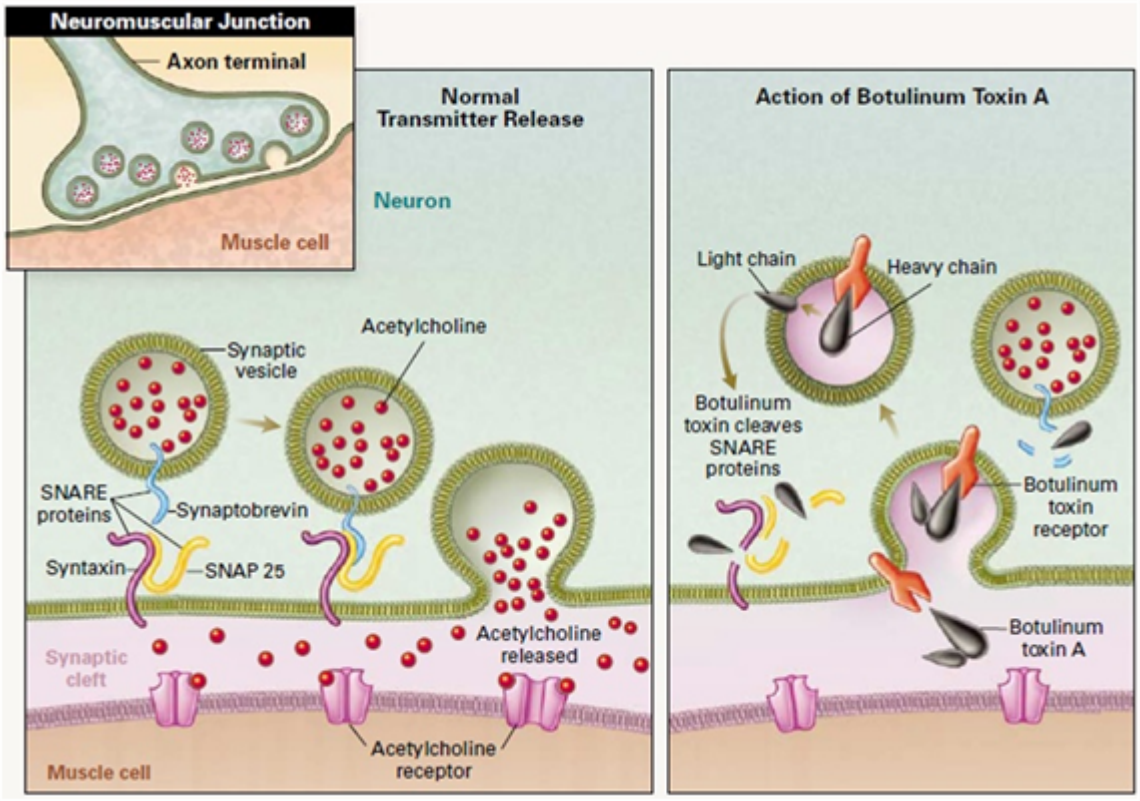

Fig 5.1 Neurotransmitter release at a neuromascular junction and cleaving of SNARE proteins by light chain of BoNT resulting in disruption of the vesicle fusion process. Acetylcholine in nerve terminals is packaged in vesicles. Normally, vesicle membranes fuse with those of the nerve terminals, releasing the transmitter into the synaptic cleft. The process is mediated by a series of proteins collectively called the SNARE proteins. Botulinum toxin, taken up into vesicles, cleaves the SNARE proteins, preventing assembly of the fusion complex and thus blocking the release of acetylcholine. (Reproduced with permission from (Rowland 2002), Copyright Massachusetts Medical Society)

The high toxicity of BoNTs makes the detection of the toxin and diagnosis of botulism a matter of great challenge. Due to the extremely low lethal dose of the toxin, it is also difficult to induce host responses detectable for diagnostics. The mouse lethality assay currently remains the only accepted standard test to confirm active BoNTs

(Benedetto 1999). On introduction of dilutions of BoNT samples in mice via intraperitoneal injections, specific botulism symptoms that finally lead to death are observed. The test is based on monitoring the mice for 48 hrs at each stage of analysis after injection of toxin. With subsequent dilutions of the sample, the maximum dilution that kills the mice as well as the minimum dilution that does not kill are estimated (Benedetto 1999). These are then used to approximate the quantity of BoNT in the sample by relating the maximum dilution which kills to the known mouse lethal dose (MLD50, 10 pg for BONT/A) (Ferreira 2001).

Fig 5.2 BoNT, if administered locally and in therapeutically safe doses, can be of cosmetic as well as therapeutic help. The picture above shows use of BOTOX® that is injected under the skin to remove wrinkles from the forehead region

The toxicity of BOTOX® is also expressed in a unit of bioactivity or potency called the biologic mouse units (U). The median lethal dose or the amount of toxin needed to kill 50% (LD50) of a group of female Swiss Webster mice that weigh 18-22 g each, constitutes one mouse unit. The human LD50 is 40 U/kg or about 2500 – 3000 U

for a 70-kg person. However, for cosmetic purposes, the usual total dose of BOTOX® that is administered during any treatment session is less than 100 U. This being about 3% of the human LD50, accidental overdosing resulting in poisoning is highly unlikely to happen. In fact, no case of systematic toxicity due to accidental injection or ingestion of BOTOX® has ever been reported (Benedetto 1999). The LD50 assay does not allow for standardization of potency units for products made by different manufacturers because of the inherent variability in conducting the assay and species differences in sensitivity to the various toxins. This poses problems in product use and has potential safety consequences which are magnified as new products enter the market. Dramatic differences in the apparent potency confound clinical dose finding and could potentially result in over or under dosing of patients. Developing a technology that can resolve issues of standardization and address variability using a high-throughput system is the key to bettering the prospects of an *in vitro* cell-based BoNT assay.

Over the years, several new methods for detection of BoNT have been developed to overcome the limitations of the mouse bioassay. The majority of these alternative *in vitro* assays are immunological methods based on binding of an antibody to the toxin. Starting with radioimmunology assays, through passive hemagglutination and immunodiffusion assays, more recently the more sensitive Enzyme-Linked Immunosorbent Assays (ELISA) have been adapted for detection of BoNT. Using specific antibody binding to the toxin, ELISA has proved to be the most commonly employed method for *in vitro* detection of all serotypes of BoNT (Čapek and others 2010). The remarkable cleavage specificity of BoNTs has enabled the widespread development of activity assays. Alongside ELISA-based assays developed for detecting

BoNT proteolysis, several methods have been successfully used for separation of BoNT cleavage products from the substrates to assay for toxin activity (Hakami and others 2010). Higher throughput speed can be achieved by automation of the process steps but this comes at the cost of sensitivity (Čapek and others 2010). An assay which has significant benefits over ELISA is the fluorescent sandwich immunoassay that can be performed on beads with more complex and expensive flow cytometry instrumentation used to detect and quantify the toxin (Čapek and others 2010). Another variation is the highly-sensitive Immuno-PCR which is an ELISA-type immunoassay that uses PCR for exponential amplification of the ELISA signal (Sano and others 1992). Easier and simpler to use assays like the hand-held immunochromatographic assay work based on a capture antibody-analyte-detection antibody interaction. They generate simple visual read-outs but have reduced detection limits (Čapek and others 2010). Systems using cross-flow immunochromatographic method and ganglioside-liposomes as detection agent show improved sensitivity (Ahn-Yoon and others 2004). Though robust and sensitive, immunological *in vitro* assays are incapable of discriminating between the active and inactive forms of BoNT and hence cannot be used in assays meant for detection of active toxin forms in clinical preparations. Endopeptidase activity based assays, like the mouse assay, can detect only active toxin species. High-throughput fluorescence endopeptidase (Frisk and others 2009) or fluorescence resonance energy transfer (FRET) technology-based assays are used for the detection of cleavage of peptide bonds. Some of these assays also have high sensitivity (Čapek and others 2010). Immunology (Ekong and others 1997) and mass spectrometry (Boyer and others 2005) are also used for detection of SNARE cleavage products. However, the critical problem

with enzymatic assays is that they are not very robust. In complex milieus, interference can lead to reduced sensitivity necessitating the need to immunoseparate the toxin. In the last decade, microchip technology has been widely adopted in assays for BoNT for relative advantages like reduced reagent consumption and semi-automated nature of operation, among others.

The few cell based BoNT assays like the fluorescent read-out assays (Thyagarajan and others 2009) or the assays based on changes in action potentials in neurons exposed to toxin (Scarlatos and others 2008), can be especially valuable as diagnostics, as they can recapitulate the natural environment in which analytes like BoNT cleave SNARE proteins to inhibit neurotransmitter secretion. However, these are usually less sensitive and require days to be executed due to time taken for cell culture and detection.

5.2 Introduction of Botulinum neurotoxin Light Chain /E (BoNT LC/E) into chromaffin cells

Currently there is no BoNT assay that is high-throughput, sensitive, easy-to-use as well as capable of differentiating the active toxin species from the inactive one. Our system offers a unique solution as it combines high-throughput with detection of active toxin. Although at present the assay is not very sensitive, there is the potential to make it more sensitive in the future, and overall, it provides for a robust platform to assay the effects of BoNT on cellular neurotransmitter secretion. The chip device boasts of an uncomplicated design capable of performing the basic tasks of cell targeting/handling and recording with ease. On the microchip platform, instead of manipulating an electrode precisely to touch the cell, the cell is targeted to individual working electrodes. The

simplicity of the design also ensures that the cell is not subjected to any other mechanical stimuli (like movement or flow as in a microfluidic channel), which might give us spurious results. The most conspicuous advantage of the system is that once the toxin is introduced into the cell, the native environment is provided for the protein to target and cleave the SNARE complex on the cell membrane, which has the potential to make the assay more sensitive than an *in vitro* assay. Our cell of choice is the chromaffin cell because they exhibit robust neurotransmitter secretion and are readily available. Our lab-on-chip device allows simultaneous targeting of dozens of cells on one device at any given time. Using specialized surface chemistry modifications, up to 70% cell targeting to individual electrodes can be achieved (Liu and others 2011). Each cell measurement typically only takes 2-5 min. Multi-channel amplifiers, being built and tested in our lab, can help in recording from multiple cells at once thus increasing the throughput.

The novel aspect of this approach is the use of the same on-chip microelectrode on which the chromaffin cell is permeabilized to record the resulting exocytosis response from. The working electrode records picoamp (pA) level currents from the oxidation of catecholamines as they are released from individual granules.

BoNTs are synthesized and released by the Clostridia as inactive ~150 kDa protein precursors. Activation requires proteolytic cleavage that generates disulfide-linked di-chain toxins made up of the ~100 kDa heavy chain which is involved in the translocation of the 50 kDa light chain (Singh 2000; Cai and others 2007). Utilization of the holotoxin in experiments is constrained due to its intrinsic toxicity and the need to activate the holotoxin, which can cause an error in the analysis of catalytic activity. These difficulties can be overcome by generating recombinant, catalytically active but

inherently non-toxic light chain proteins that allow more detailed structure–function studies of BoNT (Baldwin and others 2004). The crystal structures of BoNT/A (Lacy and others 1998), BoNT/B (Swaminathan and others 2000), and BoNT/E (Kumaran and others 2009), along with all BoNT (Hanson and others 2000; Agarwal and others 2004; Segelke and others 2004; Agarwal and others 2005; Arndt and others 2005; Arndt and others 2006) and TeNT light chains (Breidenbach and others 2005), have been determined. Overall, the LC structures are similar and provide a basis for comparative functional studies (Fu and others 2006). The rationale behind using BoNT LC/E as the model toxin to study effects on exocytosis is that LC/E induces a more thorough inhibition of neurotransmitter secretion since it dissociates SNAP-25 from syntaxin by cleaving a larger amino acid fragment of SNAP-25 i.e., BoNT LC/E has the specific advantage *in vitro* of completely abrogating vesicle fusion. In comparison, BoNT/A cleaves a shorter fragment, only partially blocking vesicle fusion, and SNAP-25 retains its interaction with plasma membrane syntaxin.

BoNTs specifically bind to peripheral nerve endings at the neuromuscular junction via the 50 kDa C-terminal half of the 100 kDa HC (the HC-fragment). Neuronal cell membranes consist of binding sites that are particularly composed of complex polysialogangliosides, glycosphingolipids, etc. When BoNT is externally administered to chromaffin cells, however, very little inhibition of neurotransmitter release occurs because chromaffin cells contain only small amounts of gangliosides and the neurotoxin or its light chain subunit must gain direct access to the interior of the chromaffin cell in order to inhibit secretion. Preincubation of intact chromaffin cells with gangliosides leads to incorporation of the glycolipids into the cell membrane, thereby facilitating entry of

the toxin (Marxen and others 1991). BoNTs are known to bind mainly to gangliosides of type GT1b (Kitamura and others 1980) and GD1a (Habermann and others 1985).

Primary chromaffin cells used in our experiments are isolated from bovine adrenal glands (Yang and others 2007). As mentioned earlier, these cells are candidates for assaying effects of BoNT for two principal reasons. First, they exhibit healthy secretion of catecholamines and are, in fact, the most widely used cell type for electrochemical studies of quantal exocytosis. They have large dense granules that enable biophysical studies of vesicles and individual fusion kinetics. Classical methods like carbon fiber amperometry have shown how these cells can be adopted as good model systems for studying the process of exocytosis. The other important aspect is that all BoNT serotypes can affect and cause widespread inhibition of neurotransmitter secretion from these specialized cells (Penner and others 1986). However, the downside is that chromaffin cells do not have the necessary cell membrane receptors to aid in uptake of BoNT (Marxen and others 1989). We plan to render cells permeable to the toxin by using i) electropermeabilization and ii) permeabilization using the well-known detergent digitonin.

5.3 Introduction of BoNT via electropermeabilization on-chip

As described in chapter 4, the same planar electrochemical microelectrode was used to stimulate the cell and record amperometric spikes that result from oxidation of released transmitter. Individual or trains of voltage pulses from the holding potential used for amperometry (~0.6 V) to test potentials of 6 V were found to trigger massive quantal release from single chromaffin cells. Since massive release indicates thorough poration of

cell membrane, a train of seven pulses to +6 V was used as the standard electropermeabilization protocol. Fig 5.3 below gives us a schematic representation of our single-cell electropermeabilization approach used to introduce BoNT into chromaffin cells on-chip. A single chromaffin cell sitting on a working electrode in a BoNT buffer solution containing BoNT LC/E is electropermeabilized by application of a voltage stimulus to the underlying electrode. Permeabilization of the plasma membrane leads to entry of BoNT LC/E from the bath solution. SNAP-25 is cleaved and when a second stimulating pulse is applied, inhibition of exocytosis can be observed from the drop in spike frequency.

Figs 5.4 and 5.5 provide sample responses to introduction of the BoNT LC/E neurotoxin via electroporation of the cell membrane using a train of seven pulses to +6 V, 0.1 ms in duration. Amperometric recordings in Figs 5.4(a) and 5.5(a) are from single representative cells during introduction of the toxin. Since electropermeabilization is partial we need to allow the electroporated cell to sit in the BoNT solution for a few minutes. This allows time for diffusion of the BoNT LC/E toxin inside the cell from the external solution. Hence appreciable deactivation of the exocytotic machinery can be expected. The initial neurotransmitter release reflects none to very low inhibition.

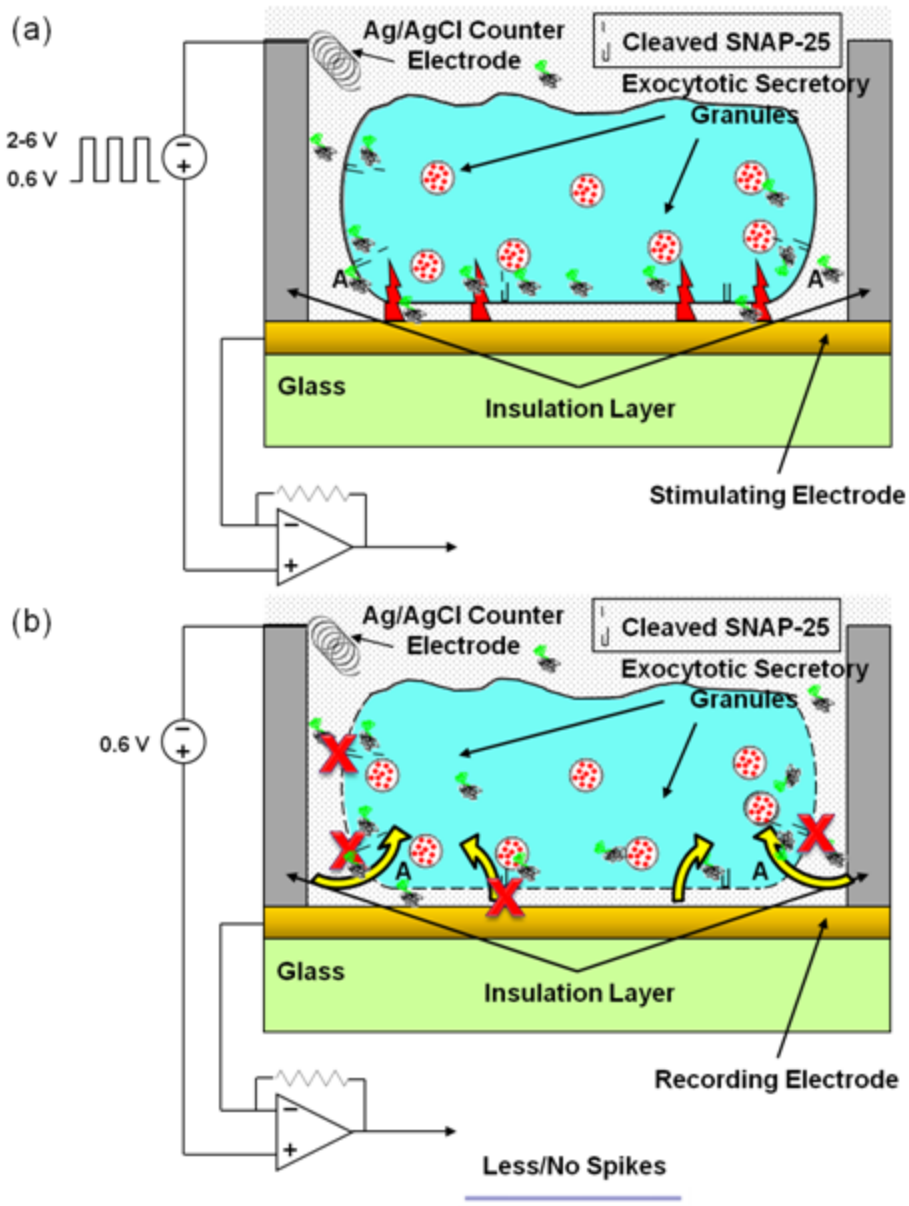

Fig 5.3 Schematic of single-cell electropermeabilization to introduce BoNT on-chip approach. First, a single chromaffin cell sitting on a working electrode in a BoNT buffer solution containing BoNT LC/E is electropermeabilized using voltage stimulation to the underlying electrode. The electropermeabilized cell allows entry of BoNT LC/E (similar to Fig 4.1). (a) Introduced BoNT LC/E cleaves SNAP-25 in the cell and when a second stimulating pulse is applied, (b) zero to few amperometric spikes are recorded from the cell showing that exocytosis has been inhibited

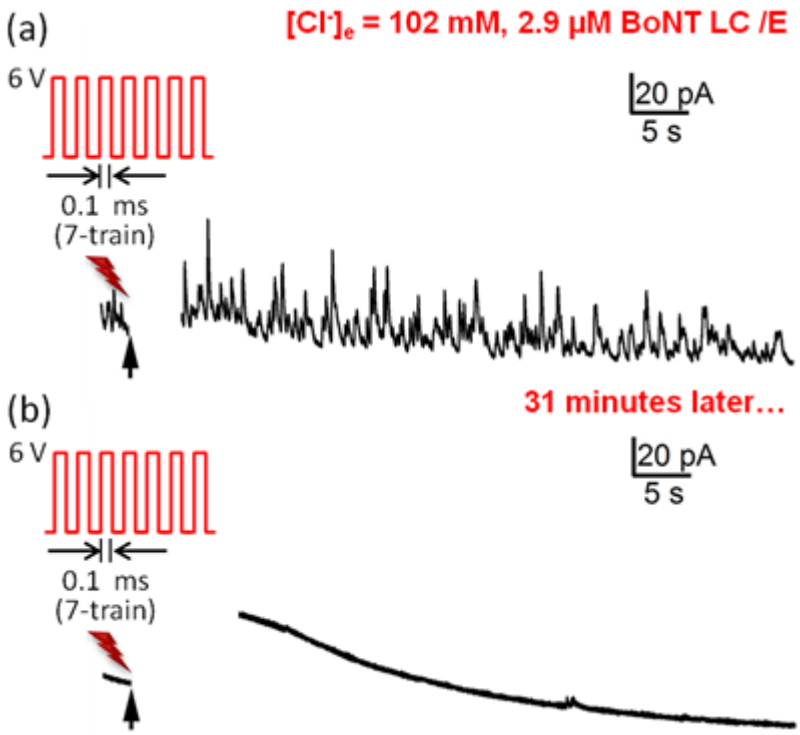

Fig 5.4 Introduction of BoNT LC/E in chromaffin cells via electropermeabilization and its effect on quantal exocytosis. (a) A high spike frequency is observed immediately after electropermeabilization in a solution containing 102 mM Cl^- and 2.9 µM BoNT LC/E. (b) A drop in frequency is noted on 2nd electropermeabilization after 31 minutes

Figs 5.4(b) and 5.5(b) show representative spikes from the respective cells after waiting periods of 31 and 23 minutes, respectively. While Fig 5.4(b) shows an appreciable drop in spike frequency, Fig 5.5(b) shows no change from before and after introduction of the toxin. Both occurrences were seen frequently in electropermeabilized chromaffin cells and data was pooled from 11 cells to study the inhibitory effect of BoNT LC/E. 8 cells showed a decrease in number of spikes from 200+ to <50 in 1 min recordings, whereas 3 cells showed a consistent secretion of ~100+ spikes (in 1 min) from before and after introduction of the toxin.

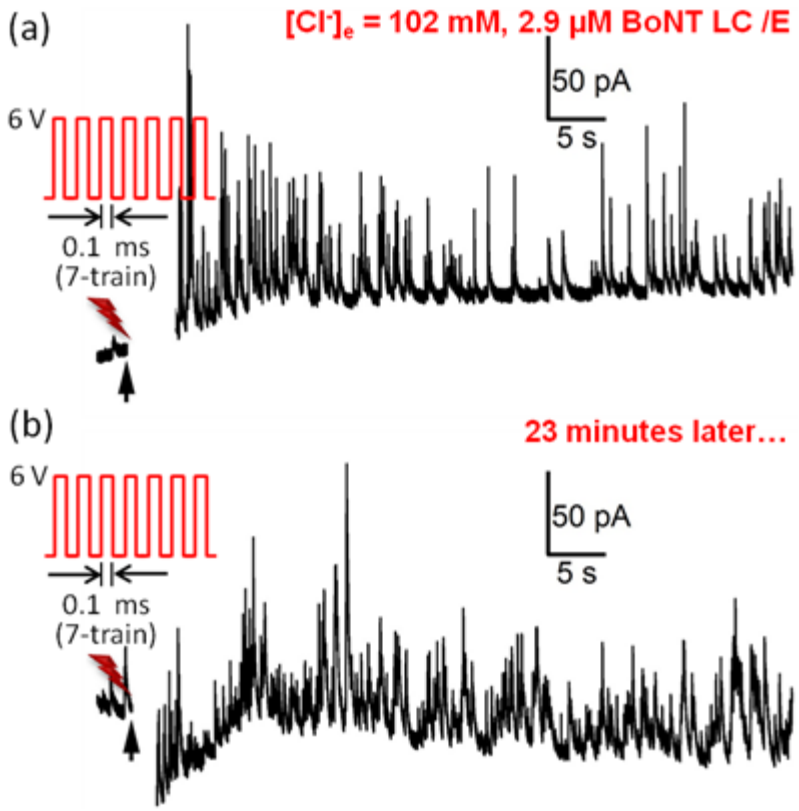

Fig 5.5 Introduction of BoNT LC/E in chromaffin cells via electropermeabilization and its effect on quantal exocytosis (contd.). (a) A high spike frequency is observed immediately after electropermeabilization in a solution containing 102 mM Cl^- and 2.9 µM BoNT LC/E. (b) However, unlike in the previous example, no drop in spike frequency is noted on 2nd electropermeabilization step after 23 minutes

It can be noted here that initially the waiting time between the first and the second electropermeabilizing pulses was kept to 5-10 minutes. However, no appreciable decrease in spike frequency was noted. Hoping to have better diffusion of the toxin inside the electropermeabilized cells, the waiting time was increased to 20-30 minutes.

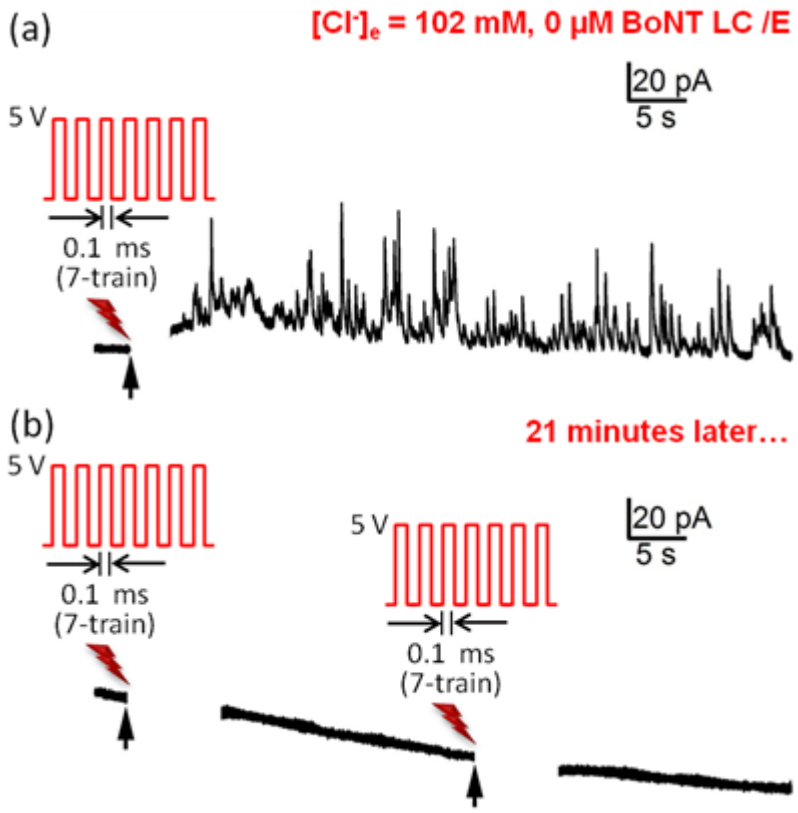

Fig 5.6 Control experiment to show that rundown due to prolonged exocytosis can occur in electropermeabilized chromaffin cells. (a) A high spike frequency is observed following electropermeabilization in a solution containing 102 mM Cl^- and 0 µM BoNT LC/E. (b) Although, there is a no toxin in the bath solution, a significant drop in spike frequency is noted on 2nd electropermeabilization after 21 min

Control experiments were performed to verify that the decrease in spike frequency in cells could primarily be attributed to the inhibitory action of the toxin on the neurotransmitter secretion machinery, and not just rundown due to the waiting period and prolonged exocytosis. These experiments consisted of electropermeabilizing cells in the absence of BoNT LC/E. Representative cells (3) showed an average decrease in exocytotic frequency from 200+ to <50 in 1 min recordings (Fig 5.6) as opposed to 2 that showed a consistent secretion of ~100+ spikes (in 1 min) from the first

electropermeabilization step to the second, proving that rundown may occur in cells over a period of time. In order to attempt to reduce rundown, cells were electroporated using milder voltage pulse protocols. Instead of the 6V/0.1 ms (7-train) pulses, 5V/0.1 ms (7-train) pulses were used since it has been shown previously that comparatively small voltage pulses lead to transient electroporation of chromaffin cells. However, representative experiments (4) showed that no appreciable change was observed in spike frequency in cells that were transiently electropermeabilized in the presence of BoNT LC/E toxin (data not shown).

Data obtained from experiments suggests that use of electropermeabilization to introduce BoNT LC/E into cells is not a robust method as reflected by absence of effective and reproducible inhibition of neurotransmitter secretion. Also, we hypothesize that electropermeabilization occurs on only a portion of the plasma membrane and hence, permeabilizing chromaffin cells more thoroughly could yield better results. Another important factor is that electropermeabilization-induced exocytosis is dependent on $[Cl^-]_e$. This Cl^--dependency paired with the absence of Ca^{2+} in the BoNT buffer solution might also affect BoNT-induced inhibition of quantal exocytosis in electropermeabilized chromaffin cells.

5.4 Introduction of BoNT via digitonin-induced permeabilization of cells

As we have seen previously, electropermeabilization can be used to render chromaffin cells permeable to exogenous molecules. Similarly, low concentrations of the detergent digitonin can be efficiently used for permeabilization and ions like Ca^{2+} as well as larger molecules like proteins can be introduced inside cells (Fiskum and others 1980).

Increase of permeability in plasma membrane of digitonin-treated chromaffin cells can elicit exocytosis and release catecholamines upon addition of micromolar Ca^{2+} to the extracellular solution (Dunn and others 1983). Electrochemical detection of exocytosis of individual chromaffin granules from digitonin-permeabilized cells has been done using carbon fiber electrodes (Jankowski and others 1992). Introduction of BoNT toxin inside chromaffin cells via digitonin-incubation or transfection has been shown to inhibit exocytosis and has been assayed using carbon fiber amperometry (Gil 1998; Graham and others 2000).

Chromaffin cells are digitonin-permeabilized in the presence of the 50 kDa BoNT light chains in order to allow the toxin to diffuse into the cell and cleave the SNARE proteins associated with secretory vesicle fusion thus causing inhibition of neurotransmitter secretion. The schematic of the process is similar to that in Fig 5.3, the only difference being that digitonin-permeabilization is used instead of electropermeabilization. To look for effects on exocytosis, 5-10 min after the permeabilized cells are exposed to the toxin in the presence of micromolar amounts of $[Ca^{2+}]_i$, the cells are amperometrically probed. A catalytic null mutant of the toxin (RYM) is used in control experiments in order to determine if only the active toxin can affect exocytosis in exposed cells. In humans, BoNTs have a median lethal dose (LD_{50}) of ~1-50 ng/kg (6.67 fM-0.33 nM) (Band and others 2010) of body weight. In whole-cell patch clamp experiments, ~400 nM of BoNT LC/E (Xu and others 1998) has been found to completely block exocytosis while in digitonin-permeabilized chromaffin cells, a maximal inhibition of 55% occurs at 310 nM neurotoxin (Bittner and others 1989). My

preliminary experiments were carried out using a solution containing 1–4 μM of BoNT LC/E.

Digitonin is a steroid glycoside which, used as a detergent, can effectively water-solubilize lipids. Hence it has found widespread use in permeabilizing cell membranes (Dunn and others 1983; TerBush and others 1988; Holz and others 1989; Tengholm and others 2000). In order to introduce BoNT via membrane poration, chromaffin cells are incubated in 8-20 μM digitonin mixed with a solution containing an active form of the light chain toxin and buffered micromolar Ca^{2+}.

Chromaffin cells are first assayed for efficiency of digitonin permeabilization. They are either exposed to 8-20 μM digitonin and 5-14.4 μM free Ca^{2+}-containing cell bath solution, or a pipette containing digitonin is brought close to the cell suspended in Ca^{2+}-containing external solution. The content of the pipette is perfused onto the cell by applying gentle pressure. Free Ca^{2+} diffuses into the cell through the permeabilized cell membrane and triggers quantal catecholamine release, which is detected by the underlying on-chip planar electrochemical microelectrode. 24 out of 36 cells exposed to 20 μM digitonin and 14.4 μM free Ca^{2+}-containing external solution showed robust exocytosis whereas 25 out of 28 cells that were exposed to 14.4 μM free Ca^{2+} only showed none to negligible neurotransmitter secretion. Representative traces of amperometric spikes from both experiments can be seen in Fig 5.7. From these preliminary results, we expect digitonin to permeabilize cells more thoroughly and irreversibly, and going forward, we have used this method in our experiments.

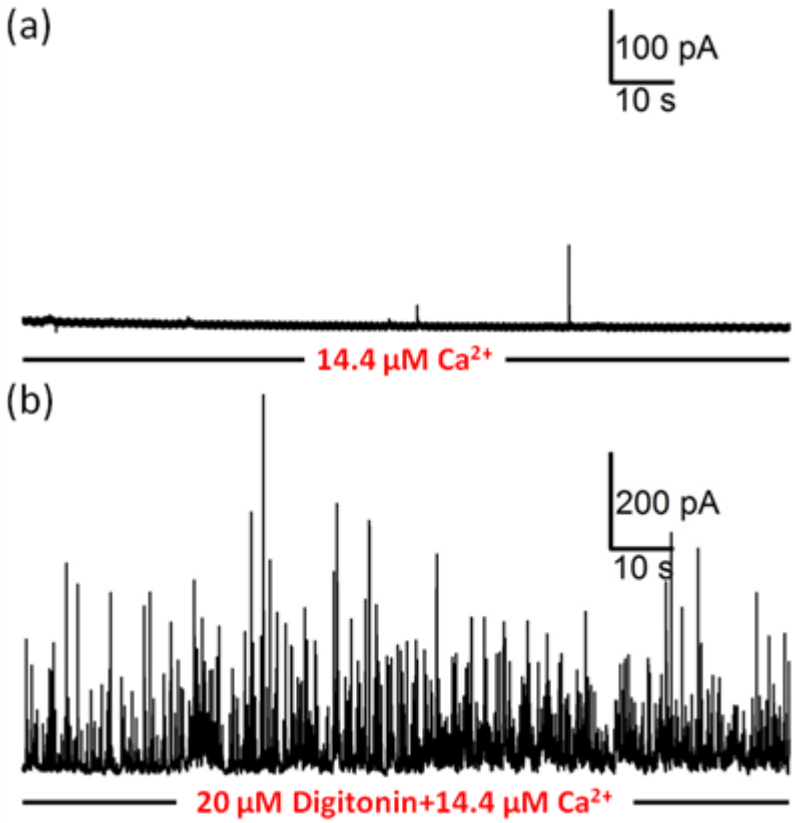

Fig 5.7 Robust quantal exocytosis in cell permeabilized by digitonin and bathed in 14.4 µM free Ca^{2+}. (a) Control cell shows few spikes when exposed to Ca^{2+} only. (b) Cell permeabilized by 20 µM digitonin shows robust exocytosis in the presence of free Ca^{2+}

Next, we employed trypan blue staining and on-chip amperometry to verify the permeabilizing ability of 10 µM digitonin on chromaffin cells. Cells are exposed to a bath solution containing 14.4 µM free Ca^{2+} and imaged using a light microscope. Exposing non-permeabilized chromaffin cells to Trypan blue shows low to minimum staining since intact cell membrane of viable cells is impermeable to the stain (data not shown).

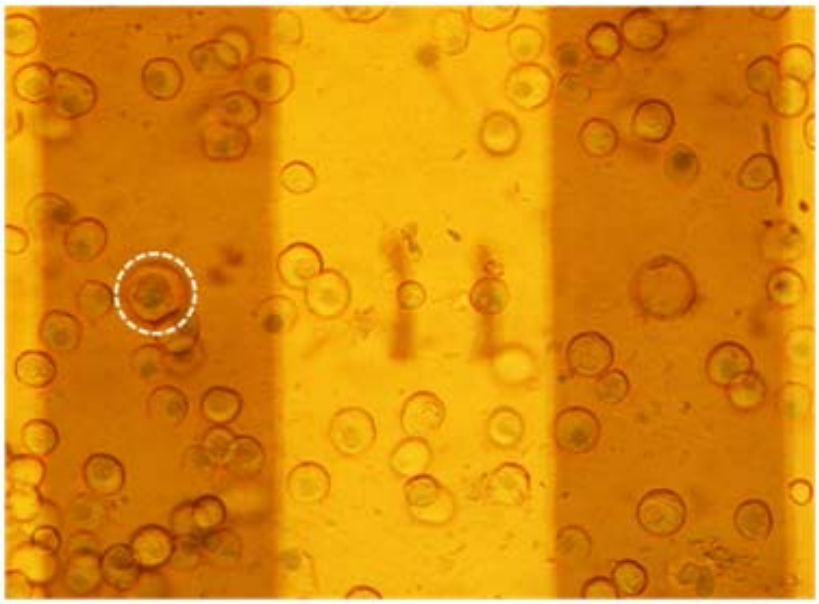

Fig 5.8 Uptake of the cell-impermeant dye Trypan blue demonstrates that digitonin induces efficient permeabilization of cells. Photomicrograph with permeabilized chromaffin cells sitting in a standard bath solution stained by trypan blue. The cell encircled in white is sitting on a working Au electrode.

In the first step, digitonin containing bath solution was added to cells on the chip. After letting the cells incubate in digitonin for a few min, Trypan blue solution was added. The cells were allowed to sit for a few more min before they were photographed. Cells are stained blue due to entrance of the dye inside the cell through the permeabilized cell membrane where it accumulates in the nucleus giving it a blue color. Fig 5.8 depicts chromaffin cells on-chip with one cell sitting directly over the electrode (white dashed circle). After a brief exposure of permeabilized cells to a trypan blue solution, ~100% of cells picked up the dye indicating that digitonin can uniformly and thoroughly permeabilize a population of chromaffin cells.

Once the permeabilization protocol was in place, light chain BoNT/E toxin in buffer was used in the external solution in order to assay its effect on exocytosis. In the first set of experiments some permeabilized cells are exposed to the toxin while others from the same batch are assayed in a toxin-free solution. After loading on the device, chromaffin cells are suspended in 1.5 μM BoNT LC/E in 10 μM digitonin-containing BoNT buffer solution and ~7.2 μM free Ca^{2+}-containing external solution. 8 cells were analyzed to obtain a total of 605 spikes giving an average secretion rate ± standard deviation of 0.63 ± 0.12 events/sec. Example traces are shown in Fig 5.9 (a) and (b). In contrast, data obtained from 6 cells assayed in ~13.9 μM free Ca^{2+}-containing external solution mixed with 10 μM digitonin showed that 1505 spikes were recorded making it at an average rate ± standard deviation of 2.07 ± 0.66 events/sec (sample traces shows in Fig 5.9 (c) and (d)). Digitonin-permeabilized cells exposed to the light chain of BoNT/E showed a 69.56% inhibition in the rate of secretion (not taking into account the increase in free Ca^{2+}-concentration from the cells exposed to the toxin to the control cells).

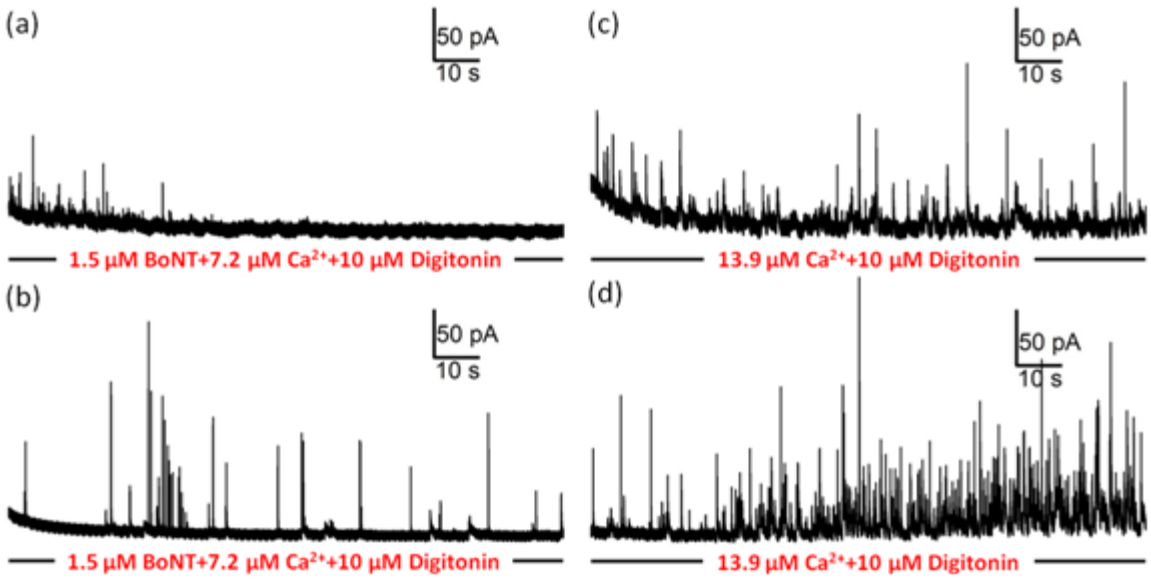

Fig 5.9 Appreciable amount of inhibition in exocytosis is seen in digitonin-permeabilized cells when they are exposed to 1.5 µM BoNT LC/E whereas digitonin-permeabilized cells in control experiments exposed to a buffered Ca^{2+} solution show vigorous exocytosis. (a) Representative trace showing how the frequency of amperometric spikes falls to zero on exposure to 1.5 µM toxin along with 10 µM digitonin and 7.2 µM Ca^{2+}. (b) A second representative trace showing consistent low spike frequency in a digitonin-permeabilized cell in a similar solution. (c) Representative trace showing uniform frequency of amperometric spikes in a control cell in 10 µM digitonin and 13.9 µM Ca^{2+}. (d) A second representative trace showing a gradual increase in spike frequency in a digitonin-permeabilized cell in the presence of 13.9 µM buffered Ca^{2+}

As a control we used an inactive form of the BoNT LC/E protein (RYM). The first set of experiments compared the responses from permeabilized cells exposed to either the RYM mutant or controls unexposed to protein. 13 cells assayed in 7.8-13 µM RYM LC/E in 8-20 µM digitonin-containing BoNT buffer solution together with ~14.4 µM free Ca^{2+}-containing external solution were analyzed to obtain a total of 1727 spikes

giving an average secretion rate of ± standard deviation of 1.11 ± 0.38 events/sec (sample traces shown in Fig 5.10 (a) and (b)).

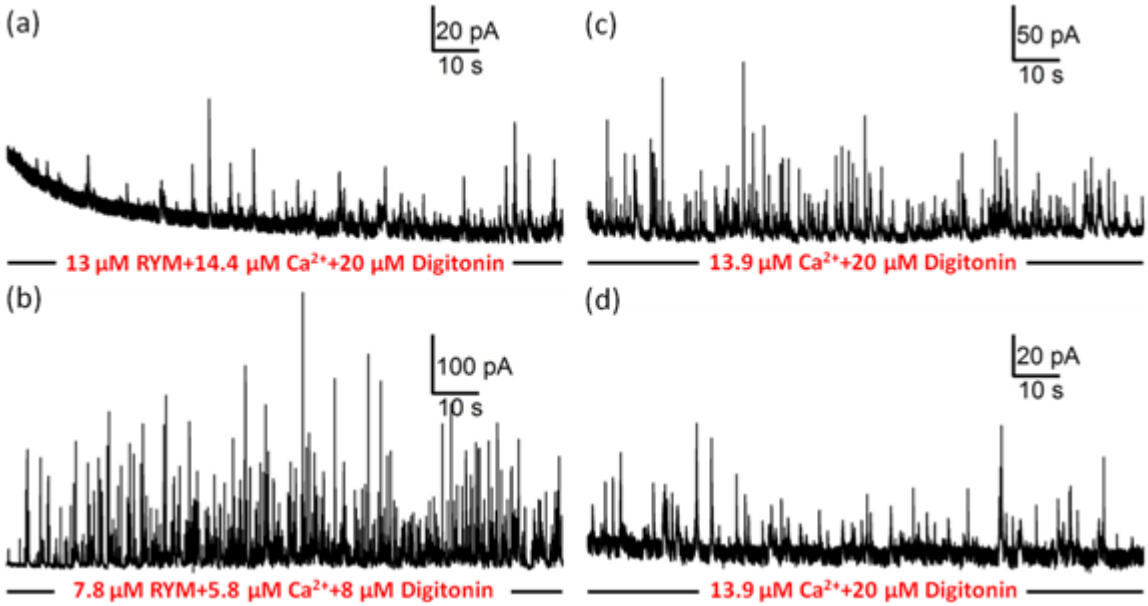

Fig 5.10 No appreciable inhibition in exocytosis is seen in digitonin-permeabilized cells when they are exposed to ~7.8-13 µM RYM. This is comparable to control experiments with digitonin-permeabilized cells exposed to buffered Ca^{2+}. (a) Representative trace showing 13 µM of the null toxin (RYM) in the presence of 20 µM Digitonin and 14.4 µM Ca^{2+} does not affect the frequency of amperometric spikes. (b) A second representative trace showing consistent high spike frequency in a 8 µM digitonin-permeabilized cell in the presence of 7.8 µM RYM and 5.8 µM Ca^{2+} in the bath. (c) Representative trace showing uniform high frequency of amperometric spikes in a target cell bathed in 20 µM Digitonin and 13.9 µM Ca^{2+} only (d) A second representative trace showing a lower but consistent spike frequency in a digitonin-permeabilized cell in a similar solution as in (c)

On the other hand, another 13 cells from the same batch assayed in ~5.76-13.9 µM free Ca^{2+}-containing external solution mixed with 8-20 µM digitonin were analyzed

to obtain a total of 1398 spikes giving an average secretion rate ± standard deviation of 0.9 ± 0.21 events/sec (representative traces shown in Fig 5.10 (c) and (d)). Therefore, not taking into account the variation in Ca^{2+}-concentration in the bath solution, the experiments showed that the RYM mutant does not have an effect on exocytosis.

The principle control experiment is done to compare the secretion rates of cells exposed to the light chain BoNT/E toxin versus the RYM inactive mutant. On being exposed to a solution with a mixture of the 1.6 μM RYM protein, 10 μM digitonin and 14.4 μM free Ca^{2+}, 1159 events were recorded from 8 cells (representative traces shown in Figs 5.11 (a) and (b)). 8 others cells from the same batch, when exposed to 1.5 μM BoNT LC/E along with 10 μM digitonin and 14.4 μM free Ca^{2+}, showed a drop in secretion such that a total of 773 events were manually counted (sample traces shown in Figs 5.11 (c) and (d)). The average rate ± standard deviation from the null protein and the BoNT were calculated to be 1.2 ± 0.12 and 0.8 ± 0.12 events/sec, respectively. Thus the active BoNT LC/E resulted in a 33% decrease in the rate of exocytosis compared to the RYM mutant. Table 2 below lists all the different combinations of solutions that were used to determine the effect of the active BoNT LC/E toxin on exocytosis as opposed to a control which is either toxin-free (digitonin and Ca^{2+} only) or contains an inactive form of the toxin (RYM). The results suggest that the digitonin-permeabilization method can be used to assay the effect of BoNT LC/E on the exocytotic machinery of chromaffin cells. T-tests were performed on all three data sets. For the BoNT LC/E vs. BoNT LC/E Null (RYM), our t-test showed a difference in the rate of neurotransmitter secretion in the presence of the toxin when compared to the rate of neurotransmitter secretion in the presence of the inactive form of the toxin ($P=0.035$ *i.e.* $P<0.05$).

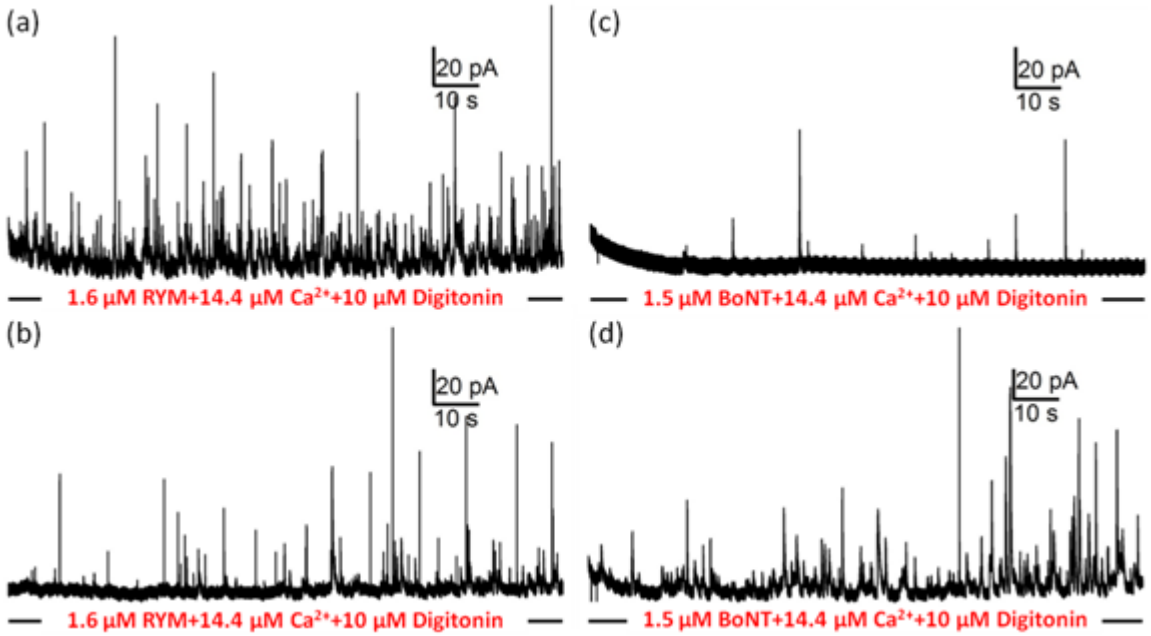

Fig 5.11 No appreciable inhibition in exocytosis is seen in digitonin-permeabilized cells when they are exposed to 1.6 µM RYM as opposed to cells that show inhibition when they are exposed to 1.5 µM BoNT LC/E. (a) Representative trace showing how the RYM doesn't affect the frequency of amperometric spikes. (b) A second representative trace showing consistent low spike frequency in a digitonin-permeabilized cell in the presence of 1.6 µM RYM, 10 µM Digitonin and 14.4 µM Ca^{2+} in the bath. (c) Representative trace showing how the frequency of amperometric spikes is very low after exposure to 1.5 µM BoNT LC/E, 10 µM Digitonin and 14.4 µM Ca^{2+}. (d) A second trace showing consistent low spike frequency in a digitonin-permeabilized cell in the presence of 1.5 µM BoNT LC/E in the bath

Table 2 Mean ± standard deviation of secretion rates observed in digitonin-permeabilized cells exposed to BoNT LC/E, its Null form RYM or a toxin-free bath solution. Also shown are the respective percentage changes in spike frequency in different sets of experiments. Data obtained from cells permeabilized on gold microelectrodes in solutions containing 5.76-14.4 μM Ca^{2+}.

	BoNT LC/E	**BoNT LC/E Null (RYM)**	**Toxin-free**
BoNT LC/E vs. Toxin-free			
# of Spikes	605 (# of cells = 8)		1505 (# of cells = 6)
Rate (spikes/sec)	0.63±0.12		2.07±0.66
Percentage Change = (2.07-0.63)/2.07 = 69.56%			
BoNT LC/E Null (RYM) vs. Toxin-free			
# of Spikes		1727 (# of cells = 13)	1398 (# of cells = 13)
Rate (spikes/sec)		1.11±0.38	0.90±0.21
Percentage Change = (0.90-1.11)/0.9 = -23.33%			
BoNT LC/E vs. BoNT LC/E Null (RYM)			
# of Spikes	773 (# of cells = 8)	1159 (# of cells = 8)	
Rate (spikes/sec)	0.80±0.12	1.20±0.12	
Percentage Change = (1.2-0.8)/1.2 = 33.33%			

5.5 Conclusion and discussion

We have already seen that electropermeabilization induced "quantal" catecholamine release is the result of formation of transient pores on the plasma membrane followed by diffusion of exogenous molecules inside the cell. Here we first tested the efficiency of electropermeabilization in introducing the light chain of BoNT/E

in single chromaffin cells. Due to various factors like the local nature of electropermeabilization and the plausible size and function of BoNT LC/Es as opposed to ions like Cl^-, it was found that this process was not a very efficient one. Another popular permeabilizing agent, digitonin was used to replace electropermeabilization in assaying BoNT LC/E. Cells were permeabilized in digitonin while being simultaneously exposed to micromolar amounts of the active or the null form of the toxin along with micromolar amount of Ca^{2+}. Results show that the rate of neurotransmitter secretion in the presence of BoNT LC/E when compared to the rate of neurotransmitter secretion in the presence of the inactive form i.e., BoNT LC/E Null (RYM), are statistically different ($P<0.05$).

Like other cell-based assays, our single-cell assay based on high-throughput electrochemical detection of quantal exocytosis is valuable as diagnostics since it provides a natural environment in which light chains of BoNT can cleave SNARE proteins to inhibit neurotransmitter secretion. However, though the method seems to be a robust one, it is currently not highly sensitive and takes 1-3 days to complete taking into account time taken for cell culture, detection on-chip and analysis of results. It can be noted that in this approach, specifically timing a stimulus is not of utmost importance and there is no requirement to porate the cells transiently in order to keep them viable over a long period of time. In fact, using multi-channel amplifiers developed by Exocytronics LLC can greatly increase the throughput of our assay. Also, since the new amplifier and headstage designed by Exocytronics comes with the option of simultaneously using 240 electrodes per chip via a multiplexing approach, a larger number of cells from the same batch can be simultaneously assayed on the same device under different experimental conditions.

CHAPTER 6

CONCLUSIONS AND FUTURE DIRECTIONS

6.1 Conclusions

The theme of this study is the development and application of electrical methods to stimulate and subsequently record quantal exocytosis from single chromaffin cells on microfabricated chips.

Some of the most widely prevalent techniques that are used to stimulate exocytosis in chromaffin cells on chips are perfusion methods that stimulate the whole population of cells on a chip. Cells are perfused with a secratogogue, leading to depolarization of the cell membrane. Prime examples are depolarization by a high K^+-solution, or application of extracellular Ba^{2+}, or the Ca^{2+} ionophore ionomycin. However, given our chip design, a perfusion system not only stimulates multiple cells but also does not allow precise timing of the stimulus. Photorelease of caged Ca^{2+} can be used to address individual chromaffin cells and stimulate them precisely, but this requires an elaborate optical setup. Electrical stimulation can elicit action potentials in excitable cells and a train of action potentials can lead to stimulation of exocytosis. So we started this project by using our microchip planar electrochemical microelectrodes to elicit action potentials in single chromaffin cells. Action potentials were elicited in an all-or-none fashion. However, on repeated stimulation, permeabilization of the membrane occurred. Since permeabilization methods have been shown to be effective ways to induce quantal neurotransmitter release from chromaffin cells, we turned our attention to optimizing this approach.

Cells could be electropermeabilized on-chip and following a voltage pulse, the electrochemical electrode was found to recover within several seconds and remain sensitive enough to record amperometric spikes of pA level currents and other typical features. Cyclic voltammograms with ferricyanide solution demonstrated that short voltage pulses of up to 10 V for 0.2 ms duration did not degrade the thin electrochemical electrodes and the same chip and same electrode could be reused for multiple recordings. Several combinations of amplitude and duration of voltage pulses were tested and a range of stimuli was found to elicit electropermeabilization and quantal release. Whereas steps to lower potentials led to transient release, larger voltage steps or pulse trains led to release lasting for longer periods. Individual cells on microelectrodes were also stained using membrane-impermeant dyes like trypan blue and propidium iodide to show that voltage pulses can electropermeabilize cells and still leave them physiologically intact for neurotransmitter secretion.

A surprising finding from these experiments was that robust exocytosis could be elicited with voltage pulses applied to cells bathed in "Ca^{2+}-free" solution. Ca^{2+}-free solutions, however, do not support substantial exocytosis when chromaffin cells are permeabilized or depolarized using other methods. Whereas extracellular Ca^{2+} is not essential, mM concentrations of Cl^- was found to be necessary to support robust quantal transmitter release in response to our electropermeabilization protocol. Bracketed experiments demonstrated that not only is Cl- important for electropermeabilization-induced exocytosis, but also there is a steep dependency of the rate of transmitter release on Cl^- between 2 and 32 mM. Neither did I see any evidence that Ca^{2+} modulated the rate of release nor evidence of release of Ca^{2+} from internal stores upon electroporation.

Further studies are needed to clarify the role of Cl^- and to determine if ClC Cl^- channels in vesicles contribute to electroporation-induced exocytosis.

Botulinum neurotoxins are potent metalloendoproteases capable of impairing transmitter release via targeting and cleaving of various SNARE proteins at specific sites and their extreme toxicity makes it necessary for the toxin to be detected in a given sample with high sensitivity and selectivity. The mouse intraperitoneal assay remains the gold standard but it is important to develop cell-based assays of BoNT that can replace the mouse lethality assay in detecting active toxin in a sample. Once electropermeabilization was established to be an effective method in stimulating exocytosis in single cells on-chip, we used our platform to develop an *in vitro* cell-based high-throughput assay to quantify BoNT. Cells were electropermeabilized in the presence of the light chain of BoNT/E. After electropermeabilization of the cells in the presence of the LC/E, cells were allowed to sit in the solution for a few minutes and amperometric spikes were recorded before and after introduction of the toxin to assay its effect. We hypothesized that our electroporation method leads to local electroporation of the cell membrane and we documented negligible difference in spike frequency upon electropermeabilization with BoNT LC/E in the external bath. The extent of cell-electroporation depends on various factors including cell-size, proximity of the cell surface to its underlying electrode, extent of cell adhesion to the electrode, etc. Due to these varied conditions, it became difficult to predict with precision the length of time that would be sufficient for the toxin to diffuse inside the cell as well as the extent of perfusion of the toxin inside the cell after electropermeabilization. Hence we increased

the waiting time between the electroporation and amperometry steps. This however led to the complication of run-down of exocytosis even in cells not exposed to the toxin.

Next we chose to use a detergent called digitonin to permeabilize cells on our device following previous studies. The permeabilization of the plasma membrane was validated by studying the uptake of the membrane-impermeant stain Trypan blue. Paired experiments were performed comparing the amount of exocytosis observed when incubating cells in either BoNT LC/E or an inactive BoNT LC/E mutant at a concentration of ~1.5 μM in the presence of digitonin and buffered Ca^{2+}. Although the BoNT null mutant experiments didn't show any dramatic decrease in spike frequency, some amount of inhibition of exocytosis was seen in digitonin-permeabilized cells exposed to the light chain /E. The percentage decrease was statistically significant *($P<0.05$)* and the platform seems to hold potential in detecting the presence of μM amount of BoNT LC/E in a given sample.

6.2 Discussion and possible future directions

6.2.1 Electropermeabilization-induced Cl^--dependent exocytosis

Exocytosis triggered by electropermeabilization of single chromaffin cells needs to be explored further in order to determine the mechanisms whereby it triggers release. It would be useful to carry out further studies using fluorescent Ca^{2+} indicators to more carefully examine possible release of Ca^{2+} from internal stores or to track exocytosis from fluorescently labeled vesicles. However, the Au electrodes used in our device are almost opaque and not suitable for fluorescent studies. Popular electrode materials including ITO, which is highly transparent, and DLC:N on ITO, which is comparatively

more translucent, can be tested for electropermeabilization efficiency using our protocols. However, in preliminary experiments I was not able to reliably induce exocytosis by applying voltage pulses to electrodes fabricated from ITO. But a set of successful amperometric recordings were made on DLC:N on ITO chips (data not shown). Future experiments testing different pulse protocols may give us more definitive results on both materials.

In electropermeabilization-induced Cl^--triggered exocytosis, the $[Cl^-]_e$-dependency of transmitter release seems to be independent of the electroporation step since manipulation of $[Cl^-]_e$ after electroporation can modulate the rate of ongoing transmitter release in a reversible manner. Ca^{2+} is observed to play little role in triggering or modulating quantal transmitter release when electropermeabilization is induced under our experimental conditions. The anion selective channel Cl_{250} was rarely observed in chromaffin granules and its activity could be observed only in the presence of calcium in the medium (Hordejuk and others 2006). The hypothesis that the dependence of vesicle release on Cl^- may be mediated by ClC Cl^- channels on the vesicle membrane (Maritzen and others 2008) can be tested by carrying out electropermeabilization-induced amperometric recordings from chromaffin cells isolated from ClC-3 knock-out mice. Capacitance measurements and amperometry showed that exocytosis of large dense-core vesicles (LDCVs) was decreased in chromaffin cells from ClC-3 knock-out mice. However, immunohistochemistry complemented with subcellular fractionation showed that ClC-3 is not detectable on LDCVs of endocrine cells and are localized to endosomes and synaptic-like microvesicles. Thus, it is thought that ClC-3 channels, though not found on large dense-core vesicles involved with exocytosis in chromaffin cells, indirectly

influence LDCV exocytosis possibly by affecting an intracellular trafficking step (Maritzen and others 2008). Known Cl^- channel blockers like 5-nitro-2-(3-phenylpropylamino)-benzoic acid (NPPB) (Pothos and others 2002) can also be used to test the hypothesis that Cl^- channels are involved in Cl^--dependent exocytosis upon electroporation. Another approach is to test which anions (e.g., I^-, F^-, SO_4^{2-}) can substitute for Cl^- in supporting exocytosis and compare this selectivity with the known permeation sequence of Cl^- channels.

Another generic application of single-cell electropermeabilization and subsequent electrical or fluorescent measurement on-chip could be in the vast field of transfection. Electroporating single cells on top of electrodes with reproducible geometry, as opposed to electropermeabilizing a population of cells in a cuvette, may induce less cell damage and be more consistent between cells. It would also require less preparation than developing viral transduction vectors. The efficiency of this proposed application could be tested by using our platform to electrotransfect chromaffin cells with a fluorescent protein like GFP and comparing it to other existing techniques like the Semliki Forest virus (SFV) gene expression system (Ashery and others 1999) or electroporation in a cuvette.

6.2.2 Cell-based assay for detection of BoNT

Our cell-based assay for the detection of Botulinum neurotoxin, while being robust and capable of high-throughput, needs considerable optimization in order to detect lower concentrations of the toxin for it to have a similar performance as the mouse bioassay. It is possible that sensitivity is lost upon loss of soluble cell components during

permeabilization with digitonin. Ideally, permeabilization would not be necessary to test the holotoxin, but chromaffin cells do not effectively take up the toxin presumably because they do not have the ganglioside receptors for the HC. A possible approach would be to engineer a cell to serve as a sensitive biosensing element to interface with our electrochemical electrode arrays. The ideal cell would have the receptor gangliosides found in motor neurons but would secrete catecholamines so that exocytosis could be readily detected with an electrochemical electrode.

Another improvement to increase throughput would be to use multichannel amplifiers, such as those being developed by Exocytronics LLC, in order to record from multiple cells simultaneously.

Using both electropermeabilization and digitonin-permeabilization in conjunction with amperometric recording from multiple cells on our biochip, a broad spectrum of high-throughput single-cell experiments can be conducted. For example, we can test drugs that target exocytosis such as reserpine, a vesicular monoamine transport blocker that decreases quantal size, or l-dopa, a catecholamine precursor that increases quantal size, to different cell lines or primary cells in order to do massive screenings of their effect on neurotransmitter release. This can help elucidate the basic mechanism of cell-to-cell communication and potentially benefit health-related research.

Solution exchange on our chips during permeabilization experiments is an important aspect and manual exchange of solutions using pipetters can be clumsy and potentially dislodge cells from their electrode wells. To achieve easier solution exchange and perfusion, microfluidic channels could be integrated into the microdevice. Using

microfluidics for solution exchange could make the process gentler, easier and faster thereby increasing the throughput of our experiments.

Another aspect of electropermeabilization or digitonin-permeabilization of cells on our multielectrode array device is that cell debris can easily foul the electrode, decrease its sensitivity, and prevent further reuse of the fabricated device – especially since the electrodes are cell-sized, they are more difficult to clean. We propose the use of Tergazyme (Alconox, NY USA), an enzyme-activated powdered detergent for laboratory, healthcare and industrial applications. Its protease enzyme removes proteinaceous soils, tissue, blood and body fluids (Alconox), and devices can either be soaked or ultrasonicated in the solution for proper cleaning.

REFERENCES

Agarwal, R., T. Binz, et al. (2005). "Structural analysis of botulinum neurotoxin serotype F light chain: Implications on substrate binding and inhibitor design." Biochemistry **44**(35): 11758-11765.

Agarwal, R., S. Eswaramoorthy, et al. (2004). "Structural analysis of botulinum neurotoxin type E catalytic domain and its mutant Glu212→Gln reveals the pivotal role of the Glu212 carboxylate in the catalytic pathway." Biochemistry **43**(21): 6637-6644.

Ahn-Yoon, S., T. R. Decory, et al. (2004). "Ganglioside-liposome immunoassay for the detection of botulinum toxin." Analytical and Bioanalytical Chemistry **378**(1): 68-75.

Albillos, A., G. Dernick, et al. (1997). "The exocytotic event in chromaffin cells revealed by patch amperometry." Nature **389**(6650): 509-512.

Alconox. "Tergazyme." from http://www.alconox.com/downloads/pdf/techbull_tergazyme.pdf.

Alvarez De Toledo, G. (1995). "Exocytotic fusion and release in dense core secretory granules." Methods and Findings in Experimental and Clinical Pharmacology **17**(SUPPL. A): 9-10.

Amatore, C., S. Arbault, et al. (2006). "Coupling of electrochemistry and fluorescence microscopy at indium tin oxide microelectrodes for the analysis of single exocytotic events." Angew Chem Int Ed Engl **45**(24): 4000-4003.

Amatore, C., S. Arbault, et al. (2008). "Electrochemical monitoring of single cell secretion: Vesicular exocytosis and oxidative stress." Chemical Reviews **108**(7): 2585-2621.

Arndt, J. W., Q. Chai, et al. (2006). "Structure of botulinum neurotoxin type D light chain at 1.65 Å resolution: Repercussions for VAMP-2 substrate specificity." Biochemistry **45**(10): 3255-3262.

Arndt, J. W., W. Yu, et al. (2005). "Crystal structure of botulinum neurotoxin type G light chain: Serotype divergence in substrate recognition." Biochemistry **44**(28): 9574-9580.

Arnon, S. S., R. Schechter, et al. (2001). "Botulinum toxin as a biological weapon: Medical and public health management." Journal of the American Medical Association **285**(8): 1059-1070.

Ashery, U., A. Betz, et al. (1999). "An efficient method for infection of adrenal chromaffin cells using the Semliki Forest virus gene expression system." European Journal of Cell Biology **78**(8): 525-532.

Baldwin, M. R., M. Bradshaw, et al. (2004). "The C-terminus of botulinum neurotoxin type A light chain contributes to solubility, catalysis, and stability." Protein Expression and Purification **37**(1): 187-195.

Band, P. A., S. Blais, et al. (2010). "Recombinant derivatives of botulinum neurotoxin A engineered for trafficking studies and neuronal delivery." Protein Expression and Purification **71**(1): 62-73.

Barbour, B. and P. Isope (2000). "Combining loose cell-attached stimulation and recording." J Neurosci Methods **103**(2): 199-208.

Barizuddin, S., X. Liu, et al. (2010). "Automated targeting of cells to electrochemical electrodes using a surface chemistry approach for the measurement of quantal exocytosis." ACS Chemical Neuroscience **1**(9): 590-597.

Barnett, D. W., J. Liu, et al. (1996). "Single-cell measurements of quantal secretion induced by α-latrotoxin from rat adrenal chromaffin cells: Dependence on extracellular Ca2+." Pflugers Archiv European Journal of Physiology **432**(6): 1039-1046.

Bashir, R. (2004). "BioMEMS: State-of-the-art in detection, opportunities and prospects." Advanced Drug Delivery Reviews **56**(11): 1565-1586.

Benedetto, A. V. (1999). "The cosmetic uses of Botulinum toxin type A." International Journal of Dermatology **38**(9): 641-655.

Berberian, K., K. Kisler, et al. (2009). "Improved surface-patterned platinum microelectrodes for the study of exocytotic events." Anal Chem **81**(21): 8734-8740.

Binz, T., S. Bade, et al. (2002). "Arg362 and tyr365 of the botulinum neurotoxin type a light chain are involved in transition state stabilization." Biochemistry **41**(6): 1717-1723.

Bittner, M. A., B. R. DasGupta, et al. (1989). "Isolated light chains of botulinum neurotoxins inhibit exocytosis. Studies in digitonin-permeabilized chromaffin cells." Journal of Biological Chemistry **264**(18): 10354-10360.

Blasi, J., E. R. Chapman, et al. (1993). "Botulinum neurotoxin A selectively cleaves the synaptic protein SNAP-25." Nature **365**(6442): 160-163.

Blumenfeld, A. M., D. W. Dodick, et al. (2004). "Botulinum neurotoxin for the treatment of migraine and other primary headache disorders." Dermatologic Clinics **22**(2): 167-175.

Boghen, D. R. (1996). "Disorders of facial motor function." Current Opinion in Ophthalmology **7**(6): 48-52.

Borges, R., M. Camacho, et al. (2008). "Measuring secretion in chromaffin cells using electrophysiological and electrochemical methods." Acta Physiol (Oxf) **192**(2): 173-184.

Boyer, A. E., H. Moura, et al. (2005). "From the mouse to the mass spectrometer: Detection and differentiation of the endoproteinase activities of botulinum neurotoxins A-G by mass spectrometry." Analytical Chemistry **77**(13): 3916-3924.

Breidenbach, M. A. and A. T. Brunger (2004). "Substrate recognition strategy for butulinum neurotoxin serotype A." Nature **432**(7019): 925-929.

Breidenbach, M. A. and A. T. Brunger (2005). "2.3 Å crystal structure of tetanus neurotoxin light chain." Biochemistry **44**(20): 7450-7457.

Bruns, D. and R. Jahn (1995). "Real-time measurement of transmitter release from single synaptic vesicles." Nature **377**: 62-65.

Burgoyne, R. D. and A. Morgan (2003). "Secretory granule exocytosis." Physiological Reviews **83**(2): 581-632.

Cahill, P. S. and R. M. Wightman (1995). "Simultaneous amperometric measurement of ascorbate and catecholamine secretion from individual bovine adrenal medullary cells." Anal Chem **67**(15): 2599-2605.

Cai, S., B. R. Singh, et al. (2007). "Botulism diagnostics: From clinical symptoms to in vitro assays." Critical Reviews in Microbiology **33**(2): 109-125.

Cans, A. S. and A. G. Ewing (2011). "Highlights of 20 years of electrochemical measurements of exocytosis at cells and artificial cells." Journal of Solid State Electrochemistry **15**(7-8): 1437-1450.

Čapek, P. and T. J. Dickerson (2010). "Sensing the deadliest toxin: Technologies for botulinum neurotoxin detection." Toxins **2**(1): 24-53.

Carabelli, V., S. Gosso, et al. (2010). "Nanocrystalline diamond microelectrode arrays fabricated on sapphire technology for high-time resolution of quantal catecholamine secretion from chromaffin cells." Biosensors and Bioelectronics **26**(1): 92-98.

Centers for Disease Control and Prevention. (2003). "Bioterrorism Agents/Diseases." Retrieved 24 Oct, 2013, from http://www.bt.cdc.gov/agent/agentlist-category.asp.

Chao, H. Y., Y. C. Wang, et al. (2004). "A highly sensitive immuno-polymerase chain reaction assay for Clostridium botulinum neurotoxin type A." Toxicon **43**(1): 27-34.

Chen, G., P. F. Gavin, et al. (1995). "Observation and quantitation of exocytosis from the cell body of a fully developed neuron in Planorbis corneus." Journal of Neuroscience **15**(11): 7747-7755.

Chen, P., B. Xu, et al. (2003). "Amperometric detection of quantal catecholamine secretion from individual cells on micromachined silicon chips." Anal Chem **75**(3): 518-524.

Chen, T. K., G. Luo, et al. (1994). "Amperometric monitoring of stimulated catecholamine release from rat pheochromocytoma (PC12) cells at the zeptomole level." Analytical Chemistry **66**(19): 3031-3035.

Chen, X., Y. Gao, et al. (2008). "Controlled on-chip stimulation of quantal catecholamine release from chromaffin cells using photolysis of caged Ca2+ on transparent indium-tin-oxide microchip electrodes." Lab Chip **8**(1): 161-169.

Chow, R. H., L. von Ruden, et al. (1992). "Delay in vesicle fusion revealed by electrochemical monitoring of single secretory events in adrenal chromaffin cells." Nature **356**(6364): 60-63.

Connolly, M. and D. De Berker (2003). "Management of Primary Hyperhidrosis: A Summary of the Different Treatment Modalities." American Journal of Clinical Dermatology **4**(10): 681-697.

De Toledo, G. A., R. Fernandez-Chacon, et al. (1993). "Release of secretory products during transient vesicle fusion." Nature **363**(6429): 554-558.

Dembek, Z. F., L. A. Smith, et al. (2007). "Botulism: cause, effects, diagnosis, clinical and laboratory identification, and treatment modalities." Disaster medicine and public health preparedness **1**(2): 122-134.

Deng, W., T. Ohgi, et al. (2001). "Characteristics of indium tin oxide films deposited by DC and RF magnetron sputtering." Japanese Journal of Applied Physics, Part 1: Regular Papers and Short Notes and Review Papers **40**(5 A): 3364-3369.

Dernick, G., G. Alvarez de Toledo, et al. (2003). "Exocytosis of single chromaffin granules in cell-free inside-out membrane patches." Nat Cell Biol **5**(4): 358-362.

Dias, A. F., G. Dernick, et al. (2002). "An electrochemical detector array to study cell biology on the nanoscale." Nanotechnology **13**: 285-289.

Dittami, G. M. and R. D. Rabbitt (2010). "Electrically evoking and electrochemically resolving quantal release on a microchip." Lab Chip **10**(1): 30-35.

Dongo, M., W. H. Tepp, et al. (2004). "Using fluorescent sensors to detect botulinum neurotoxin activity in vitro and in living cells." Proceedings of the National Academy of Sciences of the United States of America **101**(41): 14701-14706.

Dunn, L. A. and R. W. Holz (1983). "Catecholamine secretion from digitonin-treated adrenal medullary chromaffin cells." Journal of Biological Chemistry **258**(8): 4989-4993.

Ekong, T. A. N., I. M. Feavers, et al. (1997). "Recombinant SNAP-25 is an effective substrate for Clostridium botulinum type A toxin endopeptidase activity in vitro." Microbiology **143**(10): 3337-3347.

Eleopra, R., V. Tugnoli, et al. (1998). "Different time courses of recovery after poisoning with botulinum neurotoxin serotypes A and E in humans." Neuroscience Letters **256**(3): 135-138.

Elhamdani, A., H. C. Palfrey, et al. (2001). "Quantal size is dependent on stimulation frequency and calcium entry in calf chromaffin cells." Neuron **31**(5): 819-830.

Elhamdani, A., Z. Zhou, et al. (1998). "Timing of dense-core vesicle exocytosis depends on the facilitation L-type Ca channel in adrenal chromaffin cells." J Neurosci **18**(16): 6230-6240.

Evanko, D. (2005). "Primer: spying on exocytosis with amperometry." Nat Methods **2**(9): 650.

Fatt, P. and B. Katz (1950). "Membrane potentials at the motor end-plate." J Physiol **111**(1-2): 46p-47p.

Fatt, P. and B. Katz (1950). "Some observations on biological noise." Nature **166**(4223): 597-598.

Fatt, P. and B. Katz (1952). "Spontaneous subthreshold activity at motor nerve endings." The Journal of physiology **117**(1): 109-128.

Fenwick, E. M., P. B. Fajdiga, et al. (1978). "Functional and morphological characterization of isolated bovine adrenal medullary cells." Journal of Cell Biology **76**(1): 12-30.

Ferreira, J. L. (2001). "Comparison of Amplified ELISA and Mouse Bioassay Procedures for Determination of Botulinal Toxins A, B, E, and F." Journal of AOAC International **84**(1): 85-88.

Fertig, N., R. H. Blick, et al. (2002). "Whole cell patch clamp recording performed on a planar glass chip." Biophysical Journal **82**(6): 3056-3062.

Fertig, N., M. George, et al. (2003). "Microstructured apertures in planar glass substrates for ion channel research." Receptors and Channels **9**(1): 29-40.

Fertig, N., M. Klau, et al. (2002). "Activity of single ion channel proteins detected with a planar microstructure." Applied Physics Letters **81**(25): 4865-4867.

Fertig, N., C. Meyer, et al. (2001). "Microstructured glass chip for ion channel electrophysiology." Phys. Rev. **64**(4).

Finnegan, J. M., K. Pihel, et al. (1996). "Vesicular quantal size measured by amperometry at chromaffin, mast, pheochromocytoma, and pancreatic β-cells." Journal of Neurochemistry **66**(5): 1914-1923.

Fiskum, G., G. Becker, et al. (1980). "Control of steady-state free Ca2+ by mitochondria, endoplasmic reticulum, and digitonin-treated cells." Journal of Supramolecular and Cellular Biochemistry **12**(SUPPL. 4).

Frampton, J. E. and S. E. Easthope (2003). "Botulinum Toxin A (Botox® Cosmetic): A Review of its Use in the Treatment of Glabellar Frown Lines." American Journal of Clinical Dermatology **4**(10): 709-725.

Frisk, M. L., W. H. Tepp, et al. (2009). "Self-assembled peptide monolayers as a toxin sensing mechanism within arrayed microchannels." Analytical Chemistry **81**(7): 2760-2767.

Fromherz, P. and A. Stett (1995). "Silicon-Neuron Junction: Capacitive Stimulation of an Individual Neuron on a Silicon Chip." Physical Review Letters **75**(8): 1670-1673.

Fu, Z., S. Chen, et al. (2006). "Light chain of botulinum neurotoxin serotype A: Structural resolution of a catalytic intermediate." Biochemistry **45**(29): 8903-8911.

Gao, Y., S. Bhattacharya, et al. (2009). "A microfluidic cell trap device for automated measurement of quantal catecholamine release from cells." Lab on a Chip - Miniaturisation for Chemistry and Biology **9**(23): 3442-3446.

Gao, Y., X. Chen, et al. (2008). "Magnetron sputtered diamond-like carbon microelectrodes for on-chip measurement of quantal catecholamine release from cells." Biomed Microdevices **10**(5): 623-629.

Gatto-Menking, D. L., H. Yu, et al. (1995). "Sensitive detection of biotoxoids and bacterial spores using an immunomagnetic electrochemiluminescence sensor." Biosensors and Bioelectronics **10**(6-7): 501-507.

Ge, S., S. Koseoglu, et al. (2010). "Bioanalytical tools for single-cell study of exocytosis." Analytical and Bioanalytical Chemistry **397**(8): 3281-3304.

Gil, A. (1998). "Dual effects of botulinum neurotoxin A on the secretory stages of chromaffin cells." European Journal of Neuroscience **10**(11): 3369-3378.

Gillis, K. (1995). Techniques for Membrane Capacitance Measurements. Single-Channel Recording. B. Sakmann and E. Neher, Springer US**:** 155-198.

Gong, L. W., I. Hafez, et al. (2003). "Secretory vesicles membrane area is regulated in tandem with quantal size in chromaffin cells." Journal of Neuroscience **23**(21): 7917-7921.

Gonon, F., R. Cespuglio, et al. (1978). "In vivo continuous electrochemical determination of dopamine release in rat neostriatum." Comptes rendus hebdomadaires des seances de l"Academie des sciences. Serie D: Sciences naturelles **286**(16): 1203-1206.

Graham, M. E., R. J. Fisher, et al. (2000). "Measurement of exocytosis by amperometry in adrenal chromaffin cells: effects of clostridial neurotoxins and activation of protein kinase C on fusion pore kinetics." Biochimie **82**(5): 469-479.

Guglielmo-Viret, V., O. Attrée, et al. (2005). "Comparison of electrochemiluminescence assay and ELISA for the detection of Clostridium botulinum type B neurotoxin." Journal of Immunological Methods **301**(1-2): 164-172.

Habermann, E., K. Goretzki, et al. (1985). "Tetanus toxin: its interaction with tissue constituents and monoclonal antibodies." In: 7th International Conference on Tetanus: pp. 179-193 (Nistiko, G., Mastroeni, P. and Pitzura, M., Eds). Roma: Gangemi Publishing Co.

Hafez, I., K. Kisler, et al. (2005). "Electrochemical imaging of fusion pore openings by electrochemical detector arrays." Proc Natl Acad Sci U S A **102**(39): 13879-13884.

Hakami, R. M., G. Ruthel, et al. (2010). "Gaining ground: Assays for therapeutics against botulinum neurotoxin." Trends in Microbiology **18**(4): 164-172.

Hanson, M. A. and R. C. Stevens (2000). "Cocrystal structure of synaptobrevin-II bound to botulinum neurotoxin type B at 2.0 Å resolution." Nature Structural Biology **7**(8): 687-692.

Hay, J. C. and T. F. Martin (1992). "Resolution of regulated secretion into sequential MgATP-dependent and calcium-dependent stages mediated by distinct cytosolic proteins." J Cell Biol **119**(1): 139-151.

Hochstetler, S. E., M. Puopolo, et al. (2000). "Real-time amperometric measurements off zeptomole quantities of dopamine released from neurons." Analytical Chemistry **72**(3): 489-496.

Holz, R. W. (1986). "The role of osmotic forces in exocytosis from adrenal chromaffin cells." Annual Review of Physiology **VOL. 48**: 175-189.

Holz, R. W. (1988). "Control of exocytosis from adrenal chromaffin cells." Cell Mol Neurobiol **8**(3): 259-268.

Holz, R. W., M. A. Bittner, et al. (1989). "MgATP-independent and MgATP-dependent exocytosis. Evidence that MgATP primes adrenal chromaffin cells to undergo exocytosis." Journal of Biological Chemistry **264**(10): 5412-5419.

Hordejuk, R., A. Szewczyk, et al. (2006). "The heterogeneity of ion channels in chromaffin granule membranes." Cellular & Molecular Biology Letters **11**(3): 312-325.

Horrigan, F. T. and R. J. Bookman (1994). "Releasable pools and the kinetics of exocytosis in adrenal chromaffin cells." Neuron **13**(5): 1119-1129.

Jahn, R. and D. Fasshauer (2012). "Molecular machines governing exocytosis of synaptic vesicles." Nature **490**(7419): 201-207.

Jahn, R. and R. H. Scheller (2006). "SNAREs - Engines for membrane fusion." Nature Reviews Molecular Cell Biology **7**(9): 631-643.

Jankowski, J. A., T. J. Schroeder, et al. (1992). "Quantal secretion of catecholamines measured from individual bovine adrenal medullary cells permeabilized with digitonin." Journal of Biological Chemistry **267**(26): 18329-18335.

Johnson, A. S., A. Selimovic, et al. (2013). "Microchip-based electrochemical detection for monitoring cellular systems." Analytical and Bioanalytical Chemistry **405**(10): 3013-3020.

Johnson, M. A., M. Villanueva, et al. (2007). "Catecholamine exocytosis is diminished in R6/2 Huntington's disease model mice." Journal of Neurochemistry **103**(5): 2102-2110.

Kawagoe, K. T., J. A. Jankowski, et al. (1991). "Etched carbon-fiber electrodes as amperometric detectors of catecholamine secretion from isolated biological cells." Analytical Chemistry **63**(15): 1589-1594.

Kelly, R. B. (1985). "Pathways of protein secretion in eukaryotes." Science **230**(4721): 25-32.

Kim, D., S. Koseoglu, et al. (2011). "Electroanalytical eavesdropping on single cell communication." Analytical Chemistry **83**(19): 7242-7249.

Kisler, K., B. N. Kim, et al. (2012). "Transparent Electrode Materials for Simultaneous Amperometric Detection of Exocytosis and Fluorescence Microscopy." J Biomater Nanobiotechnol **3**(2A): 243-253.

Kissinger, P. T., J. B. Hart, et al. (1973). "Voltammetry in brain tissue: a new neurophysiological measurement." Brain Research **55**(1): 209-213.

Kitamura, M., M. Iwamori, et al. (1980). "Interaction between Clostridium botulinum neurotoxin and gangliosides." Biochimica et Biophysica Acta **628**(3): 328-335.

Klemic, K. G., J. F. Klemic, et al. (2002). "Micromolded PDMS planar electrode allows patch clamp electrical recordings from cells." Biosensors and Bioelectronics **17**(6-7): 597-604.

Knight, D. E. and P. F. Baker (1982). "Calcium-dependence of catecholamine release from bovine adrenal medullary cells after exposure to intense electric fields." Journal of Membrane Biology **68**(2): 107-140.

Kongsaengdao, S., K. Samintarapanya, et al. (2006). "An outbreak of botulism in Thailand: Clinical manifestations and management of severe respiratory failure." Clinical Infectious Diseases **43**(10): 1247-1256.

Kostov, Y., N. Sergeev, et al. (2009). "A simple portable electroluminescence illumination-based CCD detector." Methods in molecular biology (Clifton, N.J.) **503**: 259-272.

Kreyden, O. P. and G. Burg (2000). "[Toxin treatment of sweat pearls. A review of the treatment of hyperhidrosis with a special view of a new therapy option using botulinum toxin A]." Schweiz Med Wochenschr **130**(29-30): 1084-1090.

Kumar, P., J. T. Colston, et al. (1994). "Detection of botulinum toxin using an evanescent wave immunosensor." Biosensors and Bioelectronics **9**(1): 57-63.

Kumaran, D., S. Eswaramoorthy, et al. (2009). "Domain Organization in Clostridium botulinum Neurotoxin Type E Is Unique: Its Implication in Faster Translocation." Journal of Molecular Biology **386**(1): 233-245.

Lacy, D. B., W. Tepp, et al. (1998). "Crystal structure of botulinum neurotoxin type A and implications for toxicity." Nature Structural Biology **5**(10): 898-902.

Lehnert, T., M. A. M. Gijs, et al. (2002). "Realization of hollow SiO2 micronozzles for electrical measurements on living cells." Applied Physics Letters **81**(26): 5063-5065.

Leszczyszyn, D. J., J. A. Jankowski, et al. (1990). "Nicotinic receptor-mediated catecholamine secretion from individual chromaffin cells: Chemical evidence for exocytosis." Journal of Biological Chemistry **265**(25): 14736-14737.

Li, L. and B. R. Singh (1999). "Structure-function relationship of clostridial neurotoxins." Journal of Toxicology - Toxin Reviews **18**(1): 95-112.

Lindau, M. and G. Alvarez De Toledo (2003). "The fusion pore." Biochimica et Biophysica Acta - Molecular Cell Research **1641**(2-3): 167-173.

Liu, X., S. Barizuddin, et al. (2011). "Microwell device for targeting single cells to electrochemical microelectrodes for high-throughput amperometric detection of quantal exocytosis." Analytical Chemistry **83**(7): 2445-2451.

Madou, M. J. (2002). Fundamentals of microfabrication : the science of miniaturization. Boca Raton, Fla., CRC Press.

Maritzen, T., D. J. Keating, et al. (2008). "Role of the vesicular chloride transporter ClC-3 in neuroendocrine tissue." Journal of Neuroscience **28**(42): 10587-10598.

Marszalek, P. E., B. Farrell, et al. (1997). "Kinetics of release of serotonin from isolated secretory granules I. Amperometric detection of serotonin from electroporated granules." Biophysical Journal **73**(3): 1160-1168.

Marty, A. and E. Neher (1995). Tight-Seal Whole-Cell Recording. Single-Channel Recording. B. Sakmann and E. Neher, Springer US**:** 31-52.

Marxen, P., G. Erdmann, et al. (1991). "The translocation of botulinum A neurotoxin by chromaffin cells is promoted in low ionic strength solution and is insensitive to trypsin." Toxicon **29**(2): 181-189.

Marxen, P., U. Fuhrmann, et al. (1989). "Gangliosides mediate inhibitory effects of tetanus and botulinum A neurotoxins on exocytosis in chromaffin cells." Toxicon **27**(8): 849-859.

Mayer, M., J. K. Kriebel, et al. (2003). "Microfabricated Teflon membranes for low-noise recordings of ion channels in planar lipid bilayers." Biophysical Journal **85**(4): 2684-2695.

McCreery, R. L., R. Dreiling, et al. (1974). "Voltammetry in brain tissue: the fate of injected 6 hydroxydopamine." Brain Research **73**(1): 15-21.

McNeer, K. W., M. G. Tucker, et al. (2000). "Management of essential infantile esotropia with botulinum toxin A: Review and recommendations." Journal of Pediatric Ophthalmology and Strabismus **37**(2): 63-67.

Meunier, A., O. Jouannot, et al. (2011). "Coupling amperometry and total internal reflection fluorescence microscopy at ITO surfaces for monitoring exocytosis of single vesicles." Angewandte Chemie - International Edition **50**(22): 5081-5084.

Montecucco, C. and J. Molgó (2005). "Botulinal neurotoxins: Revival of an old killer." Current Opinion in Pharmacology **5**(3 SPEC. ISS.): 274-279.

Mosharov, E. V. and D. Sulzer (2005). "Analysis of exocytotic events recorded by amperometry." Nat Methods **2**(9): 651-658.

Neher, E. (1998). "Vesicle pools and Ca2+ microdomains: new tools for understanding their roles in neurotransmitter release." Neuron **20**(3): 389-399.

Neher, E. and A. Marty (1982). "Discrete changes of cell membrane capacitance observed under conditions of enhanced secretion in bovine adrenal chromaffin cells." Proceedings of the National Academy of Sciences of the United States of America **79**(21 I): 6712-6716.

Neher, E. and B. Sakmann (1976). "Single channel currents recorded from membrane of denervated frog muscle fibers." Nature **260**(5554): 799-802.

Neher, E. and B. Sakmann (1992). "The patch clamp technique." Sci Am **266**(3): 44-51.

Ogert, R. A., J. E. Brown, et al. (1992). "Detection of Clostridium botulinum toxin A using a fiber optic-based biosensor." Analytical Biochemistry **205**(2): 306-312.

Olofsson, J., K. Nolkrantz, et al. (2003). "Single-cell electroporation." Curr Opin Biotechnol **14**(1): 29-34.

Palade, G. (1975). "Intracellular aspects of the process of protein synthesis." Science **189**(4200): 347-358.

Pantoja, R., J. M. Nagarah, et al. (2004). "Silicon chip-based patch-clamp electrodes integrated with PDMS microfluidics." Biosensors and Bioelectronics **20**(3): 509-517.

Parpura, V. (2005). "Nanofabricated carbon-based detector." Anal Chem **77**(2): 681-686.

Parpura, V. and E. R. Chapman (2005). "Detection of botulinum toxins: Micromechanical and fluorescence-based sensors." Croatian Medical Journal **46**(4): 491-497.

Penner, R., E. Neher, et al. (1986). "Intracellularly injected tetanus toxin inhibits exocytosis in bovine adrenal chromaffin cells." Nature **324**(6092): 76-78.

Phillips, R. W. and D. Abbott (2008). "High-throughput enzyme-linked immunoabsorbant assay (ELISA) electrochemiluminescent detection of botulinum toxins in foods for food safety and defence purposes." Food Additives and Contaminants - Part A Chemistry, Analysis, Control, Exposure and Risk Assessment **25**(9): 1084-1088.

Pihel, K., Q. D. Walker, et al. (1996). "Overoxidized polypyrrole-coated carbon fiber microelectrodes for dopamine measurements with fast-scan cyclic voltammetry." Analytical Chemistry **68**(13): 2084-2089.

Poli, M. A., V. R. Rivera, et al. (2002). "Development of sensitive colorimetric capture ELISAs for Clostridium botulinum neurotoxin serotypes E and F." Toxicon **40**(6): 797-802.

Ponchon, J. L., R. Cespuglio, et al. (1979). Anal. Chem. **51**.

Pothos, E., M. Desmond, et al. (1996). "L-3,4-dihydroxyphenylalanine increases the quantal size of exocytotic dopamine release in vitro." Journal of Neurochemistry **66**(2): 629-636.

Pothos, E. N. (2002). "Regulation of dopamine quantal size in midbrain and hippocampal neurons." Behavioural Brain Research **130**(1-2): 203-207.

Pothos, E. N., V. Davila, et al. (1998). "Presynaptic recording of quanta from midbrain dopamine neurons and modulation of the quantal size." Journal of Neuroscience **18**(11): 4106-4118.

Pothos, E. N., E. Mosharov, et al. (2002). "Stimulation-dependent regulation of the pH, volume and quantal size of bovine land rodent secretory vesicles." Journal of Physiology **542**(2): 453-476.

Poulet, S., D. Hauser, et al. (1992). "Sequences of the botulinal neurotoxin E derived from Clostridium botulinum type E (strain Beluga) and Clostridium butyricum (strains ATCC 43181 and ATCC 43755)." Biochemical and Biophysical Research Communications **183**(1): 107-113.

Rivera, V. R., F. J. Gamez, et al. (2006). "Rapid detection of Clostridium botulinum toxins A, B, E, and F in clinical samples, selected food matrices, and buffer using paramagnetic bead-based electrochemiluminescence detection." Analytical Biochemistry **353**(2): 248-256.

Rowland, L. P. (2002). "Stroke, spasticity, and botulinum toxin." New England Journal of Medicine **347**(6): 382-383.

Ryttsen, F., C. Farre, et al. (2000). "Characterization of single-cell electroporation by using patch-clamp and fluorescence microscopy." Biophys J **79**(4): 1993-2001.

Said, S. Z., A. Meshkinpour, et al. (2003). "Botulinum toxin A: Its expanding role in dermatology and esthetics." American Journal of Clinical Dermatology **4**(9): 609-616.

Sano, S., C. L. Smith, et al. (1992). "Immuno-PCR: Very sensitive antigen detection by means of specific antibody-DNA conjugates." Science **258**(5079): 120-122.

Scarlatos, A., A. J. Cadotte, et al. (2008). "Cortical networks grown on microelectrode arrays as a biosensor for botulinum toxin." Journal of Food Science **73**(3): E129-E136.

Schiavo, G., F. Benfenati, et al. (1992). "Tetanus and botulinum-B neurotoxins block neurotransmitter release by proteolytic cleavage of synaptobrevin." Nature **359**(6398): 832-835.

Schiavo, G., M. Matteoli, et al. (2000). "Neurotoxins affecting neuroexocytosis." Physiological Reviews **80**(2): 717-766.

Schmidt, C., M. Mayer, et al. (2000). "A chip-based biosensor for the functional analysis of single ion channels." Angewandte Chemie - International Edition **39**(17): 3137-3140.

Schmidt, J. J., R. G. Stafford, et al. (2001). "High-throughput assays for botulinum neurotoxin proteolytic activity: Serotypes A, B, D, and F." Analytical Biochemistry **296**(1): 130-137.

Schmoranzer, J., M. Goulian, et al. (2000). "Imaging constitutive exocytosis with total internal reflection fluorescence microscopy." Journal of Cell Biology **149**(1): 23-31.

Schulte, A. and R. H. Chow (1996). "A Simple for Insulating Microelectrodes Using Anodic Electrophoretic Deposition of Paint." Analytical Chemistry **68**(17): 3054-3058.

Segelke, B., M. Knapp, et al. (2004). "Crystal structure of Clostridium botulinum neurotoxin protease in a product-bound state: Evidence for noncanonical zinc protease activity." Proceedings of the National Academy of Sciences of the United States of America **101**(18): 6888-6893.

Sen, A., S. Barizuddin, et al. (2009). "Preferential cell attachment to nitrogen-doped diamond-like carbon (DLC:N) for the measurement of quantal exocytosis." Biomaterials **30**(8): 1604-1612.

Shukla, H. D. and S. K. Sharma (2005). "Clostridium botulinum: A bug with beauty and weapon." Critical Reviews in Microbiology **31**(1): 11-18.

Simpson, L. L. (2004). Identification of the Major Steps in Botulinum Toxin Action. **44:** 167-193.

Sims, C. E. and N. L. Allbritton (2007). "Analysis of single mammalian cells on-chip." Lab on a Chip - Miniaturisation for Chemistry and Biology **7**(4): 423-440.

Singh, B. R. (2000). "Intimate details of the most poisonous poison." Nature Structural Biology **7**(8): 617-619.

Singh, B. R. (2006). "Botulinum neurotoxin structure, engineering, and novel cellular trafficking and targeting." Neurotoxicity Research **9**(2-3): 73-92.

Singh, B. R. and M. A. Silvia (1996). "Detection of botulinum neurotoxins using optical fiber-based biosensor." Advances in Experimental Medicine and Biology **391**: 499-508.

Smith, C. (1999). "A persistent activity-dependent facilitation in chromaffin cells is caused by Ca2+ activation of protein kinase C." Journal of Neuroscience **19**(2): 589-598.

Smith, R. M. and A. E. Martell (1987). "Critical stability constants, enthalpies and entropies for the formation of metal complexes of aminopolycarboxylic acids and carboxylic acids." Science of The Total Environment **64**(1–2): 125-147.

Solomon, H. M. and T. J. Lilly. (2001). "Clostridium botulinum." Bacteriological analytical manual 8th Ed.; US Food and Drug Administration: Silver Spring, MD, USA. Retrieved 25 Oct, 2013, from http://www.fda.gov/Food/FoodScienceResearch/LaboratoryMethods/ucm070879.htm.

Song, K. H. (1998). "Botulinum toxin type a injection for the treatment of frown lines." Annals of Pharmacotherapy **32**(12): 1365-1367.

Sordel, T., S. Garnier-Raveaud, et al. (2006). "Hourglass SiO2 coating increases the performance of planar patch-clamp." Journal of Biotechnology **125**(1): 142-154.

Sørensen, J. B. (2005). "SNARE complexes prepare for membrane fusion." Trends in Neurosciences **28**(9): 453-455.

Spegel, C., A. Heiskanen, et al. (2007). "On-chip determination of dopamine exocytosis using mercaptopropionic acid modified microelectrodes." Electroanalysis **19**: 263-271.

Spegel, C., A. Heiskanen, et al. (2008). "Fully automated microchip system for the detection of quantal exocytosis from single and small ensembles of cells." Lab Chip **8**(2): 323-329.

Staal, R. G. W., E. V. Mosharov, et al. (2004). "Dopamine neurons release transmitter via a flickering fusion pore." Nature Neuroscience **7**(4): 341-346.

Stanker, L. H., P. Merrill, et al. (2008). "Development and partial characterization of high-affinity monoclonal antibodies for botulinum toxin type A and their use in analysis of milk by sandwich ELISA." Journal of Immunological Methods **336**(1): 1-8.

Stett, A., V. Bucher, et al. (2003). "Patch-clamping of primary cardiac cells with micro-openings in polyimide films." Medical and Biological Engineering and Computing **41**(2): 233-240.

Sudhof, T. C. (1995). "The synaptic vesicle cycle: A cascade of protein-protein interactions." Nature **375**(6533): 645-653.

Sulzer, D. and E. N. Pothos (2000). "Regulation of quantal size by presynaptic mechanisms." Reviews in the Neurosciences **11**(2-3): 159-212.

Sun, X. and K. D. Gillis (2006). "On-chip amperometric measurement of quantal catecholamine release using transparent indium tin oxide electrodes." Anal Chem **78**(8): 2521-2525.

Swaminathan, S. and S. Eswaramoorthy (2000). "Structural analysis of the catalytic and binding sites of Clostridium botulinum neurotoxin B." Nature Structural Biology **7**(8): 693-699.

Szílagyi, M., V. R. Rivera, et al. (2000). "Development of sensitive colorimetric capture elisas for Clostridium botulinum neurotoxin serotypes A and B." Toxicon **38**(3): 381-389.

Tengholm, A., B. Hellman, et al. (2000). "Mobilization of Ca2+ stores in individual pancreatic β-cells permeabilized or not with digitonin or α-toxin." Cell Calcium **27**(1): 43-51.

TerBush, D. R., M. A. Bittner, et al. (1988). "Ca2+ influx causes rapid translocation of protein kinase C to membranes. Studies of the effects of secretagogues in adrenal chromaffin cells." Journal of Biological Chemistry **263**(35): 18873-18879.

Thyagarajan, B., N. Krivitskaya, et al. (2009). "Capsaicin protects mouse neuromuscular junctions from the neuroparalytic effects of botulinum neurotoxin." Journal of Pharmacology and Experimental Therapeutics **331**(2): 361-371.

Travis, E. R. and R. M. Wightman (1998). "Spatio-temporal resolution of exocytosis from individual cells." Annu Rev Biophys Biomol Struct **27**: 77-103.

Volland, H., P. Lamourette, et al. (2008). "A sensitive sandwich enzyme immunoassay for free or complexed Clostridium botulinum neurotoxin type A." Journal of Immunological Methods **330**(1-2): 120-129.

Wightman, R. M., J. A. Jankowski, et al. (1991). "Temporally resolved catecholamine spikes correspond to single vesicle release from individual chromaffin cells."

Proceedings of the National Academy of Sciences of the United States of America **88**(23): 10754-10758.

Wu, H. C., Huang, et al. (2001). "Detection of clostridium botulinum neurotoxin type A using immuno-PCR." Letters in Applied Microbiology **32**(5): 321-325.

Xu, T., T. Binz, et al. (1998). "Multiple kinetic components of exocytosis distinguished by neurotoxin sensitivity." Nature Neuroscience **1**(3): 192-200.

Yang, Y., T. J. Craig, et al. (2007). "Phosphomimetic mutation of Ser-187 of SNAP-25 increases both syntaxin binding and highly Ca2+-sensitive exocytosis." J Gen Physiol **129**(3): 233-244.

Yao, J. and K. D. Gillis (2012). "Quantification of noise sources for amperometric measurement of quantal exocytosis using microelectrodes." Analyst **137**(11): 2674-2681.

Yobas, L. (2013). "Microsystems for cell-based electrophysiology." Journal of Micromechanics and Microengineering **23**(8).

Zeck, G. and P. Fromherz (2001). "Noninvasive neuroelectronic interfacing with synaptically connected snail neurons immobilized on a semiconductor chip." Proc Natl Acad Sci U S A **98**(18): 10457-10462.

Zhang, Q., Y. Li, et al. (2009). "The dynamic control of kiss-and-run and vesicular reuse probed with single nanoparticles." Science **323**(5920): 1448-1453.

Zhou, Z. and S. Misler (1995). "Action potential-induced quantal secretion of catecholamines from rat adrenal chromaffin cells." J Biol Chem **270**(8): 3498-3505.

VITA

Jaya Ghosh was born in Kolkata, West Bengal, India in December, 1982. She obtained her Bachelor of Engineering degree in Instrumentation & Control Engineering from Manipal Institute of Technology (Manipal Academy of Higher Education), Manipal, Karnataka, India, in 2005. After working as a Software Engineer at Infosys Technologies Ltd., India, for two years, she came to the United States to pursue her doctoral degree in 2007. She obtained her Doctor in Philosophy degree in Biological Engineering in 2013 from University of Missouri. She will continue her biomedical research as a Postdoctoral Fellow in University of Missouri, Columbia, USA.